

**PILE DRIVING ANALYSIS — SIMULATION OF HAMMERS,
CUSHIONS, PILES, AND SOIL**

by

Lee Leon Lowery, Jr.
Assistant Research Engineer

T. J. Hirsch
Research Engineer

and

C. H. Samson, Jr.
Research Engineer

Research Report 33-9

Piling Behavior

Research Study No. 2-5-62-33

Sponsored by

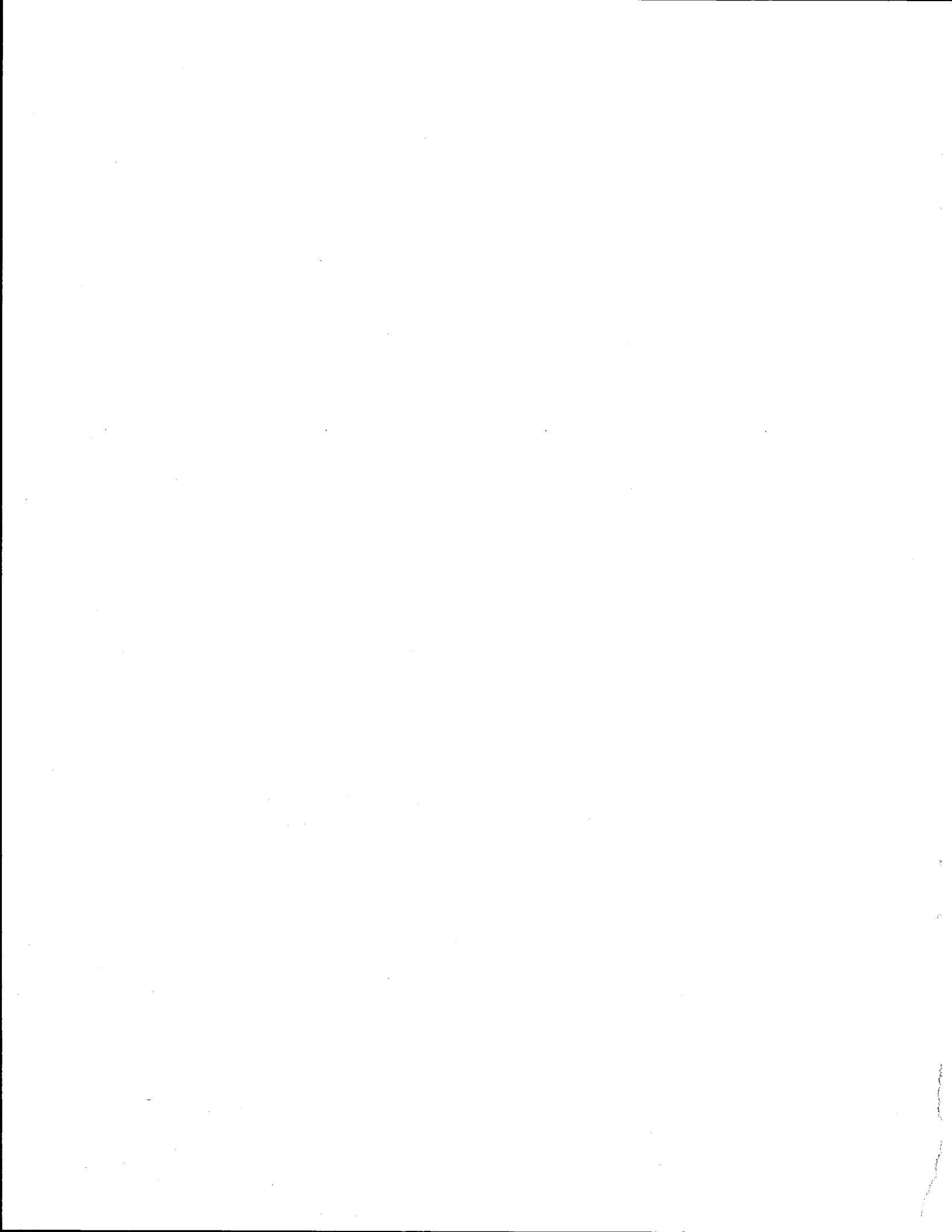
The Texas Highway Department

in cooperation with the

U. S. Department of Transportation, Federal Highway Administration
Bureau of Public Roads

August 1967

TEXAS TRANSPORTATION INSTITUTE
Texas A&M University
College Station, Texas



PREFACE

The information contained herein was developed on research study 2-5-62-33 entitled "Piling Behavior" which is a cooperative research study sponsored jointly by the Texas Highway Department and the U. S. Department of Transportation, Federal Highway Administration, Bureau of Public Roads. The broad objective of this study is to fully develop the use of a computer solution of the wave equation so that it may be used to predict driving stresses in piling and to estimate static load bearing capacity of piling.

This report concerns itself with the following specific items in the work plan as set forth in the study proposal:

1. To determine the effect of dynamic damping in concrete and steel piling on the impact longitudinal stress waves. This was accomplished by correlating theoretical stress waves with data obtained from full scale piles tested under controlled conditions.

2. To study the dynamic load-deformation properties of cushioning materials and their effect on the stress waves in piling. This was accomplished by correlating theoretical stress waves with data from full scale pile tests under controlled conditions. Theoretical results were compared with experimental data gathered for various cushion materials.

3. To evaluate the true energy output of different pile driving hammers (single acting steam hammers, double acting steam hammers, and open and closed end diesel hammers) using the wave equation to analyze portions of data obtained by the Michigan State Highway Commission and published in a report entitled "A Performance Investigation of Pile Driving Hammers and Piles."

4. To determine a uniform basis of rating pile driver energy output applicable to different type hammers.

5. To correlate the wave equation with suitable experimental test data.

During the course of investigation of the above items, the factors listed below were also found to influence the wave equation results, and therefore were also investigated and are reported herein:

1. A study of the effect of ram elasticity on piling behavior.
2. A study of the influence of parameters used to describe soil behavior.

The information reported herein is necessary in order to understand the dynamic behavior of piling and to properly simulate pile driving hammers, capblocks and cushion blocks, piles, and soils for wave equation analysis of piling behavior.

The opinions, findings and conclusions expressed in this report are those of the authors and not necessarily those of the Bureau of Public Roads.

LIST OF TABLES

Table	Page
3.1 Effect of Breaking the Ram Into Segments When Ram Strikes a Cushion	5
3.2 Effect of Breaking Ram Into Segments When Ram Strikes a Steel Anvil	5
3.3 Summary of Belleville Cases Solved by Wave Equation	7
3.4 Summary of Detroit Cases Solved by Wave Equation	8
3.5 Summary of Muskegon Cases Solved by Wave Equation	8
3.6 Effect of Cushion Stiffness on ENTHRU for BLTP-6; 10.0	9
3.7 Effect of Cushion Stiffness on FMAX for BLTP-6; 10.0	9
3.8 Effect of Cushion Stiffness on LIMSET for BLTP-6; 10.0	9
3.9 Data Reported in the Michigan Study	10
3.10 Summary of Results for Michigan Steam Hammers	12
3.11 Summary of Results for Michigan Diesel Hammers	14
3.12 Comparison of Energy Output Measured Experimentally With That Predicted by Equation 3.6, for Diesel Hammers	16
3.13 Comparison of Measured Output With That Given by Equation 3.7, for Single Acting Steam Hammers	16
3.14 Comparison of Measured Energy Output With That Predicted by Equation 3.11, for Double Acting Steam Hammers	16
3.15 Summary of Hammer Properties and Operating Characteristics	18
3.16 Effect of Removing Load Cell on ENTHRU, LIMSET, and Permanent Set of Pile	19
3.17 Effect on ENTHRU Resulting From Removing the Load Cell Assembly	20
3.18 Effect of Cushion Stiffness on Maximum Point Displacement for Case BLTP-6; 10.0 and 57.9	20
3.19 Effect of Coefficient of Restitution on ENTHRU for Case BLTP-6; 10.0 and 57.9	20
3.20 Effect of Coefficient of Restitution on Maximum Point Displacement for Case BLTP-6; 10.0 and 57.9	21
3.21 Study of Various Hammers Driving the Same Pile	21
4.1 Suspended Pile Data	22
4.2 Dynamic Cushion Properties	24
5.1 Dynamic Properties of New Cushion Blocks of Various Materials	27
6.1 Comparison of Results Found by Using Elastic-Plastic vs Non-Linear Soil Resistance Curves	32
6.2 Influence of Soil Quake at Different Soil Resistances for Case BLTP-6; 57.9 With No Soil Damping	33
6.3 Influence of Soil Damping on Different Soil Resistances for Case BLTP-6; 57.9 ($Q = 0.1$ for All Cases)	33

Pile Driving Analysis - Simulation of Hammers, Cushions, Piles, and Soil

Chapter I

INTRODUCTION

General Background

The problem of pile-driving analysis has been of great interest to engineers for many years. Ever since the first engineer proposed a method for predicting the load carrying capacity of a pile, the whole subject of pile driving has become a much debated field in engineering. In other areas new methods of analysis for structural elements and systems are constantly being proposed with little or no resulting discussion. However, the proposal of a new piling analysis is sure to stir much interest and often some rather heated discussions.

Since over four-hundred pile-driving formulas have been proposed,¹ not including the countless formula modifications which are used,² many engineers resort to the use of only one or two formulas regardless of the driving conditions encountered.³ Although many of the erroneous assumptions made in these formulas have been widely discussed,^{4,5} the fact that they omit many significant parameters which affect the problem seems to have received less attention. However, when the driving formulas omit parameters which change from case to case, the engineer has no means of determining how significant the parameter may be, nor can he tell in which direction or to what extent the change will vary the results. Thus, to obtain an accurate solution obviously requires that fewer erroneous assumptions be made regarding the dynamic behavior of the materials and equipment used in pile driving, and that all significant parameters are included in the analysis.

The first of these problems was solved when it was noted that pile driving is actually a case of longitudinal impact, governed by the wave equation rather than by statics or rigid-body dynamics.^{6,7} However, since the exact simulation and solution of the wave equation applied to piling are extremely complex for all but the simplest problems, many significant parameters still had to be neglected.

The second problem was solved by Smith⁸ who proposed a numerical solution to the wave equation, capable of including any of the known parameters involved in pile-driving analysis. This method of analysis was applicable to tapered, stepped, and composite piles, to nonlinear soil resistances and damping, to piles with cushions, followers, helmets, etc. In other words, it was a completely general method of analysis for the problem of pile driving.

It should be noted that much of the experimental work used in this report was reported by other investigators. These cases are referenced, and the problem number or name used herein will be the same as used by the original reporter. This will enable the reader to

determine any additional information about the problem being solved by referring to the original paper.

Objectives

The objectives of this research were:

1. To review and summarize Smith's original method of analysis and to derive a more general solution.
2. To determine how the numerical solution is affected by the elasticity of the ram.
3. To determine the energy output of different type pile hammers.
4. To compare results given by the wave equation with those determined by laboratory experiments and field tests.
5. To illustrate the significance of the parameters involved, including cushion stiffness and damping, ram velocity, material damping in the pile, soil damping and quake, and to determine the quantitative effect of these parameters where possible.
6. To show how the wave equation can be used to determine the dynamic or impact characteristics of the materials involved.
7. To determine the dynamic properties of the cushion subjected to impact loading.
8. To study the effect of internal damping in the pile and its significance.

Literature Review

The basic purpose of any pile driving formula is to permit the design of a functional yet economical foundation. According to Chellis,⁹ there are four basic types of driving formulas:

1. Empirical formulas, which are based on statistical investigations of pile load tests,
2. Static formulas, which are based on the side frictional forces and point bearing force on the pile, as determined by soils investigations,
3. Dynamic formulas, which assume that the dynamic soil resistance is equal to the static load capacity of the pile, and
4. The wave equation, which assumes only those material properties whose dynamic behavior is not completely understood and has not yet been determined experimentally. Each of the preceding formulas has advantages and disadvantages which have been widely noted^{10,11} and need not be restated at this time.

Isaacs is thought to have first noted that the wave equation is applicable to the problem of pile driving.¹² However, Fox¹³ was probably the first person to propose that an exact solution be used for pile-driving analysis. Shortly thereafter, Glanville, Grime, Fox, and Davies¹⁴ published the first correlations between experimental studies and results determined by the exact solution to the wave equation developed by Fox. Since this exact solution was extremely complex, they were forced to use simplified boundary conditions including zero side frictional resistance, a perfectly elastic cushion block, and an elastic soil spring acting only at the tip of the pile. However, even using these simplified boundary conditions, they obtained reasonably accurate results.

In 1940 Cummings¹⁵ discussed several errors inherent in dynamic pile-driving formulas and reviewed the previous work done using the wave equation. However, he also noted that even for the simplest problems, "the complete solution includes long and complicated mathematical expressions so that its use for a practical problem would involve laborious numerical calculations."

A practical pile-driving problem usually involves side frictional soil resistance, soil damping constants, nonlinear cushion and capblock springs, and other factors which prevent a direct solution of the resulting differential equation. However, in 1950 Smith¹⁶ proposed a mathematical model and a corresponding numerical method of analysis which accounted for the effects of many of these parameters. He has continued to update this method and published various other works.^{17,18,19,20,21}

Smith's method of analysis did not really become popular until 1960 when he published a summary of the method's application to the problem of pile-driving analysis.²² In this paper he recommended a number of material constants and the material behavior curves required to account for the dynamic action of the soil, cushion, and pile material.

Smith's method of analyzing pile-driving problems received considerable interest,²³ and two immediate applications of the wave equation were suggested:

1. The immediate application of the wave equation, using the most probable material properties to predict ultimate driving resistance and driving stresses.
2. Its use to perform extensive parameter studies in order to determine trends and to gain more insight into the behavior of pile driving, and also determine the relative significance of these parameters.

Immediately after the appearance of Smith's paper in 1960, the Bridge Division of the Texas Highway Department initiated a research project with the Texas Transportation Institute to perform exhaustive studies of the behavior of piling by the wave equation. The first report dealt with a computer program based on Smith's numerical solution.²⁴ This program was used to determine the driving stresses induced in a number of prestressed concrete piles which had failed during driving,²⁵ and later to check the conditions at similar sites at which pile breakage due to excessive driving stresses might be experienced.²⁶

Forehand and Reese²⁸ investigated the possibility of predicting the ultimate bearing capacity of piling using the wave equation, but since complete data were available for relatively few problems, they were unable to draw many firm conclusions. They also studied the dynamic action of the soil during driving and recommended some values for the soil parameters used in the wave equation.

In August, 1963 several extensions of Smith's method were presented by the writers.²⁹ Two simple cases for which "exact" solutions were known were compared with Smith's numerical solution to indicate the method's accuracy. A third section of the paper presented the results of a short parameter study which indicated how certain trends in pile driving might be determined and how to study the significance of various parameters. The results for several theoretical and field test problems were also compared.

In 1963 the writers³⁰ published a study on the methods employed in measuring dynamic stresses and displacements of piling during driving, and presented further experimental and theoretical comparisons "to demonstrate that the computer solution of the wave equation offers a rational approach to the problems associated with the structural behavior of piling during driving." This report was based on an earlier study dealing with driving prestressed concrete piles.³¹

An investigation by Hirsch³² involved a study of the variables which affected the behavior of concrete piles during driving. Over 2100 separate problems were solved and the results were presented in the form of graphs for use by design engineers.

Later publications dealt with the dynamic load-deformation properties of various pile cushion materials and other dynamic properties of materials required to simulate as closely as possible the actual behavior of a pile during driving.^{33,34,35,36}

Chapter II

A NUMERICAL METHOD OF ANALYSIS

The Basic Solution

Since 1931, it has been realized that pile driving involved theories of longitudinal impact rather than statics. However, the application of the wave equation to pile driving was restricted to very simple problems because the exact solution was complex, involved much

labor, and for most practical cases, required many simplifying assumptions.

In 1950, Smith³⁷ proposed an approximate solution based on concentrating the distributed mass of the pile, as shown in Figure 2.1a, into a series of small weights, $W(1)$ thru $W(MP)$, connected by weightless springs

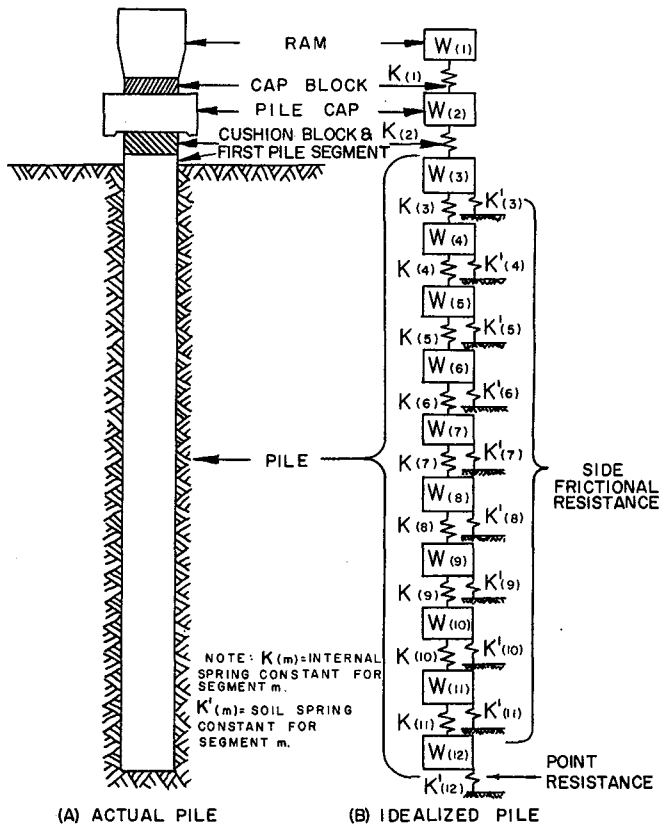


Figure 2.1. Idealization of a pile for purpose of analysis.

$K(1)$ thru $K(MP-1)$, with the addition of soil resistance acting on the masses, as illustrated in Figure 2.1b. Time also was divided into small increments. This numerical solution was then applied by the repeated use of the following equations, developed by Smith.³⁸

$$D(m,t) = D(m,t-1) + 12\Delta t V(m,t-1) \quad \text{Eq. 2.1}$$

$$C(m,t) = D(m,t) - D(m+1,t) \quad \text{Eq. 2.2}$$

$$F(m,t) = C(m,t)K(m) \quad \text{Eq. 2.3}$$

$$R(m,t) = \frac{[D(m,t) - D'(m,t)]}{K'(m) [1 + J(m)V(m,t-1)]} \quad \text{Eq. 2.4}$$

$$V(m,t) = V(m,t-1) + \frac{[F(m,t) - R(m,t)]}{g\Delta t/W(m)} \quad \text{Eq. 2.5}$$

where m is the mass number, t denotes the time interval number, Δt is the size of the time interval (sec), $D(m,t)$ is the total displacement of mass number m during time interval number t (in.), $V(m,t)$ is the velocity of mass m during time interval t (ft/sec), $C(m,t)$ is the compression of spring m during time interval t (in.), $F(m,t)$ is the force exerted by spring number m between segment numbers (m) and $(m+1)$ during time interval t (lb), and $K(m)$ is the spring rate of mass m (lb/in.). Note that since certain parameters do not change with time, they are assigned single rather than double subscripts.

The quantity $R(m,t)$ is the total soil resistance acting on segment m (lb/in.); $K'(m)$ is the spring rate of the soil spring causing the external soil resistance force on mass m (lb/in.); $D(m,t)$ is the total inelastic soil displacement or yielding during the t at segment m (in.);

$J(m)$ is a damping constant for the soil acting on segment number (m) (sec/ft); g is the gravitational acceleration (ft/sec²); and $W(m)$ is the weight of segment number m (lb).

The solution is begun by initializing the time-dependent parameters to zero and by giving the ram an initial velocity. Then an incremental amount of time Δt elapses during which the ram moves down an amount given by Equation 2.1. The displacements $D(m,I)$ of the other masses are computed in the same manner.

Equation 2.2 is then used to determine the compressions $C(m,I)$, after which the internal spring forces acting between the masses are found from Equation 2.3 and the external soil forces $R(m,I)$ are computed from Equation 2.4.

Finally, a new velocity $V(m,I)$ is determined for each mass using Equation 2.5, after which another time interval elapses. New displacements, compressions, forces, and velocities are again computed using the same equations and the cycle is repeated until the solution is obtained. Smith³⁹ and others,^{40,41} give a detailed explanation of this method of solution and the computer programming required. The dynamic behavior of various parameters will be discussed later.

Smith would have probably caused little interest had he simply given a numerical solution for the wave equation. Instead he presented a simple, physical model, easily visualized, using parameters which are readily understood. This and the simplicity of the equations required for a solution doubtlessly account for much of the wave equation's increasing popularity as a means of studying the behavior of piling.

Modifications of the Original Solution

Although the original method of analysis proposed by Smith can be used to solve many of the problems given in this report, it has been greatly extended to include other idealizations. The major additions and changes are summarized here for reference only, and are fully discussed in later chapters.

1. The relationship between soil resistance to penetration of the pile was originally limited to a series of straight lines. The revised program allows the use of any shape for this curve, as noted in Chapter VI.

2. The elastic soil deformation "Q" and the soil damping constant "J" were each limited to one value at the point of the pile and a second value for side resistance. These parameters have been generalized to include different values at each pile segment.

3. A new method by which internal damping in the pile can be accounted for is now included. This method is explained in Chapter V.

4. A second method is included to account for the coefficient of restitution of the capblock or cushionblock.

5. For correlation with experimental data, it is now possible to place forces directly on the head of the pile rather than having to calculate them from the hammer-cushion-anvil properties. This method was used extensively where the force vs time curve at the head of the pile was known; since then the hammer, cushion, and anvil properties did not influence the solution.

6. The linear force vs compression curve for various cushion materials used previously has been generalized as noted in Chapter IV.

7. The effect of gravity on the solution can now be accounted for.

8. A special "parameter study" sub-program was written and included in the general program. This feature was used to vary specific parameters or groups of

parameters between specified limits in order to study their influence on the solution, and to see if trends could be found.

9. For possible later use, several pile-driving formulas were included in the computer program.

10. The soil resistance on the point segment now uses two springs, one for the side friction acting on the side of the pile and a second spring for point bearing.

Chapter III

PILE DRIVING HAMMERS

Ram Idealization

Smith⁴² suggests that since the ram is usually short in length, in many cases it can accurately be represented by a single weight having infinite stiffness. The example illustrated in Figure 2.1 makes this assumption since $K(1)$ represents the spring constant of only the cap block, the elasticity of the ram having been neglected. He also notes that where greater accuracy is desired, or when the ram is long and slender, it can also be

divided into a series of weights and springs. However, no work has been done to determine how long the ram can be before its elasticity affects the accuracy of the solution. The most common hammers in the above class include drop, air, and steam hammers. Figures 3.1 and 3.2 show how the ram may be idealized.

In order to determine the significance of dividing the ram into a number of segments, several ram lengths ranging from 2 to 10 ft were assumed, driving a 100-ft

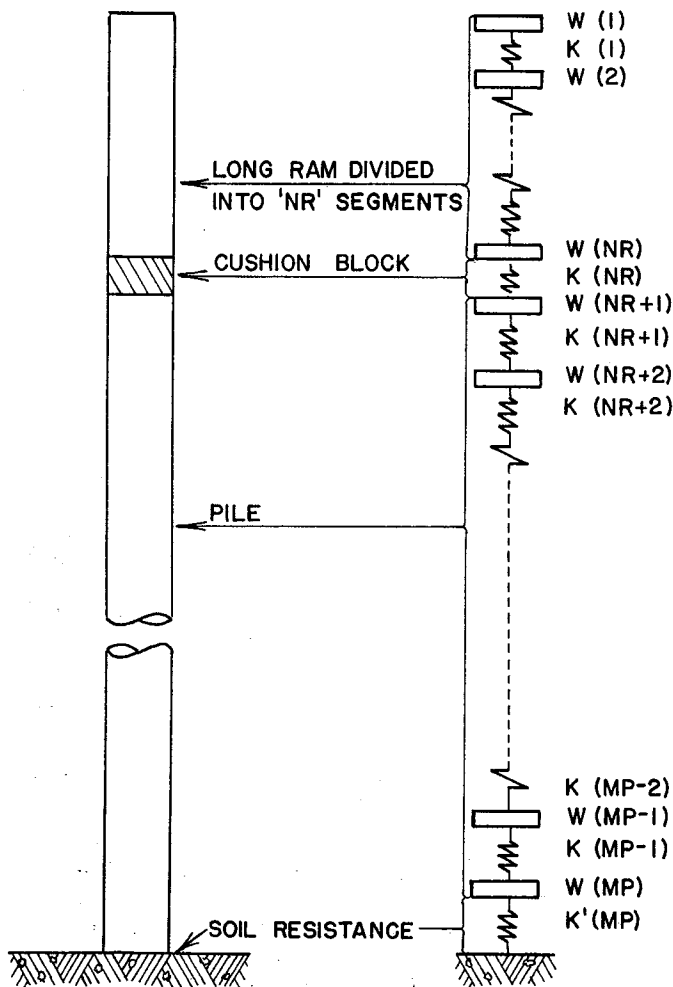


Figure 3.1. Idealization for a long ram striking directly on a cushion block.

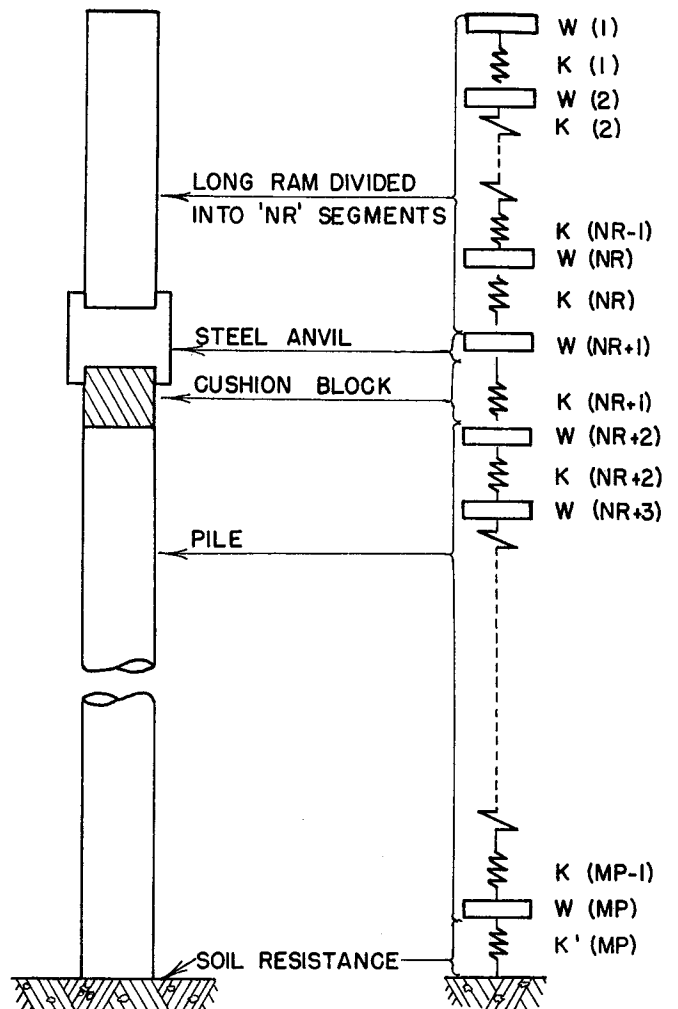


Figure 3.2. Idealization for a long ram striking directly on a steel anvil.

TABLE 3.1. EFFECT OF BREAKING THE RAM INTO SEGMENTS WHEN RAM STRIKES A CUSHION

Number of Ram Divisions	Length of Pile Segments (ft)	Maximum Compressive Force in Pile (kip)	Maximum Tensile Force in Pile (kip)	Maximum Point Displacement (in.)
1	1.25	263.1	219.0	3.057
2	1.25	262.6	218.8	3.058
10	1.25	262.9	218.5	3.059

pile with point resistance only. For this parameter study the total weight of the pile varied from 1,500 lb to 10,000 lb, while the ultimate soil resistance ranged from zero to 10,000 lb. The cushion was assumed to have a stiffness of 2,000 kip/in.

Table 3.1 lists the results found for a typical problem solved in this series, the problem consisting of a 10-ft ram traveling at 20 ft/sec, striking a cushion having a stiffness of 2,000 kip/in. The pile used was a 100-ft 12H53 steel pile, driven by a 5,000-lb ram with an initial velocity of 12.4 ft/sec. No pile cap was included in the solution, the cushion being placed directly between the hammer and the head of the pile. Since the ram was divided into very short lengths, the pile was also divided into short segments.

As shown in Table 3.1, the solution is not changed to any extent, regardless of whether the ram is divided into 1, 2, or 10 segments. The time interval Δt was held constant in each case.

In certain hammers such as a diesel hammer, the ram strikes directly on a steel anvil rather than on a cushion. This makes the choice of a spring rate between the ram and anvil difficult because the impact

occurs between two steel elements. One possible solution is to place the spring constant of the entire ram between the weights representing the ram and anvil. Also, the ram can be broken into a series of weights and springs as is the pile.

To determine when the ram in this case should be divided, a parameter study was run in which the ram length varied between 6 and 10 ft and the anvil weight from 1,000 to 2,000 lb. In each case, the ram diameter was held constant and the ram was divided into equal segment lengths as noted in Table 3.2. These variables were picked because of their possible influence on the solution.

The pile used was again a 12H53 point bearing pile with a cushion of 2,000 kip/in. spring constant placed between the anvil and head of the pile. The soil parameters used were $RU_{point} = 500$ kip, $Q = 0.1$ in., and $J = 0.15$ sec/ft. These factors were held constant for all problems listed in Table 3.2.

The most obvious result shown by Table 3.2 is that when the steel ram impacts directly on a steel anvil, dividing a long ram (6, 8 and 10 ft) into segments has a significant effect on the solution.

Energy Output of Hammer

One of the most significant parameters involved in pile driving is the velocity of the ram immediately before impact. This velocity is often used to determine the maximum kinetic energy of the hammer and its energy output rating, and must be known or assumed before the wave equation or dynamic formulas can be applied.

Although the manufacturers of pile-driving equipment furnish maximum energy ratings for their hammers, these are usually downgraded by foundation ex-

TABLE 3.2. EFFECT OF BREAKING RAM INTO SEGMENTS WHEN RAM STRIKES A STEEL ANVIL

Anvil Weight (lb)	Ram Length (ft)	Number of Ram Divisions	Length of Each Ram Segment (ft)	Maximum Compressive Force on Pile			Maximum Point Displacement (in.)	
				At Head (kip)	At Center (kip)	At Tip (kip)		
2000	10	1	10	513	513	884	0.207	
		2	5	437	438	774	0.159	
		5	2	373	373	674	0.124	
		10	1	375	375	678	0.125	
	8	1	8	478	478	833	0.183	
		4	2	359	359	648	0.117	
		8	1	360	360	651	0.118	
	6	1	6	430	430	763	0.155	
		3	2	344	344	621	0.110	
		6	1	342	342	616	0.109	
	1000	10	1	10	508	509	878	0.160
			2	5	451	451	789	0.159
5			2	381	382	691	0.151	
10			1	371	372	681	0.153	
8		1	8	487	488	846	0.151	
		4	2	443	444	785	0.144	
		8	1	369	370	675	0.134	
		10	0.8	337	338	665	0.133	
		6	1	6	457	457	798	0.137
6		3	2	361	362	666	0.128	
		6	1	316	316	562	0.109	
		10	0.6	320	320	611	0.113	

perts for various reasons. A number of conditions such as poor hammer condition, lack of lubrication, and wear seriously reduce the energy output of a hammer. In addition the energy of many hammers can be controlled by regulating the steam pressure or diesel fuel. To determine how much the rated energy of any given hammer should be reduced is not a simple task.

Chellis⁴³ discusses several reasons for this energy reduction and recommends a number of possible efficiency factors for the commonly used hammers, based on his observations and experience.

The Michigan Study of Pile Driving Hammers

In 1965 the Michigan State Highway Commission⁴⁴ completed an extensive research program designed to obtain a better understanding of the complex problem of pile driving. Though a number of specific objectives were given, one was of primary importance. As noted by Housel,⁴⁵ "Hammer energy actually delivered to the pile, as compared with the manufacturer's rated energy, was the focal point of a major portion of this investigation of pile-driving hammers." In other words, they hoped to determine the energy delivered to the pile and to compare these values with the manufacturer's ratings.

The energy transmitted to the pile was termed "ENTHRU" by the investigators⁴⁴ and was determined by the summation

$$\text{ENTHRU} = \sum F \Delta S$$

Where F , the average force on the top of the pile during a short interval of time, was measured by a specially designed load cell, and ΔS , the incremental movement of the head of the pile during this time interval, was found using displacement transducers and/or reduced from accelerometer data. It should be pointed out that ENTHRU is not the total energy output of the hammer blow, but only a measure of that portion of the energy delivered below the load-cell assembly.

Since so many variables influence the value of ENTHRU, and since some of these variables were changing during the pile driving operation (e.g., condition of the cushion, soil resistance, etc.), the investigators were not able to determine the total energy output of the hammer. As noted in the Michigan report:⁴⁶ "Hammer type and operation conditions; pile type, mass, rigidity, and length; and the type and condition of cap blocks were all factors that affected ENTHRU, but when, how, and how much could not be ascertained with any degree of certainty." However, the wave equation can account for each of these factors so that their effects can be determined.

The Michigan report also noted that ENTHRU was not actually a direct measurement of the hammer's efficiency or energy output since the forces and displacements were measured below the capblock, as shown in Figure 3.3. Thus, ENTHRU was defined as "the amount of work done on the load cell."

The maximum displacement of the head of the pile was also reported and was designated LIMSET. Oscillographic records of force vs time measured in the load cell were also reported. Since force was measured only at the load cell, the single maximum observed values for each case will be called FMAX.

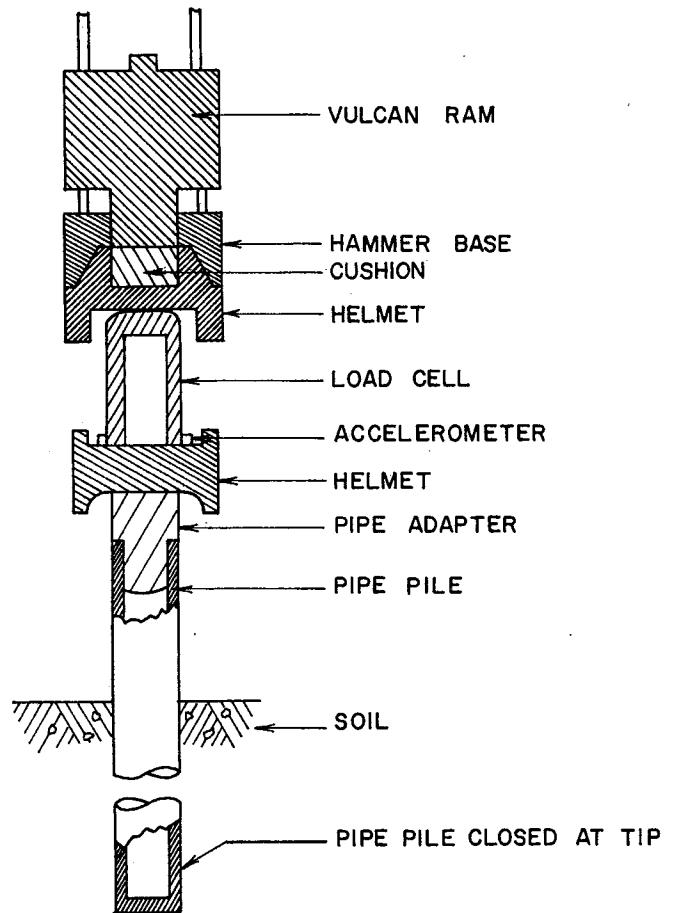


Figure 3.3. Typical pile driving assembly (after reference 44).

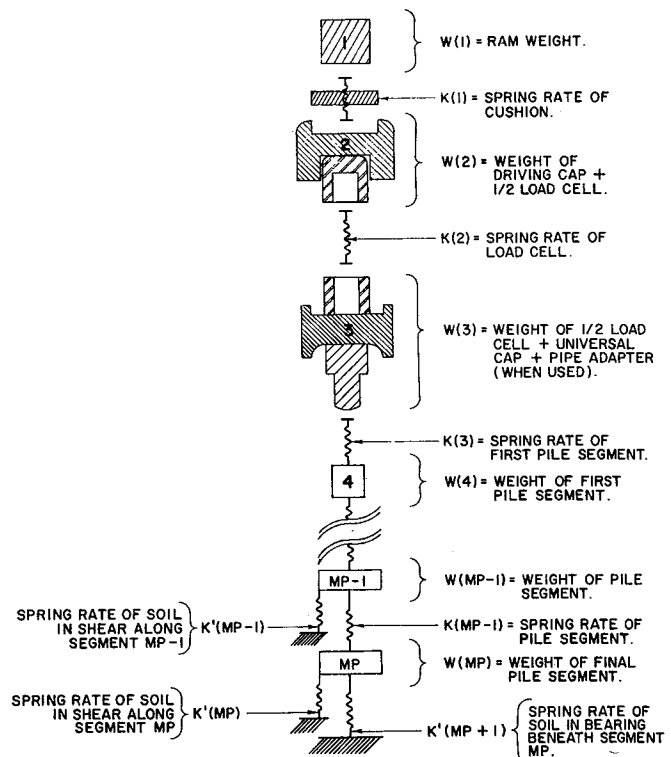


Figure 3.4. Idealization of a Vulcan hammer.

Problem Information

In selecting which of the Michigan pile problems to solve by the wave equation, it was decided to run at least two problems for each hammer used at each of the three testing sites. As shown in Table 3.3, cases selected from the Belleville site include two pile lengths for each of four different hammers. Otherwise, the problems were selected at random and the hammer energies determined are not necessarily typical of the hammer's usual operating characteristics. Similarly, the Detroit and Muskegon site problems are summarized in Tables 3.4 and 3.5. Figures 3.4 and 3.5 illustrate how these problems were idealized for purposes of analysis.

Even though the Michigan study is one of the most completely documented and fully reported research projects published concerning pile driving, certain information was not reported which must be known in order to apply the wave equation. This omission was not the result of any failure in reporting the data, but was because this information was not required by the methods of analysis used in the Michigan project and would have been difficult to measure. Two examples are the lack of information concerning the stiffness of the cushion and the velocity of the ram at impact.

Preliminary Studies

Since cushion-block information was not given, and because the cushion stiffness varies greatly during driving, a broad parameter study was made using the first case mentioned in Table 3.3. In this study, the cushion stiffness was varied by a factor of 50, from 540 kip/in. up to 27,000 kip/in. Also studied was the effect of varying the total soil resistance, RUT, using resistances of 30, 90, and 150 kip and ram velocities of 8, 12, and 16 ft/sec.

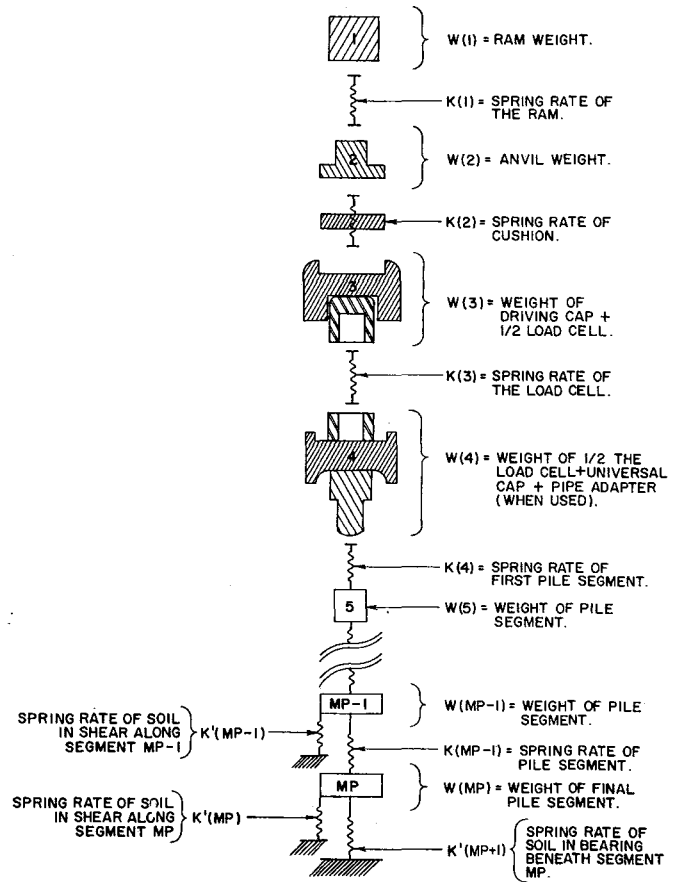


Figure 3.5. Idealization of a diesel hammer.

TABLE 3.3 SUMMARY OF BELLEVILLE CASES SOLVED BY WAVE EQUATION

Pile I.D.	Case*	Hammer**	Cushion	Type	PILE INFORMATION	
					Total Length (ft)	Embedded Length (ft)
BLTP-6	10.0	V-1	Oak	12H53	32.5	10.0
	57.9	V-1	Oak	12H53	72.5	57.9
BLTP-4	25.0	LB-312	Micarta	12 in. Pipe 0.25 in. wall	40.7	15.0
	66.4	LB-312	Micarta		81.6	56.4
BRP-4	20.0	M-DE30	Oak	12H53	40.0	20.0
	50.0	M-DE30	Oak	12H53	60.0	50.0
BLTP-5	15.0	D-D12	German Oak	12 in. Pipe 0.179 in. wall	40.0	5.0
	66.0	D-D12	German Oak		80.0	50.0

*Case number indicates pile length below ground surface and not necessarily embedment.

**Hammer designations are as follows:

- V-1 = Vulcan 1
- V-50C = Vulcan 50C
- V-80C = Vulcan 80C
- LB-312 = Link Belt 312
- LB-520 = Link Belt 520
- M-DE30 = McKiernen-Terry DE-30
- M-DE40 = McKiernen-Terry DE-40
- D-D12 = Delmag D-12
- D-D22 = Delmag D-22

TABLE 3.4. SUMMARY OF DETROIT CASES SOLVED BY WAVE EQUATION

Pile I.D.	Case*	Hammer*	Cushion	PILE INFORMATION		
				Type	Total Length (ft)	Embedded Length (ft)
DLTP-8	41.5	V-1	Oak	12H53	80.1	41.5
	80.2	V-1	Oak	12H53	97.0	80.2
DTP-5	20.0	V-50C	Micarta	12 in. Pipe 0.179 in. wall	40.0	20.0
	79.0	V-50C	Micarta		84.0	79.0
DRP-3	40.0	LB-312	Micarta	12H53	80.0	40.0
	60.0	LB-312	Micarta	12H53	80.0	60.0
DTP-13	40.0	M-DE30	Oak	12 in. Pipe 0.179 in. wall	45.0	40.0
	80.7	M-DE30	Oak		90.7	80.7
DTP-15	20.0	D-D12	German Oak	12H53	46.1	20.0
	80.5	D-D12	Oak	12H53	86.1	80.5

*See Table 3.3 for notation.

The results of this study indicate the significance of the wave equation in helping to understand the many factors that affect pile-driving behavior. The solutions for ENTHRU, FMAX, and LIMSET resulting from a change in the cushion stiffness, soil resistance, and ram velocities are given in Tables 3.6, 3.7, and 3.8, respectively. Whereas before it could not be determined "when, how, or how much," the results of this study indicate that in general for these particular problems,

1) ENTHRU is nearly independent of the cushion block stiffness used, since the cushion stiffness was increased by a factor of 50 while influencing ENTHRU only slightly,

2) FMAX is almost completely independent of the driving resistance,

3) FMAX is almost linearly related to the hammer velocity, and

TABLE 3.5. SUMMARY OF MUSKEGON CASES SOLVED BY WAVE EQUATION

Pile I.D.	Case*	Hammer*	Cushion	PILE INFORMATION		
				Type	Total Length (ft)	Embedded Length (ft)
MLTP-2	20.0	V-1	Oak	12 in. Pipe 0.250 in. wall	45.0	20.0
	53.0	V-1	Oak		60.0	53.0
MLTP-9	72.0	V-80C	Micarta	12 in. Pipe 0.250 in. wall	80.0	72.0
	127.0	V-80C	Micarta		134.0	127.0
MTP-12	30.5	LB-520	Micarta	12 in. Pipe 0.250 in. wall	40.0	30.5
	70.8	LB-520	Micarta		80.0	70.8
MTP-11	69.5	M-DE40	Oak and Plywood	12 in. Pipe 0.250 in. wall	80.0	69.5
	150.0	M-DE40			165.0	150.0
MLTP-8	31.0	D-D22	German Oak	12 in. Pipe 0.250 in. wall	40.0	31.0
	178.0	D-D22	German Oak		185.0	178.0

*See Table 3.3 for notation.

TABLE 3.6. EFFECT OF CUSHION STIFFNESS ON ENTHRU FOR BLTP-6; 10.0

		ENTHRU (kip ft)			
Ram Velocity (ft/sec)	RUT (kip)	Cushion Stiffness (kip/in.)			
		540	1080	2700	27,000
8	30	3.0	3.0	3.0	2.9
	90	3.1	3.2	3.3	2.9
	150	3.0	3.2	3.3	3.0
12	30	6.6	6.4	7.1	6.4
	90	7.0	7.1	7.2	6.4
	150	6.9	7.2	7.4	6.7
16	30	11.8	11.9	12.2	11.3
	90	12.3	12.6	12.8	11.5
	150	12.4	12.9	13.2	11.4

TABLE 3.7. EFFECT OF CUSHION STIFFNESS ON FMAX FOR BLTP-6; 10.0

		FMAX (kip)			
Ram Velocity (ft/sec)	RUT (kip)	Cushion Stiffness (kip/in.)			
		540	1080	2700	27,000
8	30	132	185	261	779
	90	137	185	261	779
	150	143	186	261	779
12	30	198	278	391	1,169
	90	205	278	391	1,169
	150	215	279	391	1,169
16	30	264	371	522	1,558
	90	275	371	522	1,558
	150	288	371	522	1,558

TABLE 3.8. EFFECT OF CUSHION STIFFNESS ON LIMSET FOR BLTP-6; 10.0

		LIMSET (in.)			
Ram Velocity (ft/sec)	RUT (kip)	Cushion Stiffness (kip/in.)			
		540	1080	2700	27,000
8	30	1.09	1.08	1.08	1.13
	90	0.44	0.44	0.45	0.45
	150	0.32	0.33	0.33	0.33
12	30	2.21	2.14	2.19	2.25
	90	0.80	0.82	0.84	0.84
	150	0.55	0.57	0.58	0.58
16	30	3.62	3.59	3.63	3.68
	90	1.30	1.31	1.32	1.34
	150	0.85	0.87	0.88	0.90

4) FMAX consistently increases as the cushion stiffness increases.

Thus for the first time, a number of trends may be established for various pile driving situations by using the wave equation.

In order to analyze other of the Michigan problems, certain data given in the Michigan report were used. This information is listed in Table 3.9.

Investigation of Steam Hammers Used in the Michigan Study

As noted in Figure 3.4, the numerical solution to the wave equation uses a series of concentrated weights and springs which closely represent the actual system involved. Time is also divided into small intervals in order to arrive at a solution.

As shown by Smith,¹ the wave equation can be used to determine (among other quantities) the displacement $D(m,t)$ of any mass "m" at time "t", as well as the force $F(m,t)$ of any mass "m" at time "t." Thus the equation for ENTHRU at any point in the system can be determined by simply letting the computer calculate the equation previously mentioned:

$$\text{ENTHRU} = \sum F \Delta S$$

or using the wave equation terms:

$$\text{ENTHRU}(m) = \sum \left[\frac{F(m,t) + F(m,t-1)}{2.0} \right] \left[D(m+1,t) - D(m+1,t-1) \right]$$

where ENTHRU(m) = the work done on any weight (m+1),

m = the mass number, and

t = the time interval number.

For example, the Michigan report determined ENTHRU(2) for the idealized system shown in Figure 3.4, since they recorded forces $F(2,t)$ in the load cell and displacements $D(3,t)$ below the load cell. For the system in Figure 3.5, ENTHRU(3) was determined.

Although it may not have been possible, ENTHRU should actually have been measured directly under the driving hammer ENTHRU(1), since ENTHRU(3) is greatly influenced by several parameters, especially the type, condition, and coefficient of restitution of the cushion, and the weights of the extra driving cap and load cell.

As will be shown later, the coefficient of restitution alone can change ENTHRU(2) by 20%, simply by changing e from 0.2 to 0.6. Nor is this variation in e unlikely since cushion condition varied from new to "badly burnt" and "chips added."

The wave equation was therefore used to analyze the problems since what was needed was a method by which the available data (ENTHRU, LIMSET, FMAX, etc.) could be used to determine the actual hammer energy involved, and also to compensate for the influence of cushion stiffness, e, additional driving cap weights, driving resistance encountered, etc.

Method Used to Correlate Theoretical and Experimental Results

In order to get the best possible correlation between experimental and theoretical solutions, an iterative method was used. This approach was suggested by the preliminary studies mentioned earlier. To demonstrate the method, an example problem, BLTP-6;10.0, will be solved.

TABLE 3.9. DATA REPORTED IN THE MICHIGAN STUDY

Driving Location	Pile I.D.	Case	Hammer* Type	Manufacturer's Maximum Rated Energy (ft lb)	ENTHRU (ft lb)	LIMSET (in.)	Permanent Set (in.)	Estimated Static Soil Resistance (kip)	
Belleville	BLTP-6	10.0	V-1	15,000	6,380	0.75	0.48	48	
		57.9	V-1	15,000	4,440	0.42	0.02	400	
	BLTP-4	25.0	LB-312	18,000	8,010	0.94	0.36	140	
		66.4	LB-312	18,000	11,200	0.92	0.02	690	
	BRP-4	20.0	M-DE-30	22,400	4,980	0.57	0.37	100	
		50.0	M-DE-30	22,400	4,470	0.41	0.12	320	
	BLTP-5	15.0	D-D12	22,500	9,040	1.86	1.43	80	
		60.0	D-D12	22,500	9,930	0.79	0.11	340	
Detroit	DLTP-8	41.5	V-1	15,000	5,760	1.22	1.00	60	
		80.2	V-1	15,000	4,540	0.54	0.50	360	
	DTP-5	20.0	V-50C	15,100	8,290	2.55	2.00	22	
		79.0	V-50C	15,100	11,420	0.82	0.09	235	
	DRP-3	40.0	LB-312	18,000	7,060	1.36	1.25	60	
		60.0	LB-312	18,000	6,620	1.41	0.77	76	
	DTP-13	40.0	M-DE30	22,400	9,100	2.21	2.00	30	
		80.7	M-DE30	22,400	9,480	1.12	0.07	265	
	DTP-15	20.0	D-D12	22,500	10,100	2.07	2.00	40	
		80.5	D-D12	22,500	5,480	0.58	0.25	120	
	Muskegon	MLTP-2	20.0	V-1	15,000	7,210	1.42	1.00	80
			53.0	V-1	15,000	4,870	0.57	0.09	200
		MLTP-9	72.0	V-80C	24,450	14,660	1.06	0.56	160
			127.0	V-80C	24,450	13,110	1.03	0.23	470
MTP-12		30.5	LB-520	30,000	14,860	1.48	1.00	40	
		70.8	LB-520	30,000	13,140	1.02	0.77	156	
MTP-11		69.5	M-DE40	32,000	16,760	1.16	0.67	160	
		150.0	M-DE40	32,000	17,900	1.41	0.05	500	
MLTP-8		31.0	D-D22	39,700	25,500	2.35	1.25	40	
		178.0	D-D22	39,700	22,050	1.71	0.04	988	

*See Table 3.3 for notation.

Since in nearly every case the condition of the cushion is unknown, the first assumption must be for the cushion rate $K(1)$. For illustrative purposes, assume that $K(1) = 180$ kip/in. and that soil resistances of 30 and 90 kip were assumed.

The next step was to run the problem with various hammer energies. As shown in Figure 3.6, for each energy input (EINPUT) the wave equation predicts a corresponding theoretical value of ENTHRU. These solutions are then used to plot the curves of Figure 3.6. Also, since each solution predicts a value for LIMSET and initial ram velocity, it is possible to plot the curves of Figure 3.7.

Returning to Figure 3.6, the question becomes what kinetic energy must the falling ram have had in order to cause a value of ENTHRU = 6,380 kip ft (the measured experimental value reported by Michigan and listed

in Table 3.9)? By entering ENTHRU = 6,380 kip ft, and assuming $RUT = 30$ kip, project to the upper curve where EINPUT is found to be 11,000 kip ft.

To further check the solution, determine the ram velocity required for 11,000 kip ft of kinetic energy from:

$$V = \sqrt{\frac{(EINPUT) (64.4)}{\text{Ram Weight}}} = 11.9 \text{ ft/sec}$$

Next, from Table 3.9, find the actual value of LIMSET (determined experimentally) and enter this value of 0.75 in. and $V = 11.9$ ft/sec in Figure 3.7.

Should the projection of these points intersect on the $RUT = 30$ kip curve, then that assumption was correct. However, this indicates a soil resistance of around 90 kip so that the $RUT = 90$ kip curve of Figure 3.6 should probably have been used.

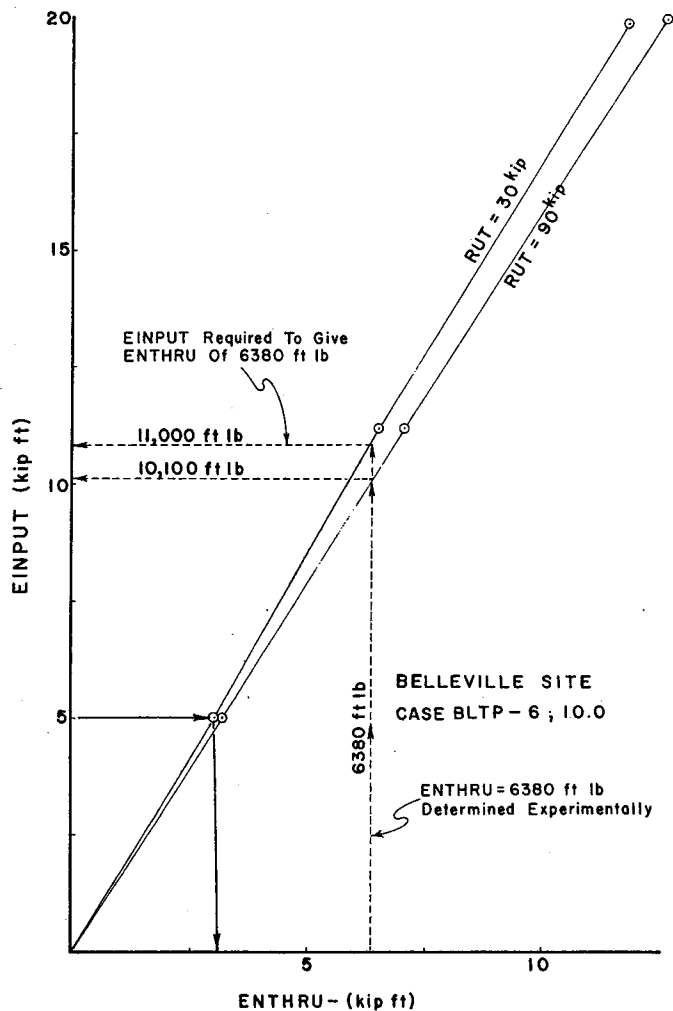


Figure 3.6. EINPUT vs ENTHRU.

Returning to Figure 3.6, the new value of EINPUT is found to be 10,100 ft lb, which gives a new ram velocity of 11.4 ft/sec. Substituting this velocity into Figure 3.7, the resulting value of RUT agrees closely with the assumed value of 90 kip.

Since the ram velocity at impact is now known, the assumed cushion stiffness of 1080 kip/in. can be checked. Holding RUT = 90 kip and the initial ram velocity = 11.4 ft/sec, and solving for the change in FMAX as the cushion stiffness varies, the curve of Figure 3.8 can be drawn. The experimental value of FMAX reported in the Michigan paper was 244 kip, which entered into Figure 3.8 gives a value of $K(1) = 900$ kip/in. Since this is close to the assumed value of 1080 kip/in., the solution was considered to be satisfactory. However, even in cases where the cushion stiffness was quite inaccurate, ENTHRU was only slightly changed when a more accurate value of $K(1)$ was used.

This solution now enables us to determine the energy output of the hammer, and other quantities. Since this hammer is rated at 15,000 ft lb and its actual output was only 10,100 ft lb the hammer must have lost 3,900 ft lb due to friction in the guides or from other causes. Thus, the hammer efficiency is $(10,100) \times (100) / 15,000 = 67$ percent. Furthermore, since only 6,380 ft

lb (ENTHRU) of the 10,100 ft lb output reached the load cell, the difference must have been lost in the helmet-cushion-load cell assembly. Thus the efficiency of this assembly must have been $(6,380) \times (100) / 10,100 = 63$ percent.

The ability to determine these efficiencies separately is important since it indicates whether the driving hammer or cushion-helmet assembly should be studied to reduce energy losses during driving.

The preceding method was used to solve each of the Michigan steam hammer cases listed in Tables 3.3, 3.4, and 3.5.

Correlation of Experimental and Theoretical Results

It is interesting to compare the final wave equation solution with the experimental results reported in the Michigan pile study. For the above case, comparisons between the experimental results and those given by the wave equation are shown in Figures 3.9 through 3.11. These figures show the experimental and theoretical forces and accelerations, displacements, and energy, vs. time, measured at the load cell. The correlations are reasonably accurate, especially during the first 0.01 sec, although the reflected compressive wave seems to be overestimated, as shown in Figure 3.9A at 0.014 sec. This did not greatly affect either the ENTHRU or dis-

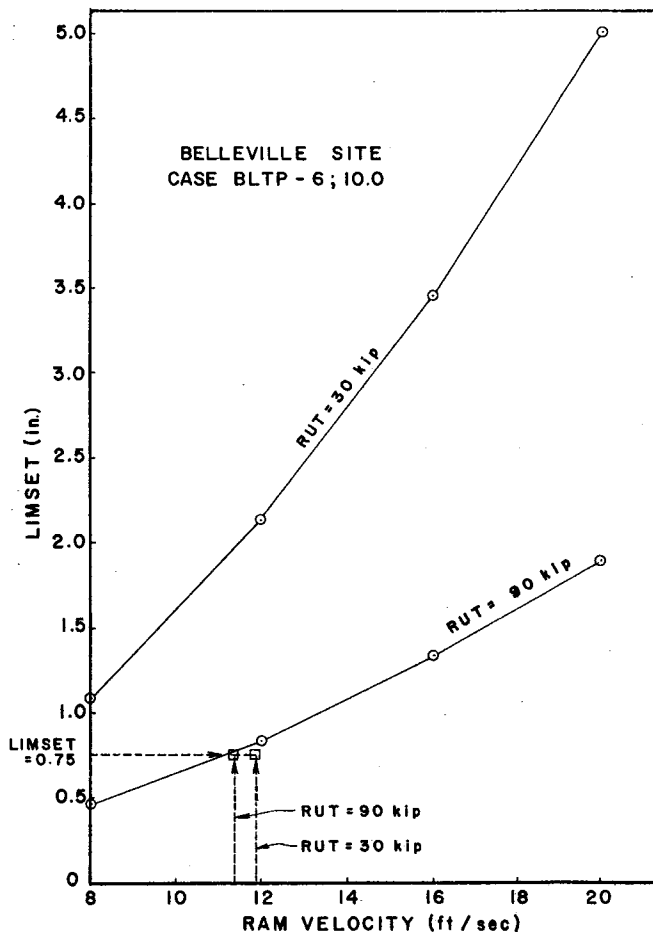


Figure 3.7. Ram velocity vs LIMSET.

BELLEVILLE SITE

CASE BLTP-6; 10.0

Ram Velocity = 11.4 ft/sec
RUT = 90.0 kip

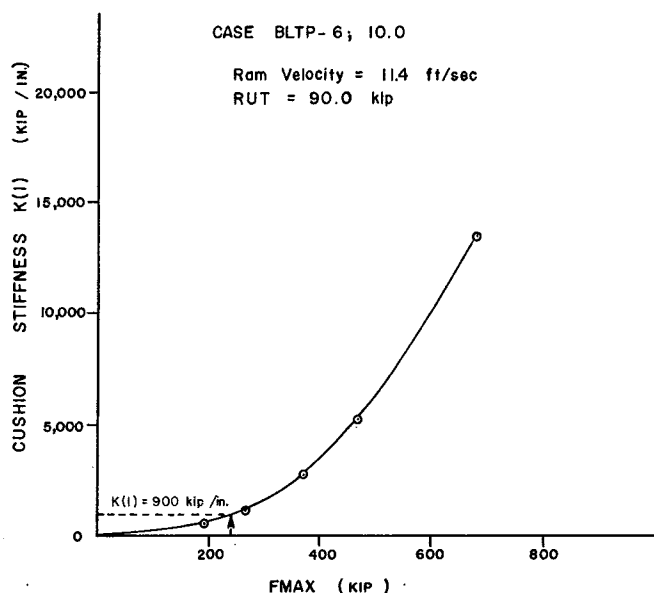


Figure 3.8. Cushion stiffness vs F_{MAX} .

placement curves, although it may have caused the rather large errors in the acceleration curve of Figure 3.9B.

A summary of the results for the steam hammer cases solved is given in Table 3.10. Listed are the energy output of the hammer, the hammer efficiencies, the ram velocity, and the total soil resistance, RUT, necessary to obtain correlation for each case.

It should be noted that there was no way to determine the soil damping or elasticity constants. Therefore, the constants recommended by Smith⁴⁷ were used. As shown by Forehand and Reese,⁴⁸ these constants affect the resulting RUT values. Therefore, the theoretical RUT values shown in Table 3.10 were not expected to agree closely with the experimental values reported in Table 3.9. However, it is interesting to note that in several cases the ratio of the soil resistance determined

experimentally to that predicted by the wave equation is reasonably constant.

Investigation of Diesel Hammers Used in the Michigan Study

Because the diesel explosive force is much smaller than the impact force, it was found to have little effect on the driving stresses.⁴¹ However, if explosive pressure is neglected, the ram velocity required to predict EN-THRU is much greater than that calculated from the free fall of the ram, even assuming 100 percent efficiency. Therefore, it was necessary to run the diesel hammer cases accounting for the explosive pressure in the hammer.

During impact between the ram and anvil the force on the anvil will reach some maximum value and then decrease. Following this impact, the diesel explosion occurs, exerting an explosive pressure and force between the ram and anvil. This behavior has been studied and reported by some of the hammer manufacturers.⁷¹ In order to simulate this action for wave-equation analysis, the explosive force acting within the diesel hammer is assumed to behave as shown in Figure 3.12. The maximum explosive force is held on the anvil for 0.01 sec after which the force is tapered to zero at 0.0125 sec. Actually, the explosive hammer force lasts considerably longer than this but its magnitude is too small to be a significant factor in pushing the pile down except during the initial driving stages when little or no soil resistance is encountered. The magnitudes of explosive pressures listed in Table 3.11 were obtained from the hammer manufacturer or were assumed.

In previous solutions, it was an easy matter to solve for the total energy of the ram at impact since only its kinetic energy, E_{INPUT} , was involved. Now, since explosive pressure is included, the total energy developed includes both kinetic and explosive energy.

This total energy, E_{TOTL} , is the sum of the energy transmitted to the anvil, E_{NTHRU1} , and the kinetic rebound energy of the ram after impact, where E_{NTHRU1} is calculated by the same method as was used for EN-

TABLE 3.10. SUMMARY OF RESULTS FOR MICHIGAN STEAM HAMMERS

Driving Location	Pile I.D.	Case	Hammer* Type	E_{INPUT} (ft lb)	$E_{NTHRU}\dagger$ (ft lb)	Hammer** Efficiency (%)	Ram-Cushion-Helmet Assembly Efficiency (%)	Ram Velocity (ft/sec)	RUT (kip)	RUT (Theoretical) RUT (Experimental) (%)
Belleville	BLTP-6	10.1	V-1	10,100	6,380	67	63	11.9	90	190
		57.9	V-1	7,000	4,440	47	63	9.5	200	50
Detroit	DLTP-8	41.5	V-1	9,700	5,760	65	60	11.2	50	83
		80.2	V-1	7,200	4,540	48	63	9.6	120	33
		20.0	V-50C	12,800	8,290	85	65	12.9	25	110
		79.0	V-50C	15,600	11,420	103	73	14.2	300+	128+
Muskegan	MLTP-2	20.0	V-1	12,200	7,210	81	59	12.5	50	62
		53.0	V-1	7,700	4,870	51	63	10.0	150	75
		72.0	V-80C	19,700	14,660	81	74	12.6	175	109
		127.0	V-80C	19,200	13,110	79	68	12.5	300	64

*See Table 3.3 for notation.

**Hammer efficiency computed on basis of the manufacturer's maximum rated output.

†Note: The problems were selected at random and the hammer energies determined are not necessarily typical of the hammer's usual operating characteristics.

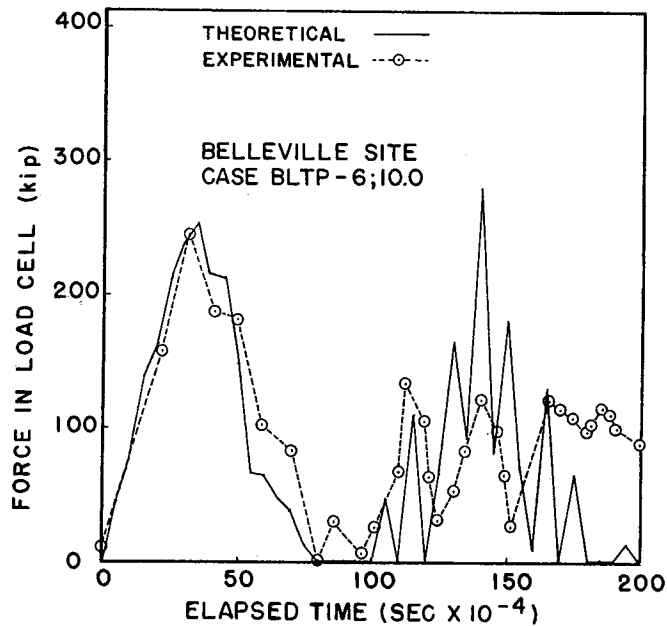
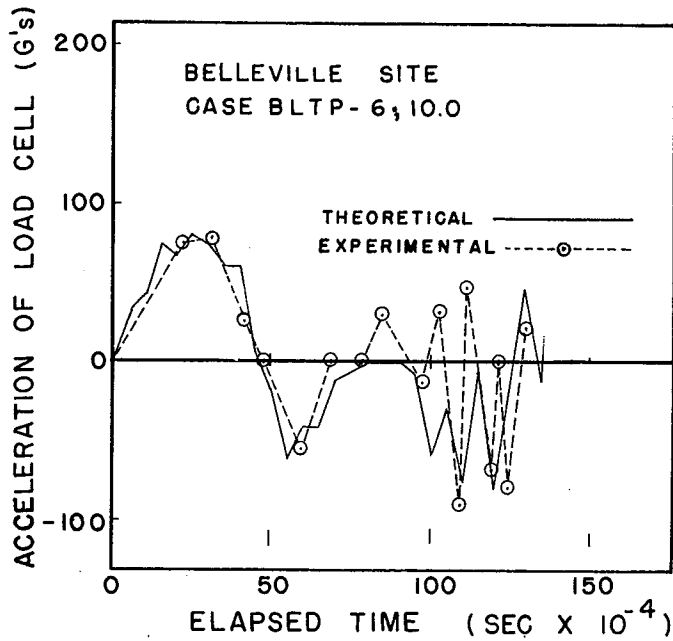


Figure 3.9. Comparison of theoretical and experimental load cell forces and accelerations.

THRU at the load cell, and the kinetic rebound energy remaining in the ram after impact is given by $WV^2/64.4$, where W is the weight of the ram and V is the rebound velocity of the ram determined by the wave equation.

The efficiencies and initial ram velocities noted in Table 3.11 were found by plotting ENTHRU and ENTHRU1 vs the initial ram velocity as shown in Figure 3.13. Plotting the values of LIMSET vs ram velocity as in Figure 3.14 then gives the total soil resistance predicted by the wave equation. This procedure was used on all diesel hammer cases, and the results are summarized in Table 3.11.

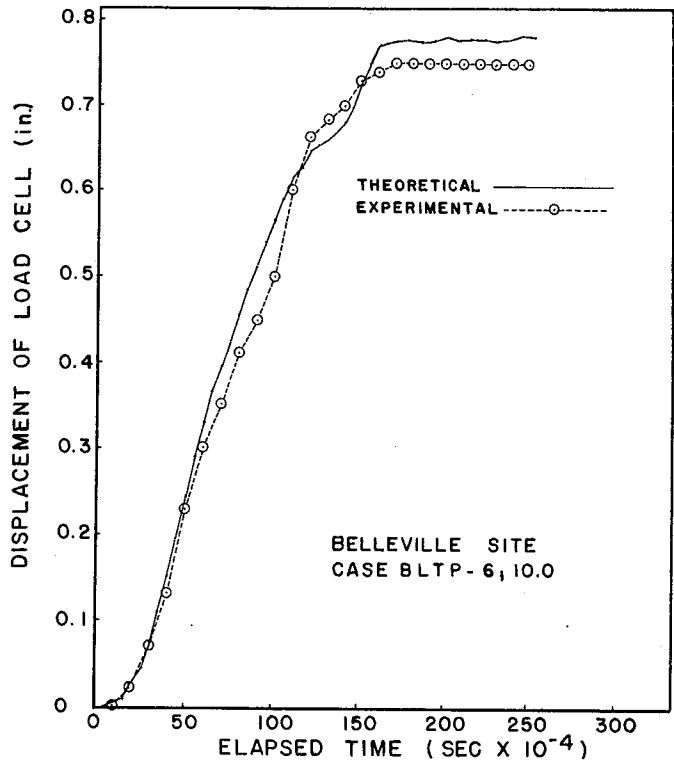


Figure 3.10. Comparison of theoretical and experimental load cell displacements.

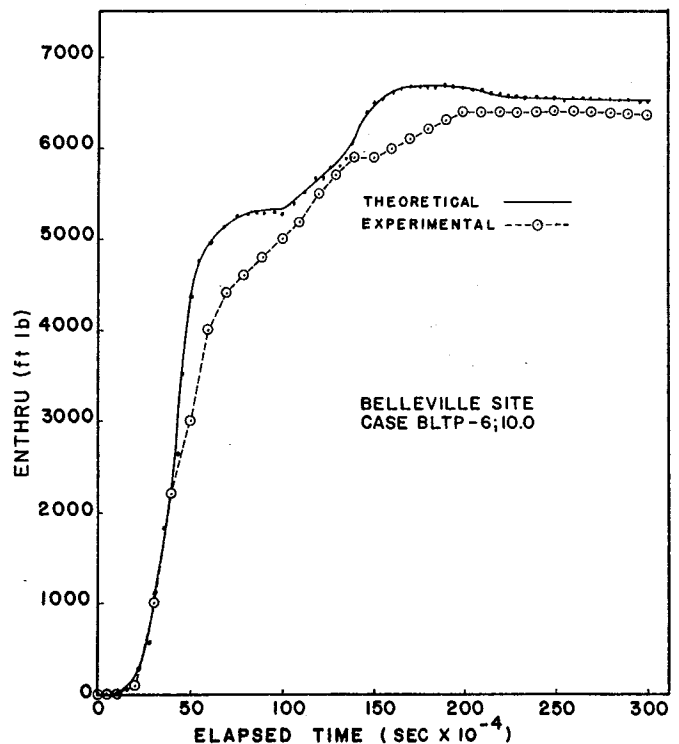


Figure 3.11. Comparison of theoretical and experimental values of ENTHRU.

TABLE 3.11. SUMMARY OF RESULTS FOR MICHIGAN DIESEL HAMMERS

Driving Location	Pile I.D.	Case	Hammer Type	Explosive Force on Anvil (kip)	ENTOTL (ft lb)	ENTHRU** (ft lb)	Hammer* Efficiency (%)	Ram-Cushion Assembly Ef- ficiency (%)	Ram Velocity at Impact (ft/sec)	RUT	
										RUT (kip)	(Theoretical) RUT (%)
Belleville	BLTP-4	25.0	LB-312	98.0	10,630	8,010	59	75	8.2	70	50
		66.4			16,030	11,200	89	70	6.4	250	36
	BRP-4	20.0	M-DE30	98.0	9,450	4,980	42	53	9.8	100	100
		50.0			9,100	4,470	41	49	10.6	200	63
	BLTP-5	15.0	D-D12	93.7	13,000	9,040	58	69	12.8	40	50
		60.0			14,730	9,930	66	67	15.0	400	118
Detroit	DRP-3	40.0	LB-312	98.0	9,270	7,060	52	76	9.8	45	75
		60.0			13,900	6,620	77	48	5.2	60	79
	DTP-13	40.0	M-DE30	98.0	14,390	9,100	64	63	13.7	35	117
		80.7			15,280	9,480	68	62	15.1	120	45
	DTP-15	20.0	D-D12	93.7	15,270	10,100	68	66	15.2	45	112
		80.5			9,430	5,480	42	58	11.6	110	92
Muskegon	MTP-12	30.5	LB-520	98.0	22,140	14,860	74	67	16.4	75	187
		70.8			21,260	13,140	71	62	14.4	70	45
	MTP-11	69.5	M-DE40	138.0	32,800	16,760	102	50	20.6	150	94
		150.0			36,850	17,900	115	49	21.5	250	50
	MLP-8	31.0	D-D22	158.7	31,600	25,500	80	81	17.8	70	175
		178.0			27,300	22,050	69	81	17.1	300	30

*Hammer efficiency based on manufacturer's maximum rated energy.

**Note: The problems were selected at random and the hammer energies determined are not necessarily typical of the hammer's usual operating characteristics.

Determination of Hammer Energy Output Diesel Hammers

At present the manufactures of diesel hammers arrive at the energy delivered per blow by two different methods. One manufacturer feels that "Since the amount of (diesel) fuel injected per blow is constant, the compression pressure is constant, and the temperature constant, the energy delivered to the piling is also constant."⁶⁹ The energy output per blow is thus computed

as the kinetic energy of the falling ram plus the explosive energy found by thermodynamics. Other manufacturers simply give the energy output per blow as the product of the weight of the ram-piston W_R and the length of the stroke h , or the equivalent stroke in the case of closed-end diesel hammers.

The energy ratings given by these two methods differ considerably since the ram stroke h varies greatly thereby causing much controversy as to which, if either,

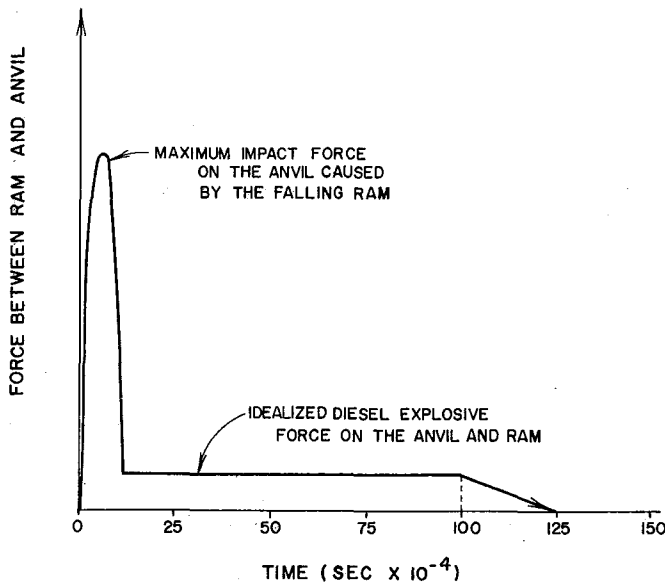


Figure 3.12. Typical force vs time curve for a diesel hammer.

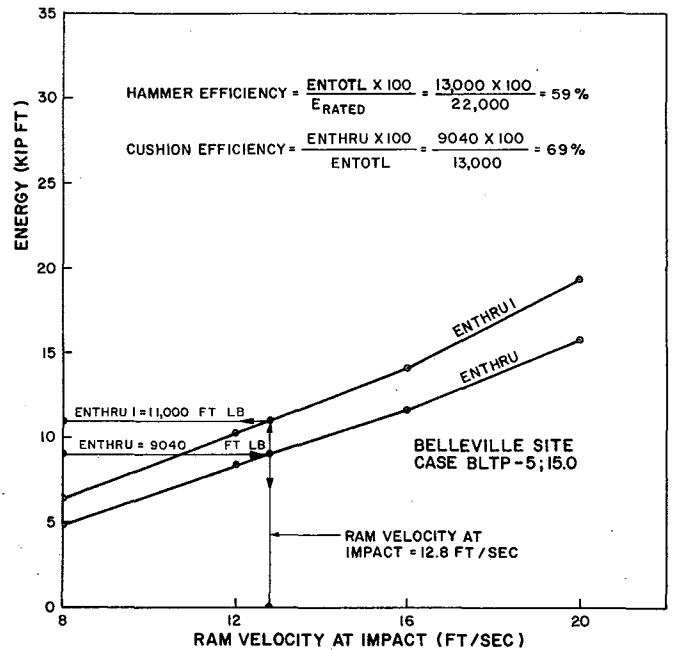


Figure 3.13. ENTHRU1 and ENTHRU vs ram velocity determined by wave equation analysis.

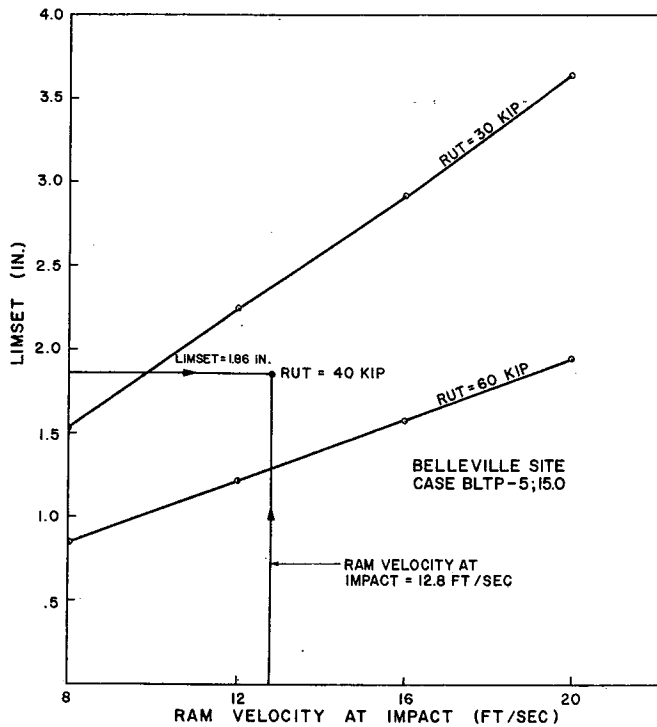


Figure 3.14. LIMSET vs ram velocity determined by wave equation analysis.

method is correct and what energy output should be used in dynamic pile analysis.

In conventional single acting steam hammers the steam pressure or energy is used to raise the ram for each blow. The magnitude of the steam force is too small to force the pile downward and consequently it works only on the ram to restore its potential energy, $W_R \times h$, for the next blow. In a diesel hammer on the other hand, the diesel explosive pressure used to raise the ram is, for a short time at least, relatively large.

While this explosive force works on the ram to restore its potential energy $W_R \times h$, the initially large explosive pressure also does some useful work on the pile given by:

$$E_e = \int F ds \quad \text{Eq. 3.1}$$

where F = the explosive force, and

ds = the infinitesimal distance through which the force acts.

Since the total energy output is the sum of the kinetic energy at impact plus the work done by the explosive force.

$$E_{\text{total}} = E_k + E_e \quad \text{Eq. 3.2}$$

where E_{total} = the total energy output per blow,

E_k = the kinetic energy of the ram at the instant of impact,

and E_e = the diesel explosive energy which does useful work on the pile.

It has been noted that after the ram passes the exhaust ports, the energy required to compress the air-fuel mixture is nearly identical to that gained by the

remaining fall of the ram.⁷⁰ Therefore the velocity of the ram at the exhaust ports is essentially the same as at impact, and the kinetic energy at impact can be closely approximated by:

$$E_k = W_R (h - d) \quad \text{Eq. 3.3}$$

where W_R = the ram weight,

h = the total observed stroke of the ram,

and d = the distance the ram moves after closing the exhaust ports and impacts with the anvil.

The total amount of explosive energy $E_{e(\text{total})}$ is dependent upon the amount of diesel fuel injected, compression pressure and temperature and therefore may vary somewhat.

Unfortunately, the wave equation must be used in each case to determine the exact magnitude of E_e since it not only depends on the hammer characteristics but also on the characteristics of the anvil, helmet, cushion, pile, and soil resistance. However, values of E_e determined by the wave equation for several typical pile problems indicates that it is usually small in portion to the total explosive energy output per blow, and furthermore, that it is on the same order of magnitude as $W_R \times d$.

Thus, Eq. 3.1 can be simplified by assuming:

$$E_e = W_R \times d \quad \text{Eq. 3.4}$$

Substituting Eqs. 3.3 and 3.4 into Eq. 3.1 gives:

$$E_{\text{total}} = E_k + E_e = W_R (h - d) + W_R d \quad \text{Eq. 3.5}$$

so that:

$$E_{\text{total}} = W_R h \quad \text{Eq. 3.6}$$

The results given by this equation are compared with the actual values found by the wave equation in Table 3.12. Note that the results are relatively constant, the average efficiency being 100%.

Steam Hammers

Again using the wave equation in conjunction with the Michigan report, Tables 3.13 and 3.14 suggest efficiency ratings of 60% for the single-acting steam hammers, and 87% for the double-acting hammer, based on an energy output given by:

$$E_{\text{total}} = W_R h \quad \text{Eq. 3.7}$$

In order to determine an equivalent ram stroke for the double-acting hammers, the internal steam pressure above the ram which is forcing it down must be taken into consideration. The manufacturers of such hammers state that the maximum steam pressure or force should not exceed the weight of the housing or casing, or the housing may be lifted off the pile. Thus the maximum downward force on the ram is limited to the total weight of the ram and housing.

Since these forces both act on the ram as it falls through the actual ram stroke h , they add kinetic energy to the ram, which is given by:

$$E_{\text{total}} = W_R h + F_R h \quad \text{Eq. 3.8}$$

where W_R = the ram weight,

F_R = a steam force not exceeding the weight

and h = the observed or actual ram stroke.

Since the actual steam pressure is not always applied at

TABLE 3.12. COMPARISON OF ENERGY OUTPUT MEASURED EXPERIMENTALLY WITH THAT PREDICTED BY EQUATION 3.6, FOR DIESEL HAMMERS

Hammer	Pile I.D.	Case	ENTOTL (ft lb)	Ram Wt. W_R (lb)	Observed Ram Stroke h (ft)	$W_R \times h$ E_{total} (ft lb)	$\frac{ENTOTL}{E_{total}}$
LB-312	BLTP-4	25.0	10,630	3,857	3.3*	12,800	.83
		66.4	16,030	3,857	3.6*	13,900	1.15
	DRP-3	40.0	9,270	3,857	2.9*	11,000	.84
		60.0	13,900	3,857	3.0*	11,600	1.20
DE-30	BRP-4	20.0	9,450**	2,800	6.6	18,500	
		50.0	9,100**	2,800	6.9	19,300	
	DTP-13	40.0	14,390	2,800	5.2	14,600	.99
		80.7	15,280	2,800	7.0	19,600	.78
D-12	BLTP-5	15.0	13,000	2,750	4.9	13,500	.96
		60.0	14,730	2,750	6.1	16,800	.88
	DTP-15	20.0	15,270	2,750	6.0	16,500	.93
		80.5	9,430**	2,750	7.0	19,300	
LB-520	MTP-12	30.5	22,140	5,070	3.7*	18,500	1.20
		70.8	21,260	5,070	4.5*	22,750	.93
DE-40	MTP-11	69.5	32,800	4,000	7.6	30,400	1.08
		150.0	36,850	4,000	8.2	32,800	1.12
D-22	MLTP-8	31.0	31,600	4,850	5.6	27,200	1.16
		178.0	27,300	4,850	5.5	26,700	1.02
							Avg. = 1.00

*Equivalent stroke derived from bounce chamber pressures.

**Experimental results for these cases appear to be quite inaccurate.

TABLE 3.13. COMPARISON OF MEASURED OUTPUT WITH THAT GIVEN BY EQUATION 3.7, FOR SINGLE ACTING STEAM HAMMERS

Pile I.D.	Case	Hammer Type	EINPUT* (ft lb)	W_R (lb)	h^{**} (ft)	E_{total} (ft lb)	$\frac{EINPUT}{E_{total}}$
BLTP-6	10.0	V-1	10,100	5,000	3	15,000	0.67
	57.9	V-1	7,000	5,000	3	15,000	0.47
DLTP-8	41.5	V-1	9,700	5,000	3	15,000	0.65
	80.2	V-1	7,200	5,000	3	15,000	0.48
MLTP-2	20.0	V-1	12,200	5,000	3	15,000	0.81
	53.0	V-1	7,700	5,000	3	15,000	0.51
							Avg. = 0.60

*EINPUT found by wave equation and listed in Table 3.10.

**The observed ram stroke h or equivalent ram stroke h_e was given in the Michigan report text.

TABLE 3.14. COMPARISON OF MEASURED ENERGY OUTPUT WITH THAT PREDICTED BY EQUATION 3.11, FOR DOUBLE ACTING STEAM HAMMERS

Pile I.D.	Case	Hammer Type	EINPUT* (ft lb)	W_R (lb)	h_e^{**} (ft)	E_{total} (ft lb)	$\frac{EINPUT}{E_{total}}$
DTP-5	20.0	V-50C	12,800	5,000	3.02	15,100	0.85
	79.0	V-50C	15,600	5,000	3.02	15,100	1.03
MLTP-9	72.0	V-80C	19,700	8,000	3.05	24,450	0.81
	127.0	V-80C	19,200	8,000	3.05	24,450	0.79
							Avg. = 0.87

*EINPUT found by wave equation and listed in Table 3.10.

**The observed ram stroke h or equivalent ram stroke h_e was given in the Michigan report text.

the rated maximum, the actual steam force can be expressed as:

$$F_R = \left(\frac{p}{P_{rated}} \right) W_H \quad \text{Eq. 3.9}$$

where W_H is the housing weight, p is the operating pressure, and P_{rated} is the maximum rated steam pressure.

The total energy output is then given by

$$E_{total} = W_R h + \left[\frac{p}{P_{rated}} W_H \right] h \quad \text{Eq. 3.10}$$

This can be reduced in terms of Eq. 3.7 by using an equivalent stroke h_e which will give the same energy output as Eq. 3.10.

Thus:

$$E_{total} = W_R h_e \quad \text{Eq. 3.11}$$

Setting Eqs. 3.10 and 3.11 equal yields

$$\begin{aligned} W_R h_e &= W_R h + \left[\frac{p}{P_{rated}} W_H \right] h \\ &= h \left[W_R + \frac{p}{P_{rated}} W_H \right] \end{aligned}$$

or solving for the equivalent stroke:

$$h_e = h \left[1 + \frac{p}{P_{rated}} \times \frac{W_H}{W_R} \right] \quad \text{Eq. 3.12}$$

Conclusions

The preceding discussion has shown that it is possible to determine reasonable values of hammer energy output simply by taking the product of the ram weight and its observed or equivalent stroke, and applying an efficiency factor listed in Tables 3.12 thru 3.14. This method of energy rating can be applied to all types of impact pile drivers with reasonable accuracy.

A brief summary of this simple procedure for arriving at hammer energies and initial ram velocities is as follows:

Open End Diesel Hammers

$$\begin{aligned} E &= W_R h (e) \\ V_R &= \sqrt{2g (h-d)} (e) \end{aligned}$$

where W_R = ram weight

V_R = initial ram velocity

h = observed total stroke of ram

d = Distance from anvil to exhaust ports

e = efficiency of open end diesel hammers, approximately 100% when energy is computed by this method.

Closed End Diesel Hammers

$$\begin{aligned} E^* &= W_R h_e (e) \\ V_R &= \sqrt{2g (h_e-d)} (e) \end{aligned}$$

*Note: For the Link Belt Hammers, this energy can be read directly from the manufacturer's chart using bounce chamber pressure gage.

where W_R = ram weight

V_R = initial ram velocity

h = equivalent stroke derived from bounce chamber pressure gage

d = distance from anvil to exhaust ports

e = efficiency of closed end diesel hammers, approximately 100% when energy is computed by this method.

Double-Acting Steam Hammers

$$\begin{aligned} E &= W_R h_e (e) \\ V &= \sqrt{2g h_e} (e) \end{aligned}$$

where W_R = ram weight

h_e = equivalent ram stroke

$$= h \left[1 + \frac{p}{P_{rated}} \times \frac{W_H}{W_R} \right]$$

h = actual or physical ram stroke

p = operating steam pressure

P_{rated} = maximum steam pressure recommended by manufacturer

W_H = weight of hammer housing

e = efficiency of double-acting steam hammers, approximately 85% by this method.

Single-Acting Steam Hammers

$$\begin{aligned} E &= W_R h (e) \\ V_R &= \sqrt{2g h} (e) \end{aligned}$$

where W_R = ram weight

h = ram stroke

e = efficiency of single-acting steam hammers, normally recommended around 75% to 85%.⁴³ In this study of the Michigan data, a figure of 60% was found. The writers feel the 60% figure is unusually low and would not recommend it as a typical value.

A summary of the properties and operating characteristics of the various hammers is given in Table 3.15.

Effects of the Experimental Measuring Devices

Another example of the application of the wave equation to the Michigan pile study is the solution of each of the previous problems, but excluding any effects of the experimental apparatus. When the question was first raised as to how the elasticity of the load cell and the additional weight of the load cell and extra driving cap might affect the results, it was decided to drive a Belleville H pile to refusal with a Delmag D-12 hammer with the load cell and extra driving cap removed. The data recorded for this pile were then compared with the data for similar piles which were driven by the same hammer but which included the extra driving cap and load cell.

The only data obtainable for the noninstrumented pile were the blow count and rate of penetration at various depths, since there was no way to measure the forces, displacements, ENTHRU, etc. It is also possible that a pipe pile might have been affected differently than the

TABLE 3.15. SUMMARY OF HAMMER PROPERTIES AND OPERATING CHARACTERISTICS

Hammer Manufacturer	Hammer Type	Maximum Rated (ft lb)	Ram Weight (lb)	Casing Weight (lb)	Anvil Weight (lb)	Maximum d (ft)	Rated Steam Pressure (psi)	Explosive Pressure (lb)	Cap Block
Vulcan	#1	15,000	5,000	4,700		3.00			
	014	42,000	14,000	13,500		3.00			
	50C	15,100	5,000	6,800		3.02	120		
	80C	24,450	8,000	9,885		3.06	120		
	140C	36,000	14,000	13,984		2.58	140		
Link Belt	312	18,000	3,857		1188	4.66	0.50	98,000	5 Micarta disks 1" x 10 7/8" dia.
	520	30,000	5,070		1179	5.93	0.83	98,000	
MKT Corp	DE20	16,000	2,000		640	8.00	0.92	46,300	nylon disk 2" x 9" dia.
	DE30	22,400	2,800		775	8.00	1.04	98,000	nylon disk 2" x 19" dia.
	DE40	32,000	4,000		1350	8.00	1.17	138,000	nylon disk 2" x 24" dia.
Delmag	D-12	22,500	2,750		754	8.19	1.25	93,700	15" x 15" x 5" German Oak
	D-22	39,700	4,850		1147	8.19	1.48	158,700	15" x 15" x 5" German Oak

H-pile tested, and that the soil conditions of the Detroit or Muskegon sites could be of influence. Furthermore, only one hammer was studied (the Delmag D-12) and the effect on the other hammers could be different. Obviously, these questions cannot be completely answered experimentally since this would mean that every time the hammer, pile type, driving location, or any other parameter changed, a similar noninstrumented pile would also have to be driven under identical conditions.

These effects are easily determined by the wave equation, simply by omitting the weights and springs corresponding to the extra driving cap and load cell shown in Figures 3.4 and 3.5. The modified idealizations are shown in Figures 3.15 and 3.16.

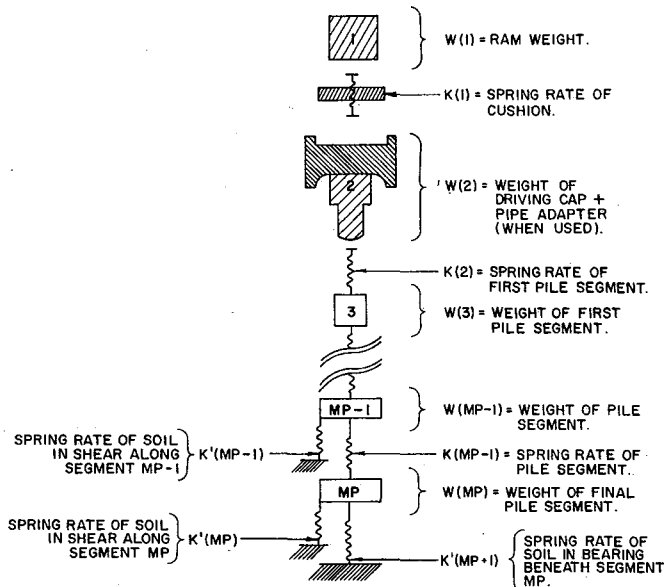


Figure 3.15. Idealization of a Vulcan hammer without measuring devices.

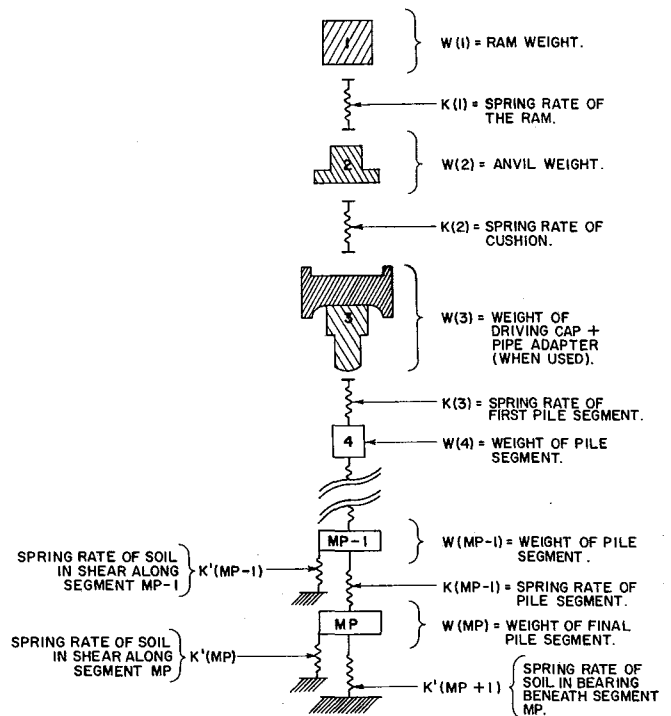


Figure 3.16. Idealization of a diesel hammer without measuring devices.

TABLE 3.16. EFFECT OF REMOVING LOAD CELL ON ENTHRU, LIMSET, AND PERMANENT SET OF PILE

Case	Ram Velocity (ft/sec)	ENTHRU (kip ft)		LIMSET (in.)		PERMANENT SET (in.)	
		With Load Cell	Without Load Cell	With Load Cell	Without Load Cell	With Load Cell	Without Load Cell
DTP-15, 80.5	8	1.5	1.6	0.27	0.34	0.23	0.25
	12	3.3	3.6	0.53	0.67	0.57	0.57
	16	5.8	6.5	1.02	1.03	0.94	0.97
	20	9.1	10.1	1.54	1.54	1.43	1.47
DLTP-8, 80.2	8	3.1	3.8	0.62	0.71	0.51	0.62
	12	7.1	8.5	1.15	1.32	1.06	1.29
	16	12.5	15.1	1.91	2.10	1.82	2.15
	20	19.5	23.6	2.70	3.08	2.65	3.13

Although no problems were solved which involved H piles driven by a Delmag D-12 hammer at the Belleville site, a similar pile was driven at Detroit for which a wave equation solution was obtained.

The results for this problem with the load cell assembly included and excluded are given in Table 3.16. This agrees with the Michigan study conclusion that for case DLTP-15;80.5 the permanent set per blow including the load cell agrees with that found when the load cell is excluded. The corresponding values for ENTHRU do not agree nearly so well.

The results for a similar problem solved at the Detroit site, DLTP-8;80.2, do not agree with this conclusion. This pile was also an H-pile, was embedded to within 0.3 ft of the first H-pile, and also had 55 kip soil resistance. However, DLTP-8;80.2 differs from the Michigan test pile in that this pile was 11 ft longer, and was driven by a Vulcan-1 hammer rather than the Delmag D-12. As shown in the lower half of Table 3.16, ENTHRU, LIMSET, and the permanent set per blow all show large changes when the measuring devices are omitted. This might be overlooked if only the experimental results for case DLTP-15;80.5 were known.

Table 3.17 shows how ENTHRU increases when the load cell assembly is removed.

Effects of Cushion Properties on Driving

Although the general effects of cushioning materials on pile driving are discussed in Chapter IV, the following discussion is given since it deals with the Michigan pile study.

As previously noted, the Michigan report states that the cushion properties influence the values of ENTHRU significantly, although "how, when, or how much" ENTHRU was affected could not be determined. It was thought that ENTHRU could be increased by using a more resistant cushion block, in the case of the Vulcan 1 and McKiernan-Terry DE-30 hammers. Although this conclusion seems reasonable, results given by the wave equation did not seem to agree. For example, as seen in Table 3.6, ENTHRU does not always increase with increasing cushion stiffness, and furthermore, the maximum increase in ENTHRU noted here is relatively small

—only about 10 percent. This effect can also be seen in Table 3.18, in which the cushion stiffness varies greatly, while the displacement of the pile point changes less than 10 percent.

However, if a different cushion is used, the coefficient of restitution will probably change too. Since the coefficient of restitution of the cushion may affect ENTHRU, a number of cases were solved with "e" ranging from 0.2 to 0.6. As shown in Tables 3.19 and 3.20, an increase in "e" from 0.2 to 0.6 normally increases ENTHRU from 18 to 20 percent, while increasing the permanent set from 6 to 11 percent. Thus, for the case shown, the coefficient of restitution of the cushion has a greater influence on rate of penetration and ENTHRU than does its stiffness. This same effect was noted in the other solutions, and the cases shown in Tables 3.19 and 3.20 are typical of the results found in other cases.

As was noted in Table 3.7, any increase in cushion stiffness also increases the driving stress. Thus, according to the wave equation, increasing the cushion stiffness to increase the rate of penetration (for example by not replacing the cushion until it has been beaten to a fraction of its original height or by omitting the cushion entirely) is both inefficient and poor practice because of the high stresses induced in the pile. It would be better to use a cushion having a high coefficient of restitution and a low cushion stiffness in order to increase ENTHRU and to limit the driving stress.

This suggests that a long micarta cushion having a relatively low spring rate, and a high coefficient of restitution might be very effective.

Comparison of Various Hammers Driving the Same Pile

One of the objectives of the Michigan pile study was to determine just how effective the various hammers actually were during driving. Therefore, every attempt was made to equalize any variables which would affect the results, such as choosing the driving location to give comparable driving conditions. However, it would be impossible to test several hammers without having some variations occur, perhaps in the soil resistance or hammer condition. Since the wave equation does not have this limitation, it can be used to advantage here.

TABLE 3.17. EFFECT ON ENTHRU RESULTING FROM REMOVING THE LOAD CELL ASSEMBLY

Driving Location	Pile I.D.	Case	ENTHRU (ft lb)		Increase ENTHRU in (%)
			With Load Cell	Without Load Cell	
Belleville	BLTP-6	10.0	6380	7500	18
		57.9	4440	5300	19
	BLTP-4	25.0	8010	8800	10
		66.4	11200	12000	8
BRP-4	20.0	4980	5750	15	
	50.0	4470	6450	44	
BLTP-5	15.0	9040	10750	19	
	60.0	9930	12300	24	
Detroit	DLTP-8	41.5	5760	6900	21
		80.2	4540	5400	19
	DTP-5	20.0	8290	10000	23
		79.0	11420	12700	12
	DRP-3	40.0	7060	7600	13
		60.0	6620	7200	11
DTP-13	40.0	9100	10850	13	
	80.7	9480	11400	20	
DTP-15	20.0	10100	11500	14	
	80.5	5480	6600	20	
Muskegon	MLTP-2	20.0	7210	8800	23
		53.0	4870	5700	17
	MLTP-9	72.0	14660	17000	16
		127.0	13110	16000	22
	MTP-12	30.5	14860	17000	14
		70.8	13140	15000	14
MTP-11	69.5	16760	22000	31	
	150.0	17900	25300	41	
MLTP-8	31.0	25500	31000	22	
	178.0	22050	26600	21	

TABLE 3.18. EFFECT OF CUSHION STIFFNESS ON MAXIMUM POINT DISPLACEMENT FOR CASES BLTP-6; 10.0 AND 57.9

Pile I.D.	RUT (kip)	Ram Velocity (ft/sec)	Maximum Point Displacement (in.)				Maximum Change (%)	
			Cushion Stiffness (kip/in.)					
			540	1080	2700	27,000		
BLTP-6; 10.0	30	12	2.20	2.14	2.22	2.26	5	
		16	3.54	3.47	3.52	3.70	6	
		20	4.66	4.93	5.00	5.01	7	
BLTP-6; 57.9	150	12	0.45	0.48	0.38	0.48	6	
		16	0.72	0.76	0.76	0.79	9	
		20	1.06	1.10	1.11	1.15	8	

TABLE 3.19. EFFECT OF COEFFICIENT OF RESTITUTION ON ENTHRU FOR CASE BLTP-6; 10.0 AND 57.9

Pile I.D.	RUT (kip)	Ram Velocity (ft/sec)	ENTHRU (kip ft)			Maximum Change (%)
			e = 0.2	e = 0.4	e = 0.6	
BLTP-6; 10.0	30	12	6.0	6.5	7.3	18
		16	10.5	11.8	12.8	18
		20	16.5	17.4	20.0	17
BLTP-6; 57.9	150	12	6.7	7.2	8.2	18
		16	11.6	12.7	14.5	20
		20	18.2	19.7	22.4	19

TABLE 3.20. EFFECT OF COEFFICIENT OF RESTITUTION ON MAXIMUM POINT DISPLACEMENT FOR CASE BLTP-6; 10.0 AND 57.9

Pile I.D.	RUT (kip)	Ram Velocity (ft/sec)	Maximum Point Displacement (in.)			Maximum Change (%)
			e = 0.2	e = 0.4	e = 0.6	
BLTP-6; 10.0	30	12	2.13	2.14	2.36	10
		16	3.38	3.47	3.58	6
		20	4.73	4.93	5.17	8
BLTP-6; 57.9	150	12	0.46	0.48	0.50	8
		16	0.73	0.76	0.81	10
		20	1.05	1.10	1.18	11

TABLE 3.21. STUDY OF VARIOUS HAMMERS DRIVING THE SAME PILE

Hammer	Ram Velocity (ft/sec)	Explosive Force (kip)	Maximum Point Displacement (in.)	Permanent Set of Pile Per Blow (in.)	Blows Per Inch
Vulcan-1	10.0	0	0.125	0.025	8
Vulcan-50C	14.5	0	0.284	0.184	3
Vulcan-80C	12.5	0	0.360	0.260	2
Link Belt 312	7.0	98.0	0.119	0.019	8
Link Belt 520	16.0	98.0	0.357	0.257	3
McKiernen-Terry DE-30	13.0	98.0	0.139	0.039	7
McKiernen-Terry DE-40	21.0	138.0	0.592	0.492	1
Delmag D-12	15.0	93.7	0.173	0.073	5
Delmag D-22	17.5	158.7	0.473	0.373	2

As an example of such a comparison, Case BLTP-6;57.9 is used, with the load cell and extra helmet omitted, and with a soil resistance of 300 kips. This pile was then analyzed by the wave equation to determine its penetration per blow when driven by each of the hammers listed in Table 3.10. In each case, the soil and pile parameters were held constant. Thus, for example, even though the values of the soil damping constant or quake may not be exact, they remained constant for each problem while experimental results would vary unless Q and J did not change at each new driving location.

Again, certain quantities had to be known for each hammer before the wave equation could be applied. For

example, the ram velocity at impact must be known, as well as the dynamic behavior of the cushion, the diesel explosive pressure in the hammer, and the length of time it exerts a force on the pile. Since the above data were not directly measured in the Michigan research program, they were being calculated from the previous data reported. The ram velocities at impact and explosive forces on the pile for the diesel hammers were based on the results given in Table 3.11, assuming the explosive force to be acting as shown in Figure 3.12. The Vulcan hammer properties were based on Table 3.10.

The results of driving this pile with the eight different hammers are listed in Table 3.21 in the form of permanent set of the pile per blow and blows per inch.

Chapter IV

CHARACTERISTIC CUSHION PROPERTIES

Introduction

Although a pile cushion serves several purposes, its primary function is to limit impact stresses in both the pile and hammer.⁵⁰ In general, it has been found that a wood or rope cushion is more effective in reducing the driving stresses than one of a relatively stiff material such as Micarta. However, a stiffer cushion is usually more durable and transmits a greater percentage of the hammer's energy to the pile.

For example, the results given in Tables 3.10 and 3.11 give an overall average efficiency of 52 percent for

cushion assemblies using wood, while the Micarta assemblies have an average efficiency of 66 percent. As shown in Table 3.7, an increase in cushion stiffness will also cause an increase in impact stresses which might damage the pile or hammer during driving. This increase in stress is particularly important when driving concrete or prestressed concrete piles.

Dynamic Stress-Strain Curves

In order to apply the wave equation to pile driving, Smith⁵¹ assumes that the cushion's stress-strain curve is

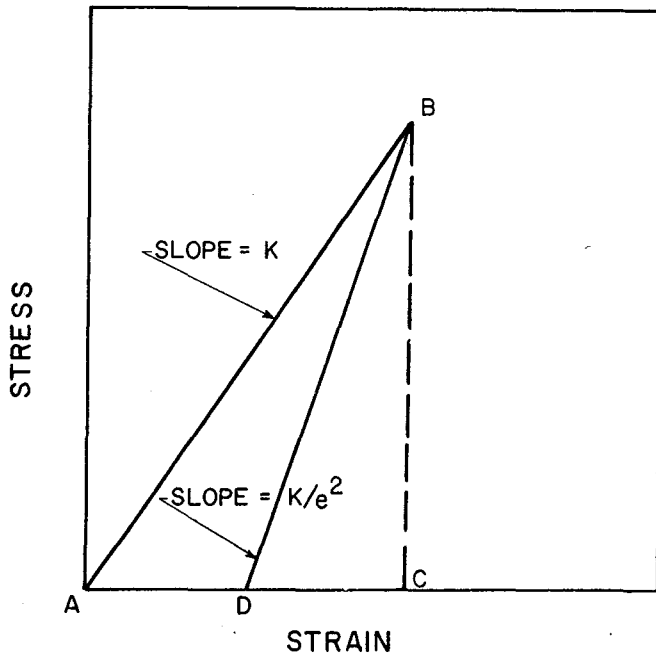


Figure 4.1. Stress-strain curve for a cushion block (after reference 51).

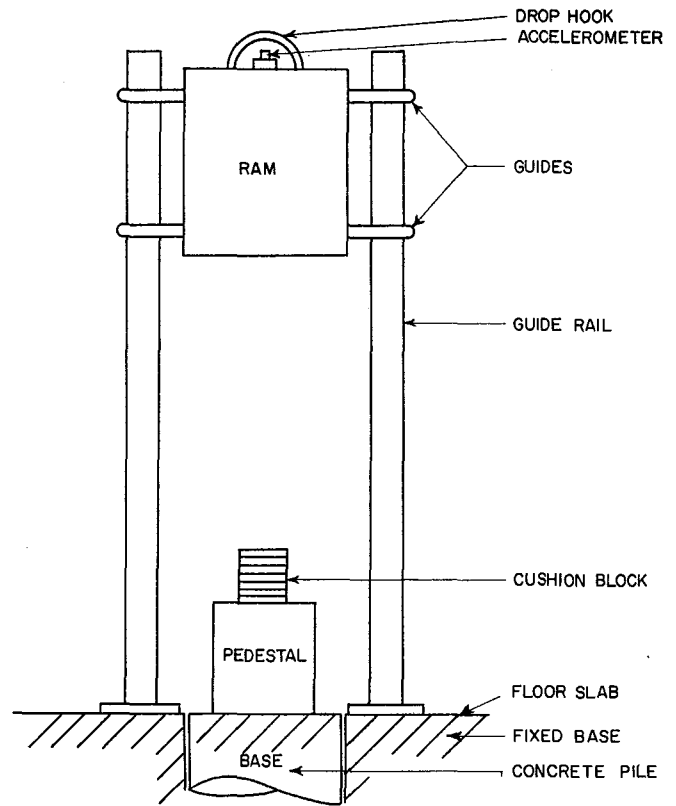


Figure 4.3. Cushion test stand.

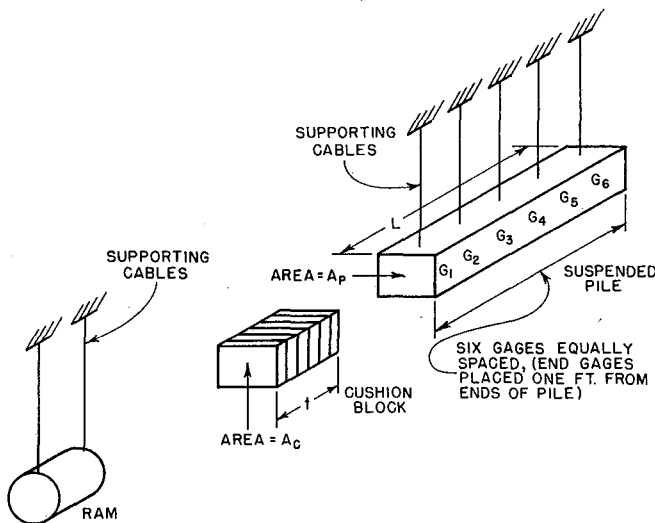


Figure 4.2. Test pile showing placement of strain gages.

a series of straight lines as shown in Figure 4.1. Even though this curve might be sufficiently accurate to predict maximum compressive stresses in the pile, the shape of the stress wave often disagrees with that of the actual stress wave.⁵² This discrepancy was at first thought to be the result of inaccurate soil data, since very little was known concerning the soil behavior during driving. It was therefore decided to suspend several test piles horizontally above the ground⁵³ as shown in Figure 4.2 to eliminate the effects of soil resistance.

Table 4.1 lists the pertinent information concerning these piles. The cushion was then hit by the ram and the resulting strains were measured at six points along the pile. Displacements and accelerations of both the ram and the head of the pile were also measured. However, even though the soil resistance had now been ex-

TABLE 4.1. SUSPENDED PILE DATA

Case	Material	E (psi)	Pile		Cushion		Ram		
			Ap (in. ²)	L (ft)	Material	Ac (in. ²)	t (in.)	Weight (lb)	Velocity (ft/sec)
LT-48	Class A Concrete	6.12x10 ⁶	254	65	Fir	62.8	9.0	4160	13.91
LT-41	Class A Concrete	6.12x10 ⁶	254	65	Micarta	89.1	9.0	4160	8.03
LT-39	Steel	30x10 ⁶	21.46	85	Oak	225.0	7.5	2128	11.42
LT-15	Class Y Concrete	*3.96x10 ⁶	225	65	Oak	225.0	9.5	2128	13.98

*E_{sonic} = 4.64x10⁶ psi

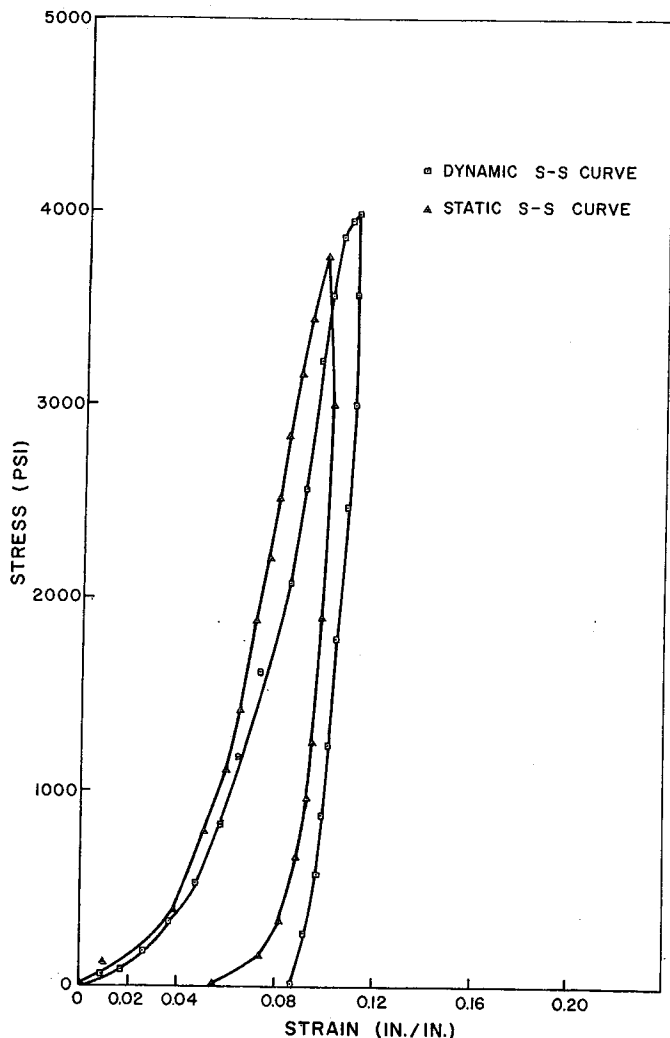


Figure 4.4. Dynamic and static stress-strain curves for a fir cushion.

cluded, the shape of the stress wave still did not agree with the theoretical shape, and so the device illustrated in Figure 4.3 was used to see if the cushion's stress-strain diagram was actually a straight line.

Using this method, the dynamic stresses and strains were measured for several cushion materials. It was later discovered that for a given material, the dynamic stress-strain curves were almost identical to the corresponding static curves. This is demonstrated in Figure 4.4 in which the dynamic and static curves for a fir cushion are compared.

Since the stress-strain curves are not linear as assumed, the shape of the theoretical stress wave in the pile is not likely to agree with the experimental shape and so the "dynamic" curves were used.

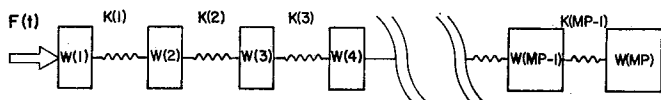


Figure 4.5. Idealized test pile with known forces applied at head of the pile.

Furthermore, it is not known how much the rigidity of the pedestal shown in Figure 4.3 affects the cushion's behavior. Therefore, the wave equation was used to check the results. The second method required the following information: 1) the stresses determined experimentally at the head of the pile vs time, 2) the velocity of the ram at impact, and 3) the physical properties of the pile system required for solution by the wave equation.

As shown in Figure 4.5, both the cushion and ram are omitted and the previously determined stresses measured experimentally at gage 1 (see Figure 4.2) are placed on the head of the pile. The wave equation is then used to determine the motion of the ram and the pile, from which the compression of the cushion at any instant of time is known. By plotting the measured cushion forces against the corresponding compressions of the cushion, the dynamic stress-strain curve may be determined. The curves obtained by this method are illustrated in Figures 4.6, 4.7, and 4.8. Comparing these with Figure 4.4, it is noted that the curves are generally similar in shape.

Dynamic Coefficient of Restitution

Although the cushion is needed to limit the driving stresses in both hammer and pile, it reduces the available hammer energy because of internal damping. The load diagram shown in Figure 4.1 illustrates this energy loss since the energy input is given by the area ABC

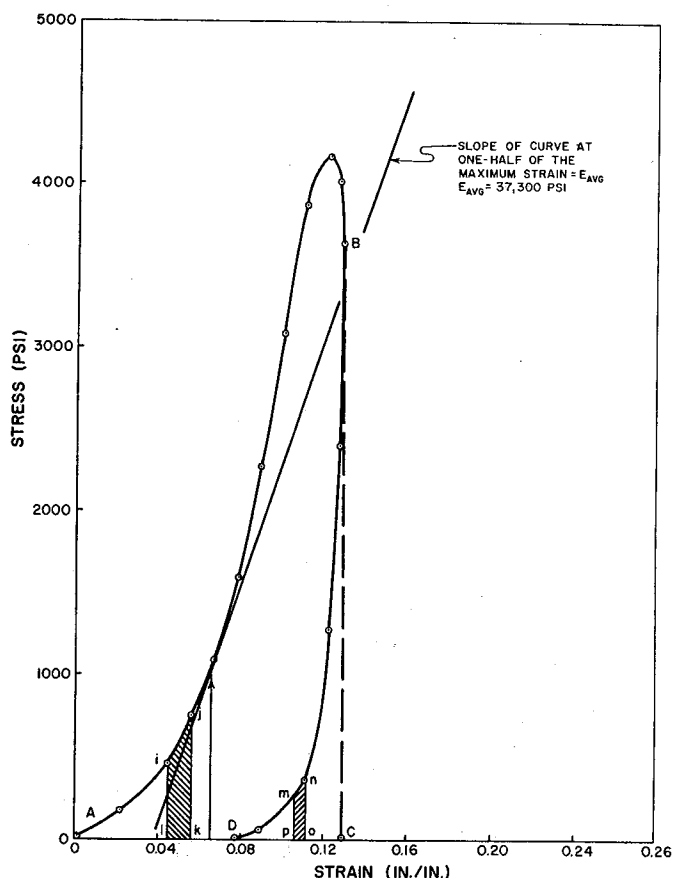


Figure 4.6. Dynamic stress-strain curve for fir cushion (Case LT-48).

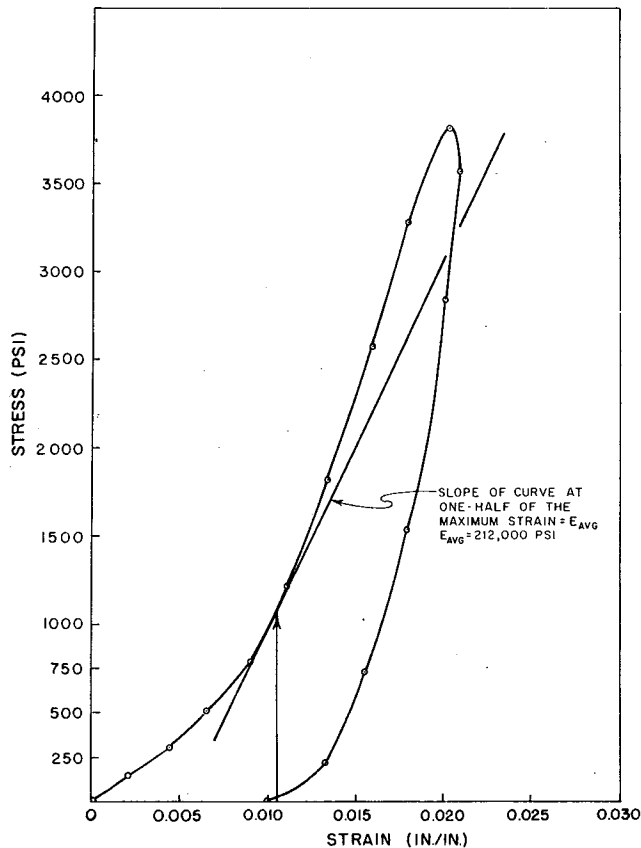


Figure 4.7. Dynamic stress-strain curve for a micarta cushion (Case LT-41).

while the energy output is given by area BCD. Usually this energy loss is accounted for by a coefficient of restitution of the cushion "e," in which

$$e = \sqrt{\frac{\text{Area under BCD}}{\text{Area under ABD}}}$$

When the dynamic stress-strain curve for the cushion is known, such as for the previous problem, the coefficient of restitution can be computed. As shown in Figure 4.6, the area under the dynamic curve ABC is computed by summing elemental areas ijkl until point B is reached (i.e., until the strain reaches a maximum), then the area under BCD is determined by summing elemental areas mnop until point D is reached.

Table 4.2 summarizes the results found for the curves of Figures 4.6, 4.7, and 4.8. These coefficients of restitution agree closely with values recommended by Hirsch.⁵⁵ It is interesting that although $e = 0.8$ is commonly recommended for a micarta capblock, these

TABLE 4.2. DYNAMIC CUSHION PROPERTIES

Case	Cushion Material	Dynamic e	Commonly Recommended e
LT-48	Fir	0.35	0.40 ⁵⁵
LT-41	Micarta	0.60	0.80 ⁴⁸
LT-39	Oak	0.47	0.48 ⁵⁵

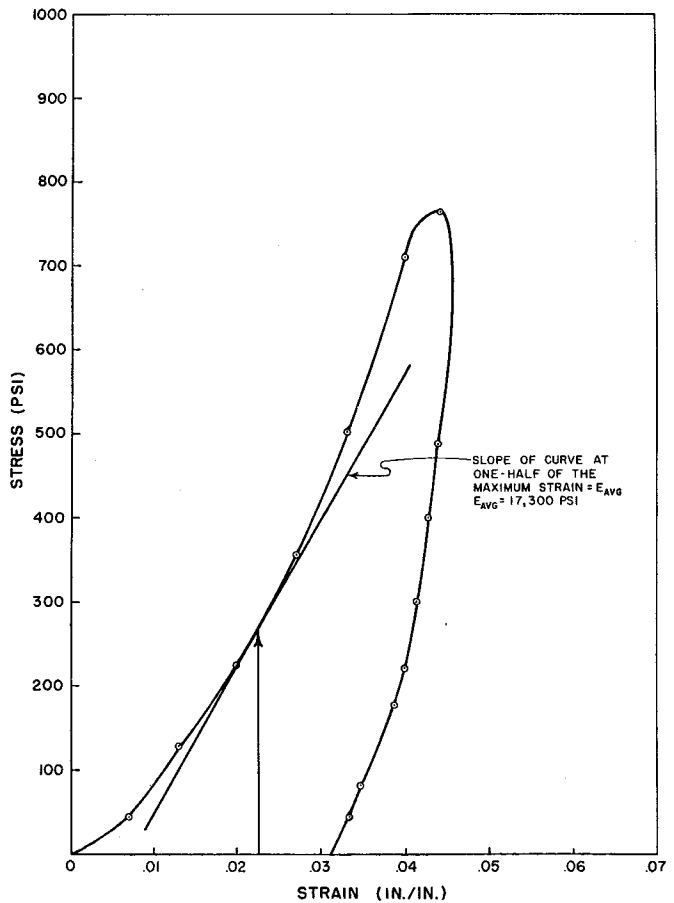


Figure 4.8. Dynamic stress-strain curve for an oak cushion (Case LT-39).

experiments indicate that e is actually much lower, probably around 0.6.

Idealized Dynamic Stress-Strain Curves

The major difficulty in using the dynamic curves derived in the previous section is that numerous points on the curve must be specified in the input data, unless the curve can be input in equation form. Although the

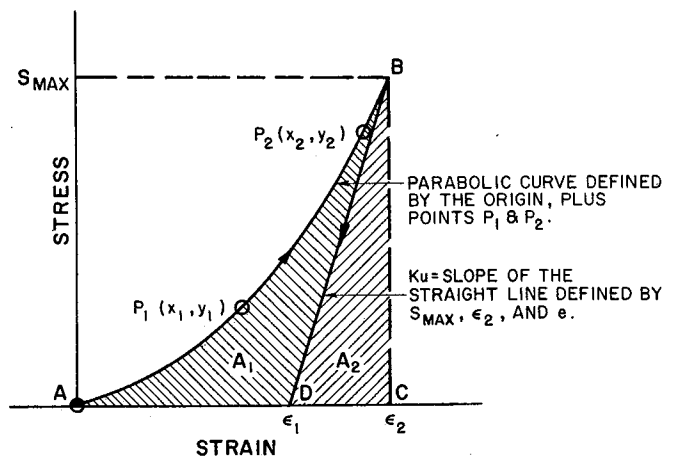


Figure 4.9. Idealized dynamic stress-strain curve for cushion (parabolic).

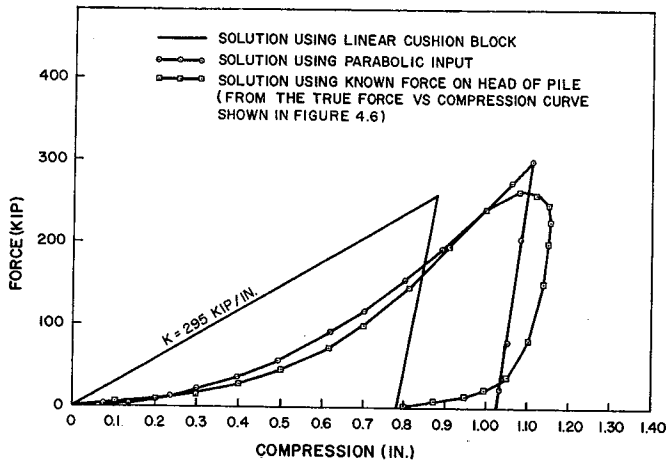


Figure 4.10. Dynamic force vs compression curves for a fir cushion (Case LT-48).

increasing load curve for each of the curves is nearly parabolic, the unloading segment is rather complex. Therefore, for convenience, the unloading segment will be approximated by a straight line having a slope such that the areas under the two curves result in the use of the correct coefficient of restitution for the cushion material being used.

Thus, the curve shown in Figure 4.9 can be defined by two different points on the loading curve (other than 0.0) and "e" of the material. The points on the curve are used to define the equation of the loading curve, and as long as the cushion strain increases, the increased input energy is computed as described earlier. When the strain in the cushion begins to decrease, the total input energy and the coefficient of restitution are used to determine the slope of the unloading curve in order to give the correct value of "e."

As shown in Figure 4.9, the total input energy is given by the area under the parabolic curve, $A_1 + A_2$, while the output energy is given by the area under the unloading curve, A_2 . Since e is defined by

$$e^2 = A_2 / (A_1 + A_2),$$

then

$$A_2 = e^2 (A_1 + A_2).$$

But A_2 is also given by

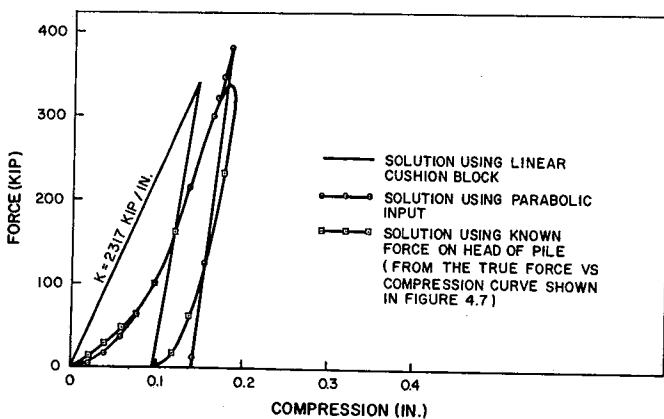


Figure 4.11. Dynamic force vs compression curve for a micarta cushion (Case LT-41).

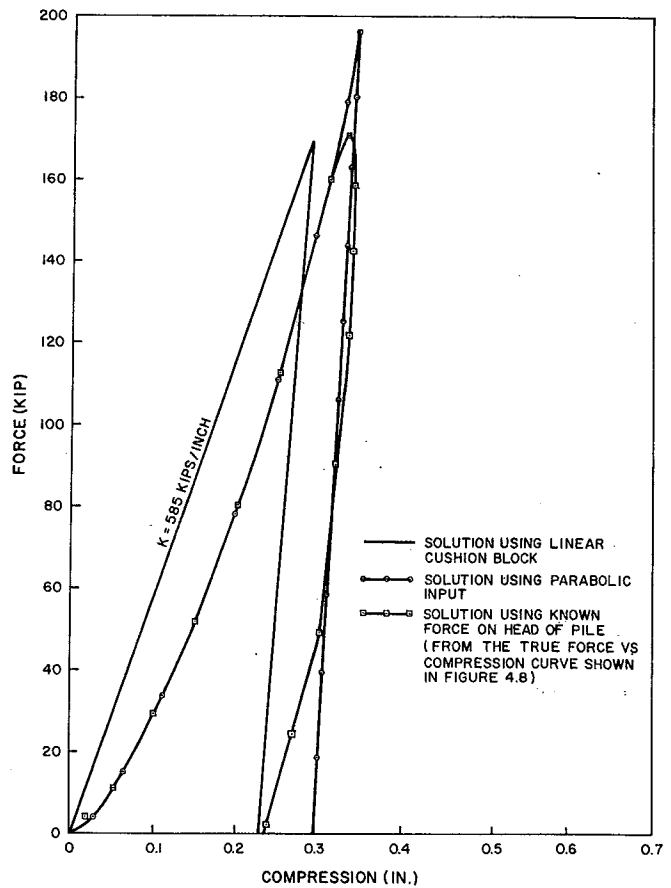


Figure 4.12. Dynamic force vs compression curve for an oak cushion (Case LT-39).

$$A_2 = \left(\frac{S_{\max} - 0}{2} \right) (\epsilon_2 - \epsilon_1)$$

$$e^2 (A_1 + A_2) = \left(\frac{S_{\max}}{2} \right) (\epsilon_2 - \epsilon_1)$$

$$(\epsilon_2 - \epsilon_1) = \frac{2e^2 (A_1 + A_2)}{S_{\max}}$$

Since the slope of the straight line BD is given by:

$$K_u = \frac{S_{\max}}{(\epsilon_2 - \epsilon_1)}$$

where K_u defines the slope of the unloading curve, e is the coefficient of restitution of the material, $(A_1 + A_2)$ is the total area under the curve ABD (calculated by the computer), and S_{\max} is the maximum stress in the cushion determined by the wave equation.

Figures 4.10, 4.11, and 4.12 compare experimental force vs compression curves obtained for the first three cases listed in Table 4.1, with those resulting from the parabolic idealization of Figure 4.9, and the straight line shown in Figure 4.1. Note that the parabolic curves closely represent the actual force-displacement curves while the linear curves are not nearly so close. In each case the parabolic curves tend to "over-shoot" the true maximum force, while the linear curve does not. The effect this has on the stress wave in the pile will be discussed in Chapter V.

Chapter V

STRESS WAVES IN PILING

Comparison of Actual and Experimental Stress Waves

As noted in Chapter IV, the shape and magnitude of the stress wave in a pile is greatly dependent upon the properties of the cushion used. This will become apparent by comparing the actual stress wave determined experimentally with results found by using the idealized cushion properties mentioned earlier.

The solution for stresses in the pile should be more accurate if the effects of the cushion and ram can be omitted. To accomplish this, the force measured at the head of the pile and the stresses at other gage points were then determined by using the wave equation. The cases solved by this method are listed in Table 4.1. Comparisons between the experimental results and wave equation solutions at two points on the pile are shown in Figures 5.1 through 5.6.

One of the major factors which influenced these comparisons was the fact that the prestressed concrete

test piles cracked while setting up the experiment. Therefore, any reflected tensile forces greater than the prestressing force opened a small gap at the crack such that the prestressing strands alone could transmit the tensile stress down the pile. This is seen by the relative agreement shown in Figures 5.1 through 5.6. Note that the stress-waves shown for the concrete piles (Figures 5.1 through 5.4) do not agree nearly so well as those for the steel pile (Figures 5.5 and 5.6).

Still, the results agree closely in each case, not only in magnitude, but also in the over-all shape of the wave, thus indicating that the numerical solution to the wave equation is quite accurate. Further, any inaccuracies are likely due to faulty assumptions concerning the dynamic behavior of other variables such as the cushion, soil, etc.

As mentioned earlier, the stress-strain curve for the cushion is normally assumed to be linear as in Figure 4.1. The true stress-strain curves shown in Figures 4.6 through 4.8 indicate that the curves are not actually

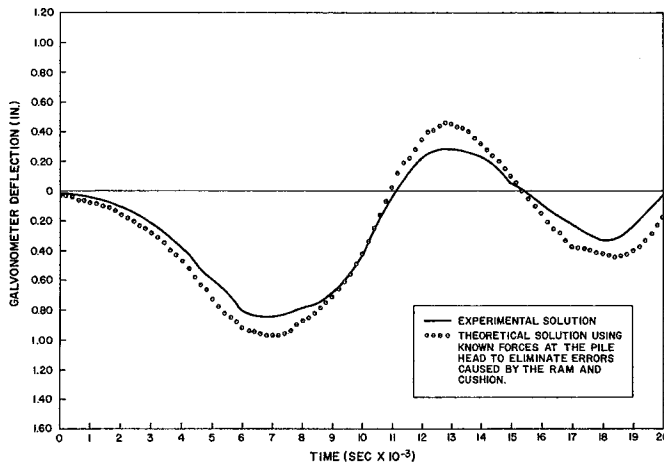


Figure 5.1. Theoretical vs experimental solution for Case LT-48, Gage #3.

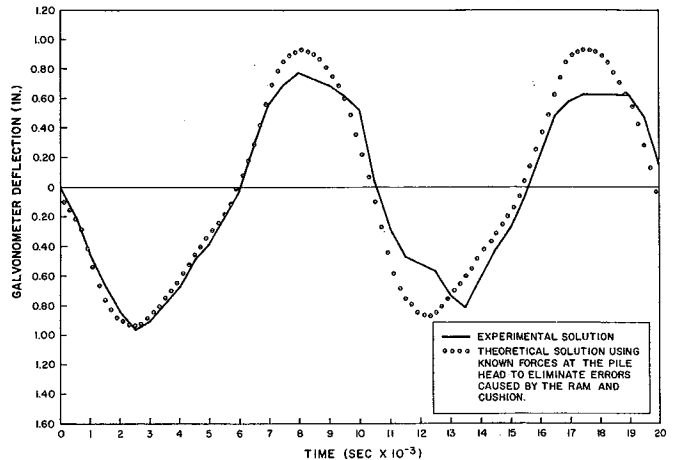


Figure 5.3. Theoretical vs experimental solution for Case LT-41, Gage #3.

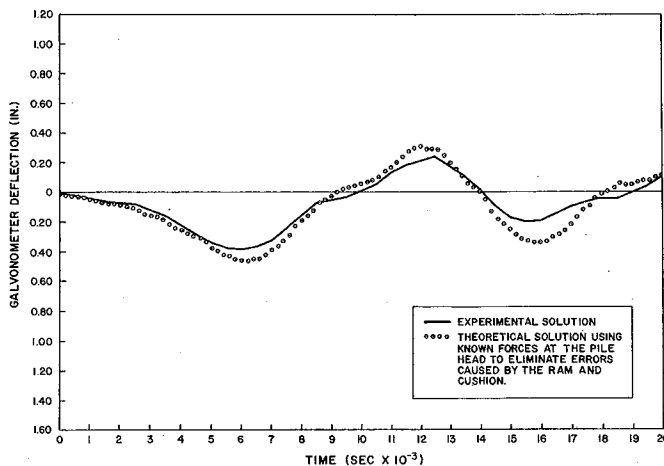


Figure 5.2. Theoretical vs experimental solution for Case LT-48, Gage #5.

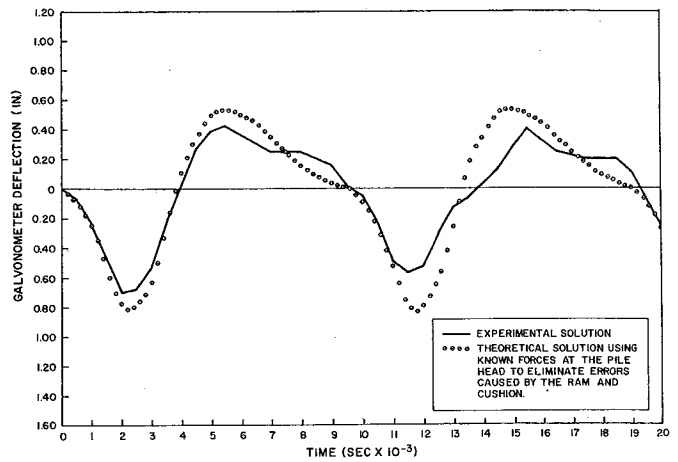


Figure 5.4. Theoretical vs experimental solution for Case LT-41, Gage #5.

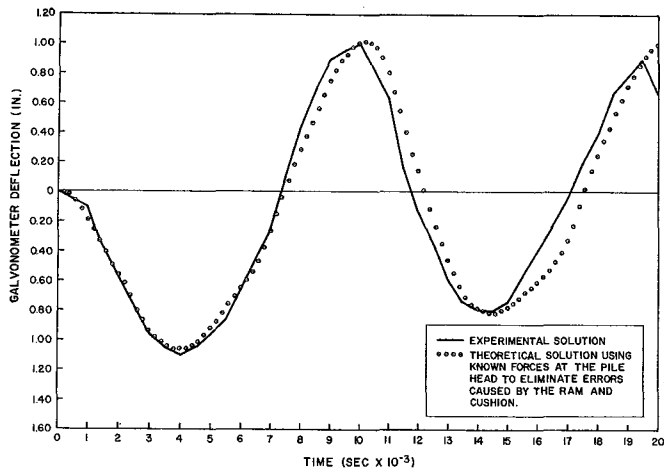


Figure 5.5. Theoretical vs experimental solution for Case LT-39, Gage #3.

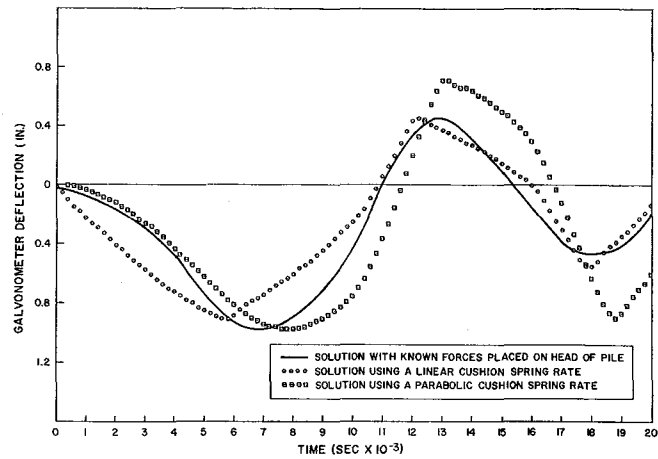


Figure 5.7. Theoretical vs experimental solution for Case LT-48, Gage #3.

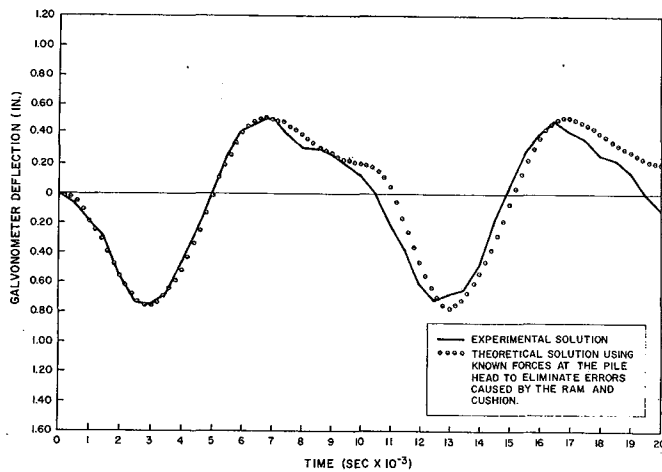


Figure 5.6. Theoretical vs experimental solution for Case LT-39, Gage #5.

linear and this assumption might therefore cause inaccuracies.

To determine how the shape of the curve affects the solution, the previous three problems were run using the cushion stress-strain curves shown in Figures 4.1 (straight line), 4.6 through 4.8 (true stress-strain curves), and 4.9 (parabolic curve). These solutions are compared in Figures 5.7 through 5.12. In each case, it is noted that the straight line solution is more accurate than the solution using the parabolic curve. This is because a simple parabolic curve was used which, even

though it agrees with the actual stress-strain curve most of the time, it cannot follow the reversed curvature at the peak of the actual curve and thus "over-shoots" the true peak force. Figures 4.10 through 4.12 show how closely the parabolic curves follow the true cushion forces, and also how far off the straight line assumption is. The parabolic curve always peaks above the true force vs compression curve, while the spring rate of the straight line can be raised or lowered so that the true maximum cushion force is not exceeded.

Thus the use of the straight-line assumption seems reasonable since it gives fairly accurate results. The linear spring constants used for the curves shown in Figures 5.7 through 5.12 were first varied between wide limits to obtain the most accurate maximum stresses. These spring rates were then used to determine what dynamic modulus of elasticity was required to give the desired spring rate, using the equation: $E_{dynamic} = (K \text{ cushion}) (\text{Length}) / (\text{Area of cushion})$. As shown in Table 5.1, these results give a lower value of E for oak than for fir, which in this case is correct since the fir capblock was highly stressed (4,170 psi) while the oak capblock was stressed only slightly (765 psi).

Further consideration of the dynamic stress-strain curves revealed that the dynamic modulus of elasticity of the capblock is almost exactly 10 percent greater than that given by the slope of the stress-strain curve (Figures 4.6 through 4.8) taken at a point halfway between zero and the maximum strain. As noted by Hirsch,⁶² the static and dynamic stress-strain curves are quite similar, so that curves like those shown in Figures 4.6 through 4.8 are easily determined for any other cushion material.

TABLE 5.1 DYNAMIC PROPERTIES OF NEW CUSHION BLOCKS OF VARIOUS MATERIALS

Case	Cushion Material	Linear Spring Rate - K (lb/in.)	Depth of Cushion (in.)	Area of Cushion (in. ²)	$E_{dynamic}$ (psi)	Slope at Midpoint of Curve (psi)	S _{MAX} in Cushion (psi)
LT-48	Fir	295,000	9.0	62.8	42,200	37,300	4170
LT-41	Micarta	2,320,000	9.0	89.1	234,000	212,000	3850
LT-39	Oak	585,000	7.5	225.0	19,500	17,300	765

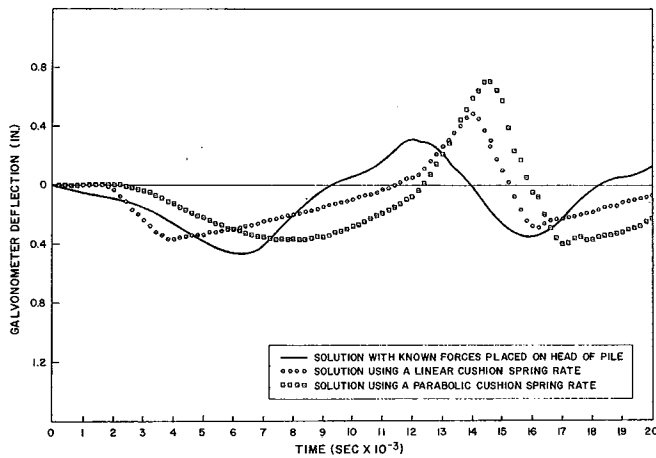


Figure 5.8. Theoretical vs experimental solution for Case LT-48, Gage #5.

It was also recommended that the dynamic modulus be increased as the cushion consolidated.⁶³

Internal Damping in Piling

As noted earlier, differences between experimental and theoretical results were assumed to be the result of inaccurate soil information. Other parameters were also varied in an attempt to obtain more accurate results,⁵⁶ one of which was the material damping or internal damping capacity of the pile material.

Smith⁵⁷ first suggested that the internal damping in the pile might prove significant, and proposed the following equation by which hysteresis in the pile could be accounted for:

$$F(m,t) = C(m,t)K(m) + \frac{BK(m)}{12\Delta t} [C(m,t) - C(m,t-1)]$$

in which B is the internal damping constant. He also recommended that B be given a value of about 0.002 in order to produce a narrow hysteresis loop. This equation was derived from the model shown in Figure 5.13

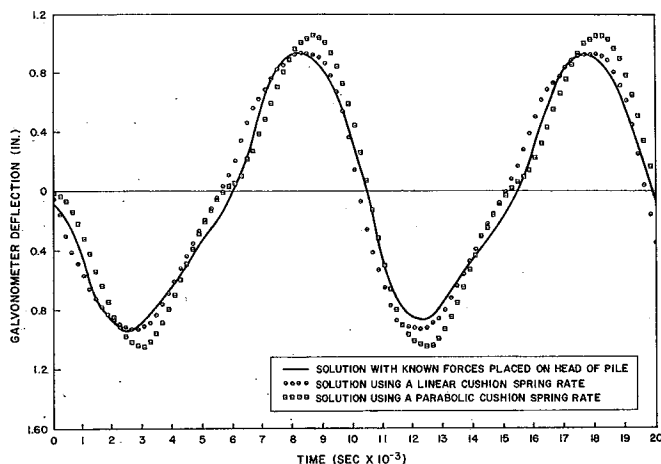


Figure 5.9. Theoretical vs experimental solution for Case LT-41, Gage #3.

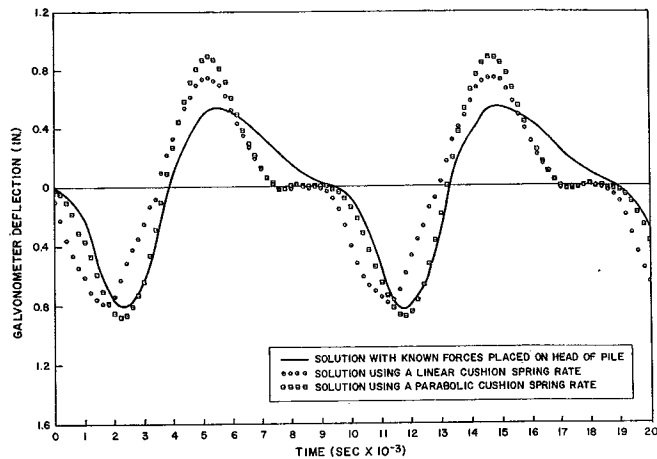


Figure 5.10. Theoretical vs experimental solution for Case LT-41, Gage #5.

(b) and if B is set equal to zero, no damping is present, as seen in Figure 5.13 (a).

The model shown in Figure 5.13 (c) has one major advantage over the previous model in that it is able to account for damping by considering the difference between the material's static modulus of elasticity E, and its sonic modulus of elasticity E_s. This is because a slowly applied load gives the dashpot time to relax without causing the spring K_s to exert a force, thereby resulting in a spring rate equal to K₀. However, when the loads are applied rapidly the dashpot has no chance to deform, resulting in a spring rate of K₀ + K_s. Thus for the model of Figure 5.13 (c), K₀ is determined from the static modulus of elasticity E, while K₀ + K_s would use the sonic value E_s.

It is interesting to note that when K_s is infinitely large, model (c) becomes equivalent to model (b), and if K_s = 0, model (c) becomes equivalent to model (a).

In order to derive the equation, Figure 5.14 is provided. Figure 5.14 (a) illustrates the damping model wherein point "m" (on the upper mass) has moved a distance x₁, point "n" (between the dashpot and spring)

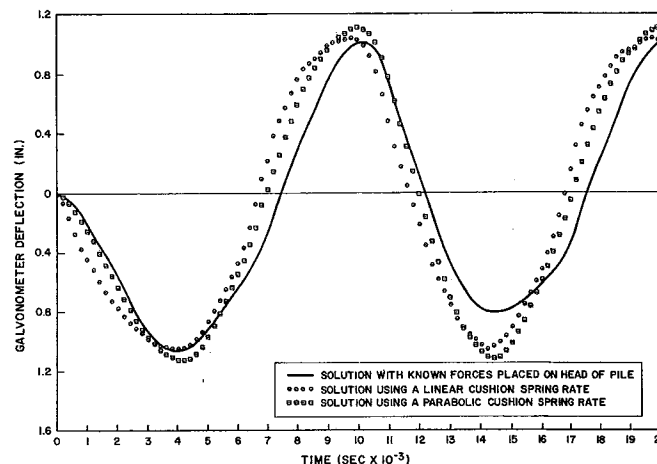


Figure 5.11. Theoretical vs experimental solution for Case LT-39, Gage #3.

has moved a distance x_2 , and point "o" (on the lower mass) has moved a distance of x_3 . Assume that at time $t = t_0$ there exists a force $F_0^{t_0}$ in the spring K_0 . There is also a force in the spring K_s given by $F_s^{t_0}$, and a force in the dashpot equal to $F_D^{t_0}$.

As shown in Figure 5.14 (b), after a single time interval passes, point m moves an additional distance Δx_1 , point na moves Δx_2 , and point o moves Δx_3 . At this time, $t = t_1 = t_0 + \Delta t$, and the forces in K_0 , K_s , and B are designated $F_0^{t_1}$, $F_s^{t_1}$, and $F_D^{t_1}$, respectively.

At time t_0 :

$$F_s^{t_0} = K_s(x_1 - x_2). \quad \text{Eq. 5.1}$$

At time $t_1 = t_0 + \Delta t_1$:

$$F_s^{t_1} = K_s[(x_1 + \Delta x_1) - (x_2 + \Delta x_2)].$$

$$F_s^{t_1} = K_s[(x_1 - x_2) + (\Delta x_1 - \Delta x_2)]. \quad \text{Eq. 5.2}$$

Substituting Equation 5.1 into 5.2:

$$F_s^{t_1} = F_s^{t_0} + K_s(\Delta x_1 - \Delta x_2). \quad \text{Eq. 5.3}$$

By definition, at all times:

$$F_D^{t_1} = B \frac{(\Delta x_2 - \Delta x_3)}{\Delta t}. \quad \text{Eq. 5.4}$$

Because point n must be in equilibrium:

$$F_s^{t_1} = F_D^{t_1}. \quad \text{Eq. 5.5}$$

Substituting Equation 5.3 and 5.4 into 5.5:

$$F_D^{t_0} + K_s(\Delta x_1 - \Delta x_2) = B \frac{(\Delta x_2 - \Delta x_3)}{\Delta t}$$

$$F_D^{t_0} + K_s \Delta x_1 = K_s \Delta x_2 + \frac{B \Delta x_2}{\Delta t} - \frac{B \Delta x_3}{\Delta t}$$

$$F_D^{t_0} \Delta t + K_s \Delta x_1 \Delta t + B \Delta x_3 = \Delta x_2 (K_s \Delta t + B).$$

Solving for Δx_2 :

$$\Delta x_2 = \frac{F_D^{t_0} \Delta t + K_s \Delta x_1 \Delta t + B \Delta x_3}{K_s \Delta t + B} \quad \text{Eq. 5.6}$$

Substituting Equation 5.6 into 5.4 produces:

$$F_D^{t_1} = \frac{F_D^{t_0} + K_s (\Delta x_1 - \Delta x_3)}{(K_s \Delta t / B) + 1} \quad \text{Eq. 5.7}$$

The solution begins by setting $F_D^{t_0}$ equal to zero, and calculating it for the next time interval from Equation 5.7. The quantity K_s is a constant and $(\Delta x_1 - \Delta x_3)$ is simply the change in compression during a single time interval. Therefore, returning to the earlier terminology, Equation 5.7 can be written:

$$DF(I, t+1) = \frac{DF(I, t) + DK(I) [C(I, t+1) - C(I, t)]}{[DK(I) \Delta t / B] + 1.0} \quad \text{Eq. 5.8}$$

where $DF(I, t)$ is the damping force in dashpot number "I" during time interval "t," $DK(I)$ is the dynamic spring rate of damping spring "I," $C(I, t)$ is the compression in spring I during time interval number t, Δt is the time increment, and B is a damping constant.

The static force in spring I will be computed as before, by

$$F(I, t+1) = K(I) [C(I, t+1)]. \quad \text{Eq. 5.9}$$

Thus by adding the Equations 5.8 and 5.9, the total force acting on each mass can be determined for the next time interval.

Since as far as is known this derivation does not appear elsewhere, the boundary conditions for the damp-

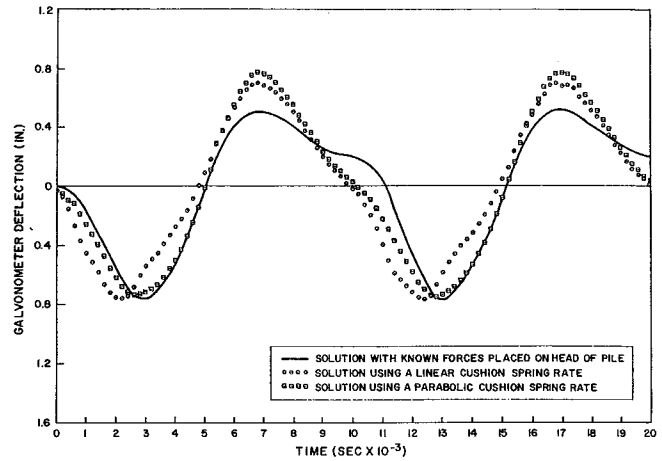


Figure 5.12. Theoretical vs experimental solution for Case LT-39, Gage #5.

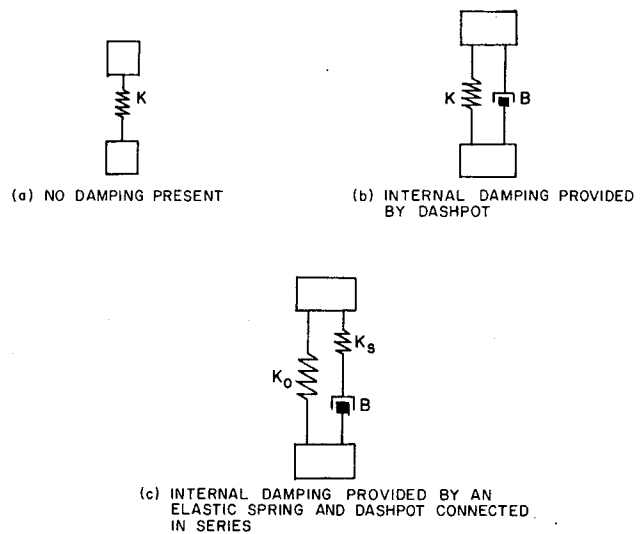


Figure 5.13. Various idealizations for the spring segment of a pile.

ing force given by Equation 5.7 were checked. From Equation 5.7,

$$(a) \text{ Letting } K_s = 0 : F_D^{t_1} = \frac{F_D^{t_0} + 0}{1 + 0} = F_D^{t_0}.$$

This is correct since F_D begins at zero and cannot increase in magnitude when $K_s = 0$.

$$(b) \text{ Letting } K_s = \infty : F_D^{t_1} = \frac{F_D^{t_0} + \infty}{\infty + 1} = \infty / \infty.$$

Since this is indeterminate,

$$F_D^{t_1} = K_s \rightarrow \infty \frac{\frac{d}{dK_s} [F_s^{t_0} + K_s (\Delta x_1 - \Delta x_3)]}{\frac{d}{dK_s} [K_s \Delta t + 1]}$$

$$= K_s \rightarrow \infty \frac{0 + (\Delta x_1 - \Delta x_3)}{\Delta t / B + 0} = \frac{B (\Delta x_1 - \Delta x_3)}{\Delta t}.$$

This checks since it is the equation found when $K_s = \infty$ and only the dashpot remains. In this case the models of Figures 5.13 (b) and (c) would be identical

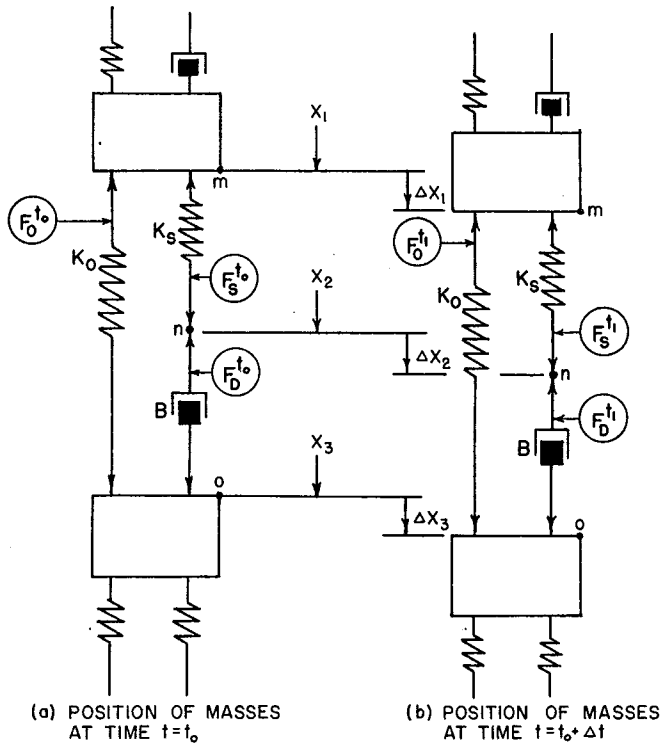


Figure 5.14. Idealized pile segment with standard linear solid damping.

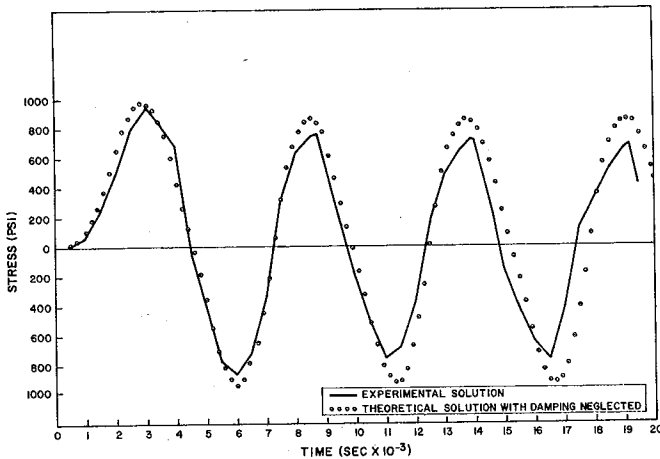


Figure 5.15. Comparison of experimental and theoretical solutions for stresses at Gage #3 with damping omitted (Case LT-15).

$$(c) \text{ Letting } B = 0 : F_D^{t_1} = \frac{F_D^{t_0} + K_s(\Delta x_1 - \Delta x_3)}{1 + \frac{K_s \Delta t}{0}}$$

$$= \frac{1}{\infty} = 0.$$

This checks since if the dashpot has no damping ability, the damping force must be zero.

$$(d) \text{ Letting } B = \infty : F_D^{t_1} = \frac{F_D^{t_0} + K_s(\Delta x_1 - \Delta x_3)}{\frac{K_s \Delta t}{\infty} + 1}$$

$$= F_D^{t_0} + K_s(\Delta x_1 - \Delta x_3)$$

$$\text{But } F_D^{t_0} = F_s^{t_0} = K_s(x_1 - x_2).$$

Substituting this into the previous equation one finds

$$F_D^{t_1} = [K_s][(x_1 - x_2) + (\Delta x_1 - \Delta x_2)]$$

$$= [K_s][(x_1 + \Delta x_1) - (x_2 + \Delta x_2)]$$

$$= [K_s][\text{Total compression at time } t].$$

This is correct since it is the equation for the spring and when $B = \infty$, the dashpot is "locked" and no damping occurs.

$$(e) \text{ Letting } \Delta t = 0 : F_D^{t_1} = \frac{F_D^{t_0} + K_s(\Delta x_1 - \Delta x_3)}{0 + 1}$$

This result agrees because it gives the same result as letting $B = \infty$. (See part (d) above.)

$$(f) \text{ Letting } \Delta t \rightarrow \infty : F_D^{t_1}$$

$$= \frac{F_D^{t_0} + K_s(\Delta x_1 - \Delta x_3)}{\infty + B} = 0.$$

This checks because the force stored in the damping spring would be released by relaxation of the dashpot if $\Delta t = \infty$.

(g) Let $\Delta x_1 = \Delta x_2$ and assume that the damping spring has an initial force stored at $t = t_0$. Although this force should diminish with time, it cannot go to zero during a single time interval, unless $\Delta t = \infty$.

$$F_D^{t_1} = \frac{F_D^{t_0} + K_s(0)}{\frac{K_s \Delta t}{B} + 1.0} = \frac{F_D^{t_0}}{\frac{K_s \Delta t}{B} + 1.0}$$

This is correct since the force in the spring is reduced, but will never actually reach zero unless $\Delta t = \infty$.

Figures 5.15 through 5.18 compare the effects of damping in a pile using the damping models shown in Figure 5.13. The results given are for test pile number LT-15 which is described in Table 4.1. This particular pile was of lightweight concrete with $E = 3.96 \times 10^6$ and $E_s = 4.63 \times 10^6$ psi. This problem was chosen since E_s was relatively larger than E , indicating the possibility of rather high damping.

However, one is often more interested in the maximum stresses found in the pile, which usually occurs during the first or second pass of the stress wave along the pile. During this time the effects of damping are small and can usually be neglected.

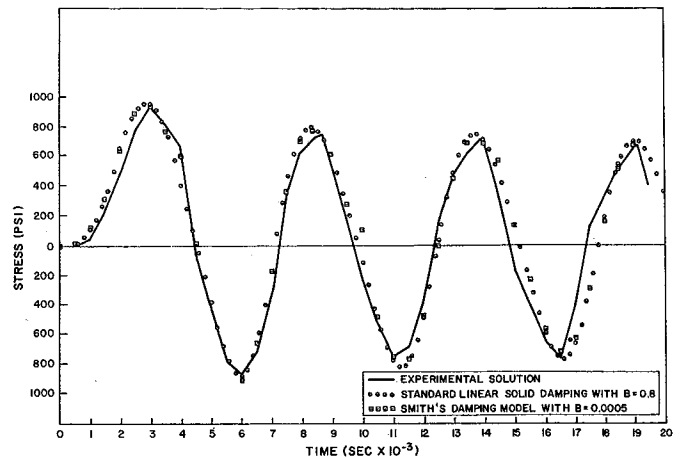


Figure 5.16. Comparison of experimental and theoretical solutions for stresses at Gage #3 for different damping models (Case LT-15).

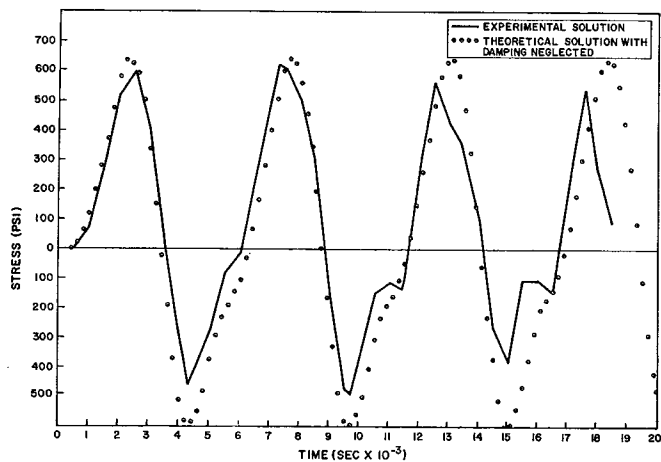


Figure 5.17. Comparison of experimental and theoretical solutions for stresses at Gage #5 with damping omitted (Case LT-15).

This conclusion may not be accurate for timber piles since wood has a much higher damping capacity than either the steel or concrete piles for which experimental data were available. This higher damping capacity might affect the results earlier in the solution which might in turn lower the accuracy of the results. Nevertheless, if more testing should indicate that the damping models are accurate for timber piling too, then the problem, or rather the uncertainties of damping effects will no longer be a problem.

In any case, if the wave is to be studied for an extended period of time, damping in the pile cannot be

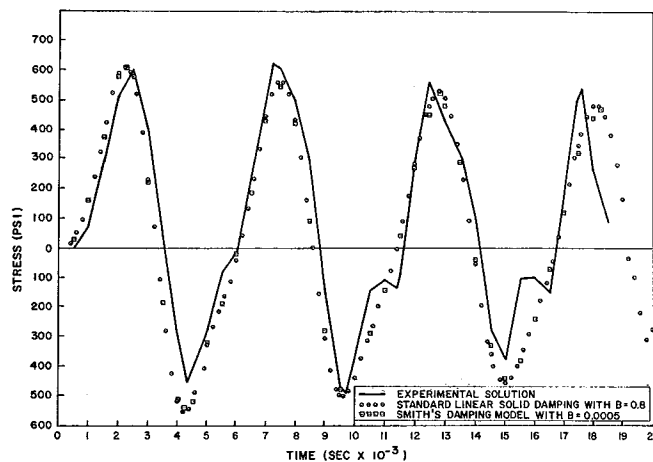


Figure 5.18. Comparison of experimental and theoretical solutions for stresses at Gage #5 for different damping models (Case LT-15).

neglected. This is illustrated in Figures 5.15 and 5.17 where fairly large errors resulted when damping was neglected. On the other hand, Figures 5.16 and 5.18 suggest that in certain cases damping should be accounted for using either of the damping models of Figure 5.13.

The most surprising result of this study is not the accuracy of the damping models, but rather that both models give nearly identical results even though Smith's model is extremely simple while the other is rather complex. Again, this may also prove incorrect for timber piling or other piling which has a large damping capacity. For example, one of the above methods might be more accurate than the other.

Chapter VI

SOIL PROPERTIES

Idealized Soil Resistance Curves

The load-deformation characteristics assumed for the soil in Smith's numerical solution are shown in Figure 6.1 (a). This curve excludes the damping effects of the soil caused by rapid loading, and illustrates only the soil resistance caused by static loading. As shown, the two parameters required to define the load-deformation curve are the ground quake " $Q(m)$ " and the ultimate static soil resistance " $R_u(m)$."

When the soil is located along the side of the pile, it is assumed to resist any rebound of the pile as well as any downward motion. This is typified by the curve OABCDEF. However, the soil located at the tip of the pile can only exert upward forces, as represented by the curve OABCFCB.

The spring rate for the curve between point O and A may now be determined from

$$K'(m) = \frac{R_u(m)}{Q(m)}$$

In order to include the damping effects of the soil, a third variable $J(m)$ is defined as the damping constant of soil spring " m ." Thus the total resistance of

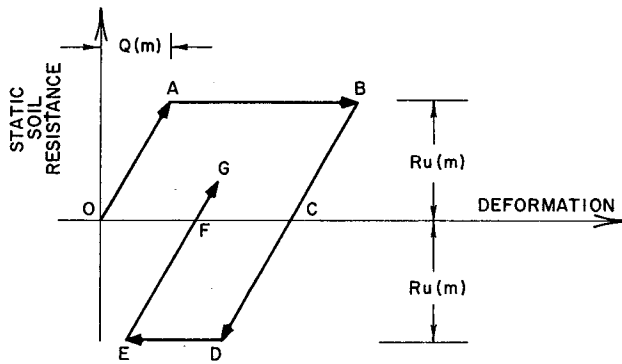
the soil, including the effect of loading rate, is given by

$$R(m,t) = [D(m,t) - D'(m,t)] K'(m) [1 + J(m)V(m,t-1)]$$

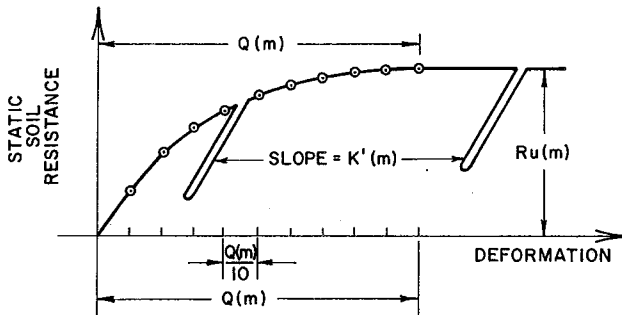
where m denotes the segment number of the pile, t is the time interval number, $D(m,t)$ is the displacement of segment m at time interval number t , $K'(m,t)$ is the plastic deformation of the soil, $J(m)$ is the soil damping constant, $K'(m)$ is the soil spring constant, $V(m,t)$ is the velocity of mass number m at time interval number t , and $R(m,t)$ is the soil resistance acting on that element at time t .

In cases in which more accurate soil data are available, the general soil resistance curve of Figure 6.1 (b) may be used to advantage. This curve also uses the variables $Q(m)$ and $R_u(m)$, but the curve no longer must be linear. In this case, the ground quake $Q(m)$ is divided into ten equal segments, and the static soil resistances corresponding to these ten points comprise the input data required to establish the curve. Also, as shown in Figure 6.1 (b), the slope of the unloading curve is given by $K'(m)$. A more complete discussion of the use of this method is given in the appendix.

To check out the programming changes involved in this method, several problems were first solved using



(a) ELASTIC-PLASTIC OR "LINEAR" SOIL RESISTANCE CURVE



(b) GENERALIZED SOIL RESISTANCE CURVE

Figure 6.1. Load-deformation characteristics assumed for the soil.

the regular elastic-plastic curve of Figure 6.1 (a). These problems were then solved again using the generalized soil resistance method with soil resistance values lying on the same curve, the two solutions then being checked for identical results.

A number of other problems were also solved to see what changes might result when the shape of the soil resistance curve was altered. For example, the linear soil resistance curve used in a problem originally solved by Smith⁵⁸ is shown in Figure 6.2 (a). This problem was then solved using the nonlinear curve of Figure 6.2 (b).

The solutions for these two problems, shown in Table 6.1, are typical of the results found for the other cases studied, in that a rather large change in the soil curve changed the results only slightly. In this case,

TABLE 6.1. COMPARISON OF RESULTS FOUND BY USING ELASTIC-PLASTIC VS NONLINEAR SOIL RESISTANCE CURVES

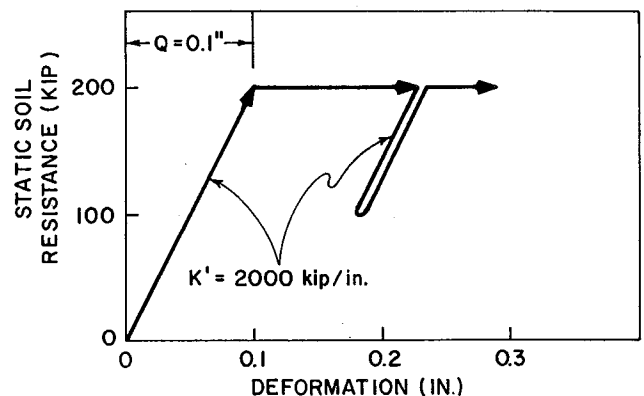
Type of Soil Resistance	Maximum Force (kip)			Maximum Point Displacement (in.)
	At Head of Pile	At Center of Pile	At Point of Pile	
Elastic Plastic	290	300	405	0.203
Nonlinear	290	301	370	0.218
Percent Change	0.0	+0.3	-8.7	+7.4

for example, although the soil quake was doubled and the curve made nonlinear, the maximum change in stress was less than 9 percent, and the permanent set increased less than 8 percent. Only a drastic change in the soil resistance curve was found to cause an appreciable difference in the solution.

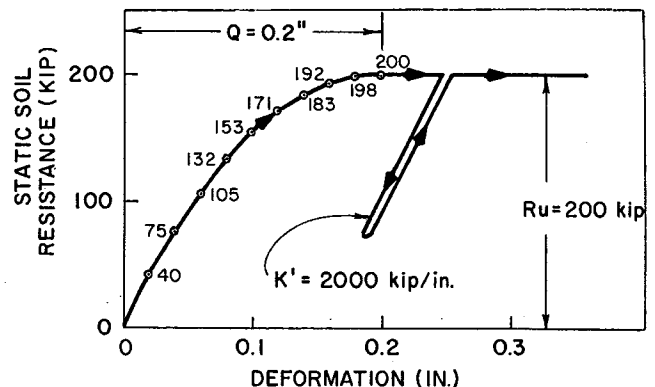
Therefore, if the soil resistance curve for the problem even slightly resembles the curve of Figure 6.2 (a), the linear resistance equation will probably be satisfactory. Whenever it becomes necessary, the nonlinear soil resistance can be used as explained in the appendix.

Significance of the Soil Quake "Q"

The properties of the soil under the action of dynamic loading are probably the least understood of the many variables affecting the problem.⁶⁴ Although a number of values for the soil quake may be used, the value $Q = 0.1$, recommended by Chellis⁶⁵ is probably the most widely accepted for general use, except when a more accurate value can be determined. As might be expected, the trouble stems mainly from the large number of variables influencing the value of Q at any given driving location, the most obvious of course being the type of soil encountered. Much work is presently being done to define these factors and to more accurately determine the actual values for both "Q" and "J" to increase the solution's accuracy.^{66,67}



(a) ELASTIC-PLASTIC SOIL RESISTANCE CURVE (AFTER REFERENCE 58)



(b) GENERALIZED SOIL RESISTANCE CURVE

Figure 6.2. Soil resistance vs deformation curves.

While it is beyond the scope of this paper to attempt to determine values for Q , it is interesting to see how the value of Q affects the solution. After a number of the Michigan research problems with varying values of Q were studied, Case BLTP-6; 57.9 was chosen as being fairly representative. The problems were solved with Q ranging from 0.1 to 0.5, as seen in Table 6.2. To determine whether Q would have similar effects at all magnitudes of soil resistance, $R_{u\text{total}}$ was also varied. The results of this parameter study are given in Table 6.2.

One of the trends noted in Table 6.2 is the small effect Q has on the maximum compressive force found in the pile. The effect on tensile force is more pronounced, although no conclusion could be reached as to whether the tensile stress will increase or decrease as Q changes since the results did not indicate an apparent trend. Maximum ENTHRU values are also relatively independent of the soil quake, with ENTHRU tending to decrease as the soil quake increases.

The most pronounced and consistent trend is the marked increase in maximum point displacement corresponding to increasing values of Q . It is also noted that the percent increase in maximum point displacement is relatively small for a small soil resistance, but greatly increases as the total soil resistance becomes large. This is also shown in Figure 6.3. Similar results

TABLE 6.2. INFLUENCE OF SOIL QUAKE AT DIFFERENT SOIL RESISTANCES FOR CASE BLTP-6; 57.9 WITH NO SOIL DAMPING

Total Soil Resistance (kip)	Q (in.)	Maximum Point Displacement (in.)	Maximum ENTHRU (kip ft)	Maximum Compressive Force (kip)	Maximum Tensile Force (kip)
50	0.1	1.49	6.80	225	109
	0.2	1.51	6.80	222	109
	0.3	1.51	6.73	221	114
	0.4	1.54	6.71	221	119
	0.5	1.58	6.69	221	124
100	0.1	0.84	6.96	230	68
	0.2	0.88	6.88	224	85
	0.3	0.90	6.86	223	97
	0.4	0.93	6.84	222	98
	0.5	0.97	6.83	222	97
150	0.1	0.56	7.10	235	91
	0.2	0.57	7.05	227	90
	0.3	0.61	6.93	225	128
	0.4	0.64	6.88	223	163
	0.5	0.69	6.85	223	188
200	0.1	0.41	7.21	240	79
	0.2	0.44	7.13	230	67
	0.3	0.48	7.06	226	77
	0.4	0.52	6.99	224	107
	0.5	0.56	6.90	224	118
300	0.1	0.22	7.28	250	82
	0.2	0.30	7.24	234	108
	0.3	0.36	7.16	229	111
	0.4	0.42	7.10	225	59
	0.5	0.47	7.05	224	73
400	0.1	0.11	7.30	260	127
	0.2	0.21	7.28	239	114
	0.3	0.29	7.24	233	158
	0.4	0.36	7.18	228	158
	0.5	0.41	7.12	226	102

were found for the other Michigan cases studied, except that the tensile force often varied substantially more than indicated for the case of Table 6.2.

Significance of the Soil Damping

Michigan Case BLTP-6;57.9 was also chosen to illustrate the damping effects of the soil. These damping constants were given values ranging from 0.0 to 0.5, and as was done in the previous section, the total soil resistance was varied from 50 to 400 kip to see if trends found at low resistances would also be noted when the soil resistance was large. Since the soil damping constants most commonly used are those recommended by Smith,⁶⁸ i.e., a soil damping constant of 0.05 sec/ft along the side of the pile and 0.15 sec/ft at the point of the pile, the variation of $J = 0.0$ to 0.5 very likely covers the values typical for many conditions and soils. These results are given in Table 6.3.

As was previously determined for Q , the soil damping constants also have little effect on the maximum ENTHRU values. The maximum compressive forces do

TABLE 6.3. INFLUENCE OF SOIL DAMPING ON DIFFERENT SOIL RESISTANCES FOR CASE BLTP-6; 57.9 ($Q = 0.1$ FOR ALL CASES)

Total Soil Resistance (kip)	J (sec/ft)	Maximum Point Displacement (in.)	Maximum ENTHRU (kip ft)	Maximum Compressive Force (kip)	Maximum Tensile Force (kip)
50	0.0	1.49	6.80	225	109
	0.1	1.11	6.89	221	68
	0.2	0.85	7.03	221	41
	0.3	0.72	7.21	221	18
	0.4	0.63	7.23	222	6
	0.5	0.56	7.25	222	5
100	0.0	0.84	6.96	230	68
	0.1	0.58	7.12	222	31
	0.2	0.49	7.20	223	11
	0.3	0.43	7.25	223	14
	0.4	0.38	7.27	224	12
	0.5	0.34	7.28	225	17
150	0.0	0.56	7.10	235	91
	0.1	0.42	7.23	223	23
	0.2	0.34	7.26	224	21
	0.3	0.28	7.28	225	26
	0.4	0.24	7.27	239	24
	0.5	0.21	7.26	251	22
200	0.0	0.41	7.21	223	79
	0.1	0.28	7.28	225	35
	0.2	0.22	7.28	239	37
	0.3	0.18	7.25	255	31
	0.4	0.15	7.22	267	27
	0.5	0.13	7.20	274	26
300	0.0	0.22	7.28	250	82
	0.1	0.12	7.23	272	53
	0.2	0.09	7.18	286	41
	0.3	0.08	7.14	293	33
	0.4	0.07	7.11	298	31
	0.5	0.07	7.07	302	30
400	0.0	0.11	7.20	260	127
	0.1	0.07	7.13	308	61
	0.2	0.06	7.07	313	41
	0.3	0.05	7.02	314	35
	0.4	0.05	6.96	314	33
	0.5	0.05	6.90	314	33

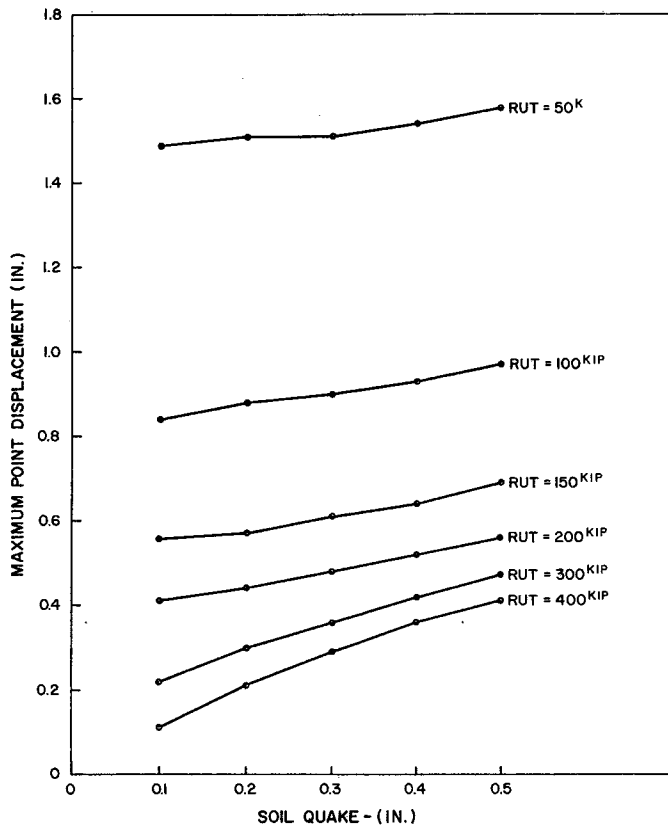


Figure 6.3. Maximum point displacement vs quake (Case BLTP-6; 57.9).

have a tendency to increase as J increases, especially when the soil resistance is large. While the tensile forces still do not follow any definite pattern, they are somewhat more regular than those determined by varying "Q."

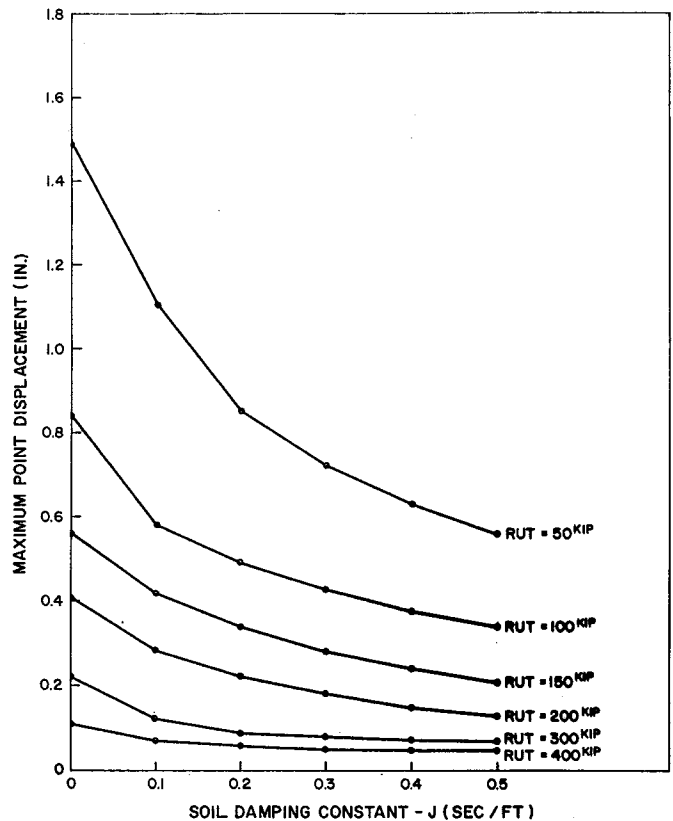


Figure 6.4. Maximum point displacement vs soil damping constant (Case BLTP-6; 57.9).

The maximum point displacements again show the most consistent trend as J is varied, as shown in Figure 6.4. The other cases studied showed this same trend, i.e., as J increases, the maximum displacement decreases rapidly.

Chapter VII

CONCLUSIONS

The correlation between the numerical solution and the experimental data presented in Chapter V indicates the potential accuracy of Smith's method, but the problem involves so many important parameters that it is extremely important to know as much as possible about their actual behavior.

As shown in Chapter III, it is possible to determine valuable information from the wave equation even though exact values for some of these parameters are unknown. For example, several problems can be solved in which the unknown parameter varies between upper and lower limits as was done to determine the effect of the ram's elasticity. This study shows that only for steel on steel impact does the elasticity of the ram affect the solution.

In order to study the Michigan data over 5,000 problems had to be solved because certain key informa-

tion such as the ram velocity was not reported. Still, it was possible to study the behavior of the pile-driving hammers discussed. For example, the efficiency of the cushion assembly was remarkably consistent, in that they were nearly independent of the type of pile, pile length, and soil resistance. The correlation between the wave equation and the field data shown in Chapter III further illustrates that Smith's method is accurate, especially when the required data are known and need not be assumed.

Much of the value of this method of analysis is its flexibility. As illustrated in Chapter III, the wave equation can be used for any number of studies which otherwise would not be possible.

It was shown that the stress-strain curve for a cushion is not a straight line. Instead, it follows a curve which is closely parabolic. However, a straight line

which has a slope equal to that of the true stress-strain curve taken at a point halfway between zero and the maximum strain gives accurate results. The cushion's dynamic coefficient of restitution was found to agree with commonly recommended values.

The effect of internal damping in the concrete and steel piles was shown to be negligible in these cases, although it can be accurately accounted for by the wave equation if desired.

The data from the Michigan Study of Pile Driving Hammers were extrapolated to evaluate the true energy output of different pile driving hammers. It was found that the energy output for all types of hammers (steam

and diesel) can be determined by the simple equation:

$$E = W_R \times h \times e$$

where E = energy output in ft-lb

W_R = ram weight in lb,

h = ram stroke or equivalent stroke in ft,
and

e = hammer efficiency (found to be 60% for the Vul. No. 1, 87% for the Vul. 50C and 80C, and 100% for the diesel hammers investigated by the Michigan Study).

This is believed to be a most significant finding in view of the existing controversy over the manufacturers' rated energies for diesel hammers.

Recommendations

RECOMMENDATIONS FOR FURTHER RESEARCH

The following areas are recommended for further research:

1. A complete evaluation of the data collected by the Michigan State Highway Commission, including correlation of hammer energy, permanent set of pile per blow, etc. This would require a major research effort because of the quantity of data reported. Also, because certain variables were not determined, several theoretical solutions must be solved for each attempt correlation until the unknown parameter can be "pinned down" with reasonable accuracy. For example, the solutions for over 5,000 problems were required to complete the 28-case study made in Chapter III.

2. A study to determine how to improve the effi-

ciency of the pile-driving hammers presently in use. This type of research should be most interesting to the hammer manufacturers since present equipment could be optimized to drive piling faster and/or reduce the driving stresses during driving. The possibility that today's pile-driving hammers are as efficient as possible through trial and error is remote.

3. Further research is needed to insure that the damping models proposed in Chapter IV are also accurate for timber piling, and to determine what damping constants should be used.

4. Major research efforts are needed to investigate every aspect of the soil resistance acting on the pile during driving.

References

1. Smith, E. A. L., "Pile Driving Analysis by the Wave Equation," Proc. ASCE, Aug., 1960, p. 35.
2. Federal Construction Council, "Foundation Piling," Building Research Advisory Board, National Academy of Sciences—National Research Council, Publication 987, 1962, p. 28.
3. Ibid, p. 8.
4. Cummings, A. E., "Dynamic Pile Driving Formulas," *Journal of Boston Soc. of Civil Engrs.*, Jan., 1940.
5. Forehand, P. W. and J. L. Reese, "Pile Driving Analysis Using the Wave Equation," Master of Science in Engineering Thesis, Princeton University, 1963, p. 5.
6. Isaacs, D. V., "Reinforced Concrete Pile Formula," *Inst. Aust. Eng. J.*, Vol. 12, 1931, p. 415.
7. Fox, E. N., "Stress Phenomena Occurring in Pile Driving," *Engineering* (London) Vol. 134, 1932, p. 312.
8. Smith, E. A. L., "Pile Driving Analysis by the Wave Equation," Proc. ASCE, Aug., 1960.
9. Chellis, R. D., "Pile Foundations," McGraw-Hill Book Co., New York, 1951, p. 20.
10. Fox, E. N., "Stress Phenomena Occurring in Pile Driving," *Engineering* (London) Vol. 134, 1932.
11. Taylor, D. W., "Fundamentals of Soil Mechanics," John Wiley & Sons, New York, 1956, p. 770.
12. Isaacs, D. V., "Reinforced Concrete Pile Formula," *Inst. Aust. Eng. J.*, Vol. 12, 1931, p. 312.
13. Fox, E. N., "Stress Phenomena Occurring in Pile Driving," *Engineering* (London) Vol. 134, 1932, p. 263.
14. Glanville, W. H., G. Grime, E. N. Fox, and W. W. Davies, "An Investigation of the Stresses in Reinforced Concrete Piles during Driving," British Bldg. Research Bd. Tech. Paper No. 20, D. S. I. R., 1938.
15. Cummings, A. E., "Dynamic Pile Driving Formula," *Journal of Boston Soc. of Civil Engrs.*, Jan., 1940, p. 6.
16. Smith, E. A. L., "Pile Driving Impact," Proceedings, Industrial Computation Seminar, September, 1950, International Business Machines Corp., New York, N. Y., 1951, p. 44.
17. Smith, E. A. L., "Impact and Longitudinal Wave Transmission," Transactions, ASME, August, 1955, p. 963.
18. Smith, E. A. L., "What Happens When Hammer Hits Pile," *Engineering News Record*, McGraw-Hill Publishing Co., Inc., New York, N. Y., September 5, 1957, p. 46.
19. Smith, E. A. L., "Tension in Concrete Piles During Driving," *Journal*, Prestressed Concrete Institute, Vol. 5, 1960, pp. 35-40.
20. Smith, E. A. L., "The Wave Equation Applied to Pile Driving," Raymond Concrete Pile Co., 1957.
21. Smith, E. A. L., "Pile Calculations by the Wave Equation," *Concrete and Constructional Engr.*, London, June, 1958.
22. Smith, E. A. L., "Pile Driving Analysis by the Wave Equation," Proc. ASCE, Aug., 1960.
23. Smith, E. A. L., "Pile Driving Analysis by the Wave Equation," Transactions, ASCE, Vol. 127, 1962, Part I, p. 1171.
24. Samson, Charles H., Jr., "Pile Driving Analysis by the Wave Equation (Computer Procedure)," Report of the Texas Transportation Institute, Texas A&M University, May, 1962.
25. Samson, Charles H., Jr., "Investigation of Behavior of Piles During Driving, Lavaca Bay Causeway," Unpublished Report of TTI to Texas Highway Dept., 1962.
26. Samson, Charles H., Jr., "Pile Stress Analysis—Harbor Island Bay Bridge," Unpublished Report of the Texas Transportation Institute, July, 1962.
27. Hirsch, T. J., "Stresses in Long Prestressed Concrete Piles During Driving," Report of the Texas Transportation Institute, Texas A&M University, September, 1962.
28. Forehand, P. W. and J. L. Reese, "Pile Driving Analysis Using the Wave Equation," Master of Science in Engineering Thesis, Princeton University, 1963.
29. Samson, C. H., Jr., T. J. Hirsch, and L. L. Lowery, "Computer Study of Dynamic Behavior of Piling," *Journal of the Structural Division*, ASCE, Vol. 89, No. ST4, Proc. Paper 3608, August, 1963.
30. Hirsch, T. J., C. H. Samson, Jr., and L. L. Lowery, "Driving Stresses in Prestressed Concrete Piles," Structural Eng. Conf. of ASCE, San Francisco, Oct., 1963.
31. Hirsch, T. J., "Field Tests of Prestressed Concrete Piles During Driving," Report of the Texas Transportation Institute, Texas A&M University, August, 1963.
32. Hirsch, T. J., "Computer Study of Variables which Affect the Behavior of Concrete Piles During Driving," Report of the Texas Transportation Institute, Texas A&M University, August, 1963.
33. Samson, C. H., Jr., F. C. Bundy, and T. J. Hirsch, "Practical Applications of Stress-Wave Theory in Piling Design," Presented to the annual Texas Section ASCE meeting, San Antonio, Texas, October, 1963.
34. Hirsch, T. J., and C. H. Samson, Jr., "Driving Practices for Prestressed Concrete Piles," Report of the Texas Transportation Institute, Texas A&M University, April, 1965.
35. Hirsch, T. J., "Fundamental Design and Driving Considerations for Concrete Piles," 45th Annual Meeting of Highway Research Board, Washington, D. C., January, 1966.
36. Hirsch, T. J., and Thomas C. Edwards, "Impact Load-Deformation Properties of Pile Cushioning Materials," Report of the Texas Transportation Institute, Texas A&M University, July 1965.

37. Smith, E. A. L., "Pile Driving Impact," Proceedings, Industrial Computation Seminar, September, 1950, International Business Machines Corp., New York, N. Y., 1951.
38. Smith, E. A. L., "Impact and Longitudinal Wave Transmission," Transactions, ASME, August, 1955.
39. Smith, E. A. L., "Pile Driving Analysis by the Wave Equation," Proc. ASCE, Aug., 1960.
40. Forehand, P. W., and J. L. Reese, "Pile Driving Analysis Using the Wave Equation," Master of Science in Engineering Thesis, Princeton University, 1963.
41. Samson, C. H., Jr., T. J. Hirsch, and L. L. Lowery, "Computer Study of Dynamic Behavior of Piling," *Journal of the Structural Division*, ASCE, Vol. 89, No. ST4, Proc. Paper 3608, August, 1963.
42. Smith, E. A. L., "Pile Driving Analysis by the Wave Equation," Transactions, ASCE, Vol. 127, 1962, Part I, p. 1152.
43. Chellis, R. D., "Pile Foundations," McGraw-Hill Book Co., New York, 1951, p. 29.
44. Michigan State Highway Commission, "A Performance Investigation of Pile Driving Hammers and Piles," Office of Testing and Research, Lansing, March, 1965.
45. Housel, W. S., "Pile Load Capacity: Estimates and Test Results," *Journal of the Soil Mechanics and Foundations Division*, ASCE, Proc. Paper 4483, September, 1965.
46. Michigan State Highway Commission, "A Performance Investigation of Pile Driving Hammers and Piles," Office of Testing and Research, Lansing, March, 1965, p. 330.
47. Smith, E. A. L., "Pile Driving Analysis by the Wave Equation," Transactions, ASCE, Vol. 127, 1962, Part I.
48. Forehand, P. W. and J. L. Reese, "Pile Driving Analysis Using the Wave Equation," Master of Science in Engineering Thesis, Princeton University, 1963.
49. Michigan State Highway Commission, "A Performance Investigation of Pile Driving Hammers and Piles," Office of Testing and Research, Lansing, March, 1965, p. 246.
50. Hirsch, T. J., and Thomas C. Edwards, "Impact Load-Deformation Properties of Pile Cushioning Materials," Report of the Texas Transportation Institute, Texas A&M University, July, 1965, p. 1.
51. Smith, E. A. L., "Pile Driving Analysis by the Wave Equation," Transactions, ASCE, Vol. 127, 1962, Part I, p. 1162.
52. Samson, C. H., Jr., T. J. Hirsch, and L. L. Lowery, "Computer Study of Dynamic Behavior of Piling," *Journal of the Structural Division*, ASCE, Vol. 89, No. ST4, Proc. Paper 3608, August, 1963.
53. Hirsch, T. J., and Thomas C. Edwards, "Impact Load-Deformation Properties of Pile Cushioning Materials," Report of the Texas Transportation Institute, Texas A&M University, July, 1965.
54. Hirsch, T. J., and Thomas C. Edwards, "Impact Load-Deformation Properties of Pile Cushioning Materials," Report of the Texas Transportation Institute, Texas A&M University, July, 1965.
55. *Ibid.* p. 29.
56. Samson, C. H., Jr., T. J. Hirsch, and L. L. Lowery, "Computer Study of Dynamic Behavior of Piling," *Journal of the Structural Division*, ASCE, Vol. 89, No. ST4, Proc. Paper 3608, August, 1963.
57. Jacobsen, L. S., "Steady Forced Vibrations as Influenced by Damping," ASME Transactions, Vol. 52, 1930, p. 168.
58. Smith, E. A. L., "Pile Driving Analysis by the Wave Equation," Transactions, ASCE, Vol. 127, 1962, Part I, p. 1167.
59. Samson, C. H., Jr., T. J. Hirsch, and L. L. Lowery, "Computer Study of Dynamic Behavior of Piling," *Journal of the Structural Division*, ASCE, Vol. 89, No. ST4, Proc. Paper 3608, August, 1963, p. 417.
60. *Ibid.* p. 427.
61. *Ibid.* p. 429.
62. Hirsch, T. J., and Thomas C. Edwards, "Impact Load-Deformation Properties of Pile Cushioning Materials," Report of the Texas Transportation Institute, Texas A&M University, July, 1965, p. 21.
63. *Ibid.* p. 20.
64. Samson, C. H., Jr., T. J. Hirsch, and L. L. Lowery, "Computer Study of Dynamic Behavior of Piling," *Journal of the Structural Division*, ASCE, Vol. 89, No. ST4, Proc. Paper 3608, August, 1963, p. 418.
65. Chellis, R. D., "Pile Foundations," McGraw-Hill Book Co., New York, 1951, p. 23.
66. Chan, P. A., "A Laboratory Study of Dynamic Load-Deformation and Damping Properties of Sands Concerned with a Pile-Soil System," a dissertation, Texas A&M University, unpublished, January, 1967.
67. Hirsch, T. J., and Thomas C. Edwards, "Use of the Wave Equation to Predict Pile Load Bearing Capacity," Report of the Texas Transportation Institute, Texas A&M University, unpublished, August, 1966.
68. Samson, C. H., Jr., F. C. Bundy, and T. J. Hirsch, "Practical Applications of Stress-Wave Theory in Piling Design," Presented at the annual Texas Section ASCE meeting, San Antonio, Texas, October, 1963, p. 1162.
69. Rand, Mogens, "Explosion Adds Driving Force to Diesel Hammer," *Engineering Contract Record*, December, 1960.
70. Rand, Mogens, "Test Performed with the Delmag Diesel Hammer, Type D-12," December 13, 1955, Publication of the Department of Mechanical Engineering, University of Toronto.
71. Rand, Mogens, "How the Diesel Pile Hammer Works," *Roads & Streets*, May, 1961.

Appendix A

PROGRAM INPUT DATA

CARD 101 (Required)

ID1 and ID2	— All "ID" values are for identification only and can be either alphabetic or numeric.
1/Δt	— Time interval. If left blank, Δtcr/2 will be used. (1/sec)
MP	— Total number of segments in the system to be analyzed.
VELMI	— Initial velocity of the ram. (ft/sec)
MH	— Element number of the first pile segment.
NR	— Number of divisions of the ram.
EEM(NR)	— Coefficient of Restitution of spring number NR, directly under ram.
EEM(NR+1)	— Coefficient of Restitution of spring number NR+1.
GAMMA(NR)	— The minimum force in the spring beneath the ram once that force has reached a maximum. (kip) For example, if the diesel hammer explosive pressure causes 158.7 kip minimum force in this spring, set GAMMA(NR) = 158.7 kip. If the minimum force the spring can transmit is zero (for example, when no tensile force can exist between the ram and anvil) set the corresponding GAMMA(I) = 0.0. If the spring represents a continuous body such as the spring between any two pile segments, it can transmit tensile forces between the elements. This is signified by setting GAMMA(I) equal to any negative value, usually -1.0 kip.
GAMMA(NR+1)	— Same as above, but for spring number NR+1.
NSTOP	— Total number of time intervals the program is to run.

NOP(I)	VALUE	FUNCTION
NOP(1)		Used to read cards 103-106 and print out the data for problem identification.
	= 1	No identification card is to be used.
	= 2	Read and print a single ID card. (card 103)
	= 3	Read and print two ID cards. (cards 103 and 104)
	= 4	Read and print ID cards 103, 104, and 105.
	= 5	Read and print ID cards 103, 104, 105, and 106.
NOP(2)		Used to specify the input method for the segment weights WAM(I).
	= 1	Read one weight for each segment (card series 200).
	= 2	Read the segment weights for only the first five and last five segments of the pile system from a single card (card 200), and equate all remaining segment weights to the sixth weight in the system. (NOP(2) = 2 is used when a large number of equal weights are present except for the first or last few weights.)

NOP(I)	VALUE	FUNCTION
NOP(3)		Used to specify the input method for the internal spring stiffness. (XKAM(I).
	= 1	Read one stiffness for each internal spring from card series 300.
	= 2	Read the stiffness values for only the first five and last five internal springs on a single card 300, and assign the fifth value to all remaining internal springs. (NOP(3) = 2 is used under the same conditions as NOP(2) = 2.
NOP(4)		Used to specify what soil resistance distribution act along the pile.
	= 1	Read RUM(I) for each element from card series 400, and set the point bearing soil resistance RUM(MP+1) equal to RUP.
	= 2	Set all side resistances equal to zero, and set RUM(MP+1) = RUP.
	= 3	Distribute RUT-RUP uniformly along the side of the pile from segment MO thru MP, and set RUM(MP+L) = RUP.
	= 4	Distribute RUT-RUP triangularly along the pile between segments MO and MP, and set RUM(MP+1) = RUP.
	= 5	Read one 450 series card for each mass upon which a nonlinear resistance vs displacement curve acts. If a linear curve also happens to be acting on an element, it must also be input on a 450 series card.
NOP(5)		Used to specify the input method for GAMMA(I). Note: The significance of GAMMA(I) is discussed in the "500 card series."
	= 1,2	Read GAMMA1 and GAMMA2 from card 101 and assign GAMMA1 to internal spring number NR, and assign GAMMA2 to spring number NR+1. Then set GAMMA(I) of the remaining springs to -1.0.
	= 3	Same as for NOP(5)=2, except that GAMMA(NR+2) is also set equal to 0.0.
	= 4	Same as for NOP(5)=2, except GAMMA(NR+2)=0.0 and GAMMA(NR+3)=0.0. This option is used when a large number of elements such as an anvil, follower, load cell and pile cap are encountered, since these elements cannot transmit a tensile force to the next element. This option can be used to set up to eight consecutive values of GAMMA(I)=0.0 by setting NOP(5)=8.
	= 9	Read GAMMA(I) for each spring from card series 500.

NOP(I)	VALUE	FUNCTION
NOP(6)		Used to specify the input method for EEM(I).
	= 1	Read EEM1 and EEM2 from card 101 set EEM(NR)=EEM1, and EEM(NR+1)=EEM(2). Then set EEM(I) for all other springs equal to 1.0 (perfectly elastic).
	= 2	Read EEM(I) for each spring from card series 600.
NOP(7)		Used to specify the input method for BEEM(I).
	= 1	Set all BEEM(I)=0.0.
	= 2	Read BEEM(I) for each spring from card series 700.
NOP(8)		Used to specify the input method for VEL(I).
	= 1	Read VELMI from card 101 and set VEL(I,t=0) for all segments of the ram (usually one segment) equal to VELMI. Set all other VEL(I)=0.0.
	= 2	Read VEL(I) for each segment from card series 800.
NOP(9)		Used to specify input method for Q(I).
	= 1	Read QSIDE and QPOINT from card 102 and set all Q(I) along side of the pile equal to QSIDE. Set Q(MP+1) under pile tip equal to QPOINT.
	= 2	Read Q(I) for each element including Q(MP+1) from card series 900.
NOP(10)		Used to specify input method for SJ(I).
	= 1	Read SIDEJ and POINTJ from card 102. Set all SJ(I) along side of pile equal to SIDEJ and SJ(MP+1) under pile tip equal to POINTJ.
	= 2	Read SJ(I) for each element including SJ(MP+1) from card series 1000.
NOP(11)		Used to specify the input method for DYNAMK(I).
	= 1	Set all DYNAMK(I)=0.0.
	= 2	Read DYNAMK(I) for each spring from card series 1100.
NOP(12)		Used to specify input method for A(I).
	= 1	Read AREA from card 102 and set all A(I) equal to AREA.
	= 2	Read A(I) for each internal spring from card series 1200.
NOP(13)		Used to specify which method of internal damping is to be used in the pile.
	= 1	Use Smith's method (refer to Figure 5.13b).
	= 2	Use standard linear solid method (refer to Figure 5.13c).
NOP(14)		Used to specify how the force in the cushion after impact is to be determined.
	= 1	Calculate cushion forces from the wave equation applied to the moving ram after impact.

NOP(I)	VALUE	FUNCTION
	= 2	In this case, the force at the head of the pile at all times is known, probably by experimental methods, and this force curve is to be applied at the head of the pile. The force at each time interval FORCIN(t) is read from card series 1300 (kip).
	= 3	Same as when NOP(14)=2, except that galvanometer readings rather than forces at each time interval are input and the cushion forces are determined by the computer. In this case, the information on the 1400 header card is needed, followed by the galvanometer deflection at each time interval from card series 1400.
NOP(15)		Used to specify how gravity is to be accounted for in the solution.
	= 1	The effect of gravity is to be neglected.
	= 2	Gravity is to be considered, with the initial displacement of each segment, D(I,O), and the initial soil resistances RAM(I,O) assumed to be zero.
	= 3	Gravity is to be considered, and D(I,O) and RAM(I,O) are to be approximated by Smith's suggested method. ⁶⁰
	= 4	Gravity is to be considered, and the values for D(I,O) and RAM(I,O) are computed by Samson's suggested method. ⁶¹
NOP(16)		Used to specify the number of problems to be solved using the basic data given on cards 101 through the 1700 card series.
	= 1	Only one problem is to be solved using this set of data.
	= 2	Run more than one problem with changes in these data as specified on card 1600.
NOP(17)		Used to specify whether the ultimate pile capacities predicted by various pile driving equations are desired.
	= 1	No capacities are to be computed.
	= 2	Using the information from card 1700 and the information provided by the wave equation solution, solve for the ultimate resistance to failure as predicted by several popular pile driving equations.

CARD 102 (Required)

ID3	— Identification.
ID4	— Identification.
RUT	— The total static soil resistance acting on the pile (kip).
RUP	— The total static soil resistance acting beneath the point (kip).
MO	— Number of first element upon which soil resistance acts.
QSIDE	— Soil quake along side of pile, if a single value exists. If not, set QSIDE=0.0 (in.).
QPOINT	— Soil quake beneath pile point (in.).
SIDEJ	— Soil damping factor in shear along the side of the pile if a single value exists. If not, set SIDEJ=0.0 (sec/ft).

- POINTJ — Soil damping factor in compression beneath the pile point (sec/ft).
- NUMR — Number of elements for which the soil spring does not have a linear stress-strain curve.
- IPRINT — Print frequency. For example, if the solution at every 5th time interval is wanted, set IPRINT=5.
- AREA — A constant used to convert the forces into stresses or other more convenient values (such as changing lb. to kip by setting AREA=1000.0).
- NS1-NS6 — The element numbers for which solutions vs time interval will be printed. Maximum values and other information are always printed for each element after NSTOP time intervals have elapsed.

CARDS 103-106 (Required only if NOP(1)=2,3,4,5)

If NOP(1)=1, no identification card will be read. If NOP(1)=2, read card 103 containing 72 columns of alphabetic or numeric identification and print this information above the problem. If NOP(1)=3, read and print two identification cards, up to a maximum of four cards (NOP(1)=5).

200 CARD SERIES (Required)

IDW1, IDW2 — Throughout this Input, variables beginning with the letters "ID" are for identification, in this case to help identify what segment weights are being used.

WAM(I) — The weight of element number I (kip). a) If NOP(2)=1, the computer will read MP segment weights, ten segment weights to a card from cards 201-230, up to a maximum of 300 segments. For example, if the system is divided into 37 segments, four 200 series cards must be included in the data: 201 through 204. b) If NOP(2)=2, in this case the pile must have a constant weight per foot along its length. Since the pile is usually divided into equal segment lengths, only a few of the element weights are different. Therefore, only the top five weights (the ram, anvil, . . .) and the bottom five weights (. . ., pile segment, pile point) must be read from the card 200. The computer then sets all other element weights equal to the sixth value punched in the card.

300 CARD SERIES (Required)

IDK1, IDK2 — Identification.

XKAM(I) — The internal spring rate of spring I (kip/in.).
 a) If NOP(3)=1, the computer reads MP-1 spring rates from cards 301-330.
 b) If NOP(3)=2, the first and last five XKAM(I) are read from card 300, and the remaining XKAM(I) are set equal to the sixth XKAM(I) value, i.e., XKAM(MP-4).

400 CARD SERIES (Required if NOP(4)=1)

IDRL1, IDRL2 — Identification.

RUM(I) — The ultimate static resistance of the soil acting on pile segment I (kip). a) If NOP(4)=1, read MP ultimate soil resistances, from cards 401-430, and set RUM(MP+1) equal to RUP.

- b) If NOP(4)=2, set all side friction=0.0 and set RUM(MP+1)=RUP.
- c) If NOP(4)=3, distribute (RUT-RUP) uniformly along the pile starting from segment number MO to number MP, and set RUM(MP+1)=RUP.
- d) If NOP(4)=4, distribute (RUT-RUP) triangularly between MO and MP set RUM(MP+1)=RUP.
- e) If NOP(4)=5, read NUMR cards, each of which can define a linear or nonlinear force-displacement curve for the soil (see card series 450).

450 CARD SERIES (Required if NOP(4)=5)

When NOP(4)=5, the soil resistance vs displacement curve is nonlinear. This requires ten soil resistances to be read for each soil spring, one for each displacement corresponding to a multiple of Q/10. As shown on data card 451, I is the number of the element upon which the nonlinear resistance is acting, XKIM(I) is the unloading spring rate (kip/in.), and R(I,J) are the soil resistances (kip) at each of the displacements Q/10, 2Q/10, . . . , 9Q/10, Q. Whenever NOP(4)=5, one 450 series card is required for each element upon which soil resistance acts.

500 CARD SERIES (Required when NOP(5)=2)

IDG1, IDG2 — Identification.

GAMMA(I) — The minimum force possible in spring I after a peak compressive force has passed, except that any negative GAMMA(I) is construed to mean that that spring can transmit a tensile force of any magnitude (kip).

600 CARD SERIES (Required when NOP(6)=2)

IDE1, IDE2 — Identification.

EEM(I) — The coefficient of restitution for MP-1 internal springs. This determines the slope of the unloading curve (dimensionless).

700 CARD SERIES (Required when NOP(7)=2)

IDB1, IDB2 — Identification.

BEEM(1) — The damping coefficient of the MP-1 internal springs (in. sec/ft).

800 CARD SERIES (Required when NOP(8)=2)

IDV1, IDV2 — Identification.

VEL(I) — The initial velocities of each of the MP weights (ft/sec).

900 CARD SERIES (Required when NOP(9)=2)

IDQ1, IDQ2 — Identification.

Q(I) — The soil "quake" for MP+1 soil springs (in.).

1000 CARD SERIES (Required when NOP(10)=2)

IDJ1, IDJ2 — Identification.

SJ(I) — The soil damping factor for MP+1 soil spring (sec/ft).

1100 CARD SERIES (Required when NOP(11)=2)

IDDK1, IDDK2 — Identification.

DYNAMK(I) — The dynamic spring rate of MP-1 internal springs (kip/in.).

1200 CARD SERIES (Required when NOP(12)=2)

IDA1, IDA2 — Identification.

A(I) — The cross-sectional area of each of the MP-1 internal springs (in.²).

1300 CARD SERIES (Required when NOP(13)=2)

FORCIN(INTV) — The force acting on the head of the pile (kip) at time interval INTV, for NSTOP intervals with a maximum NSTOP equal to 100 time intervals.

- 1400 CARD SERIES (Required when NOP(14)=2)
- CARD 1400 — Header Card.
- APILE — The area of the head of the pile (in.²).
- EMODUL — The modulus of elasticity of the pile (kip/in.²).
- RGAGE — The strain gage resistance (ohm).
- RCAL — Calibration resistance (ohm).
- ACTIVG — Number of active gages.
- GFACTR — Gage factor for the gages used.
- D1 — Displacement of the galvanometer trace when RCAL is thrown into the bridge at the head of the pile (in.).
- D2 Through D5 — Galvo displacements corresponding to RCAL at any other four strain gage points (in.).
- CARDS 1401 UP TO 1410
- DGALVI(INTV) — The galvanometer deflection for the gage at the head of the pile, at interval number INTV (in.).
- CARD 1500 (Required when NOP(15)=4)
- F1 and F2 — Forces known to lie on the true dynamic force vs compression curve of the cushion (kip).
- C1 and C2 — The cushion compressions corresponding to F1 and F2, respectively (in.).
- CARD 1600 (Required when NOP(16)=2)
- NOPP(I) — When a number of cases are to be solved for which only a few parameters will change, NOPP(I) designates which parameter to vary and how many different values it should be assigned. For example: NOPP(1)=5 indicates that five problems are to be solved, for which only the ram's initial velocity will vary. Each NOPP(I) controls a single variable as shown in Table A.1.
- DV1 Through DK1 — These parameters control the percent change in the variables mentioned above. For example, assume

that the effects of ram velocities of 10, 12, 14, 16, 18, and 20 ft/sec are being studied. The value of DV1 would be (12 ft/sec - 10 ft/sec) / 10 ft/sec or DV1=0.20. In this case, NOPP(1) would equal 6 since 6 separate problems are to be run. The variables controlled by DV1 to DK1 are also listed in Table A.1.

TABLE A.1. LIST OF PARAMETER VARIATIONS AND THEIR CONTROLLING OPTIONS

Controlling Option	Per Cent Increase in Original Value	Parameter Controlled
NOPP(1)	DV1	VELMI (Initial ram velocity)
NOPP(2)	DW1	W(1)
NOPP(3)	DW2	W(2)
NOPP(4)	DW1	W(3) through W(MP)
NOPP(5)	DK1	XKAM(1)
NOPP(6)	DK2	XKAM(2)
NOPP(7)	DK1	XKAM(3) through XKAM(MP-1)
NOPP(8)	DQI	QSIDE
NOPP(9)	DQP	QPOINT
NOPP(10)	DJI	SIDEJ
NOPP(11)	DJP	POINTJ
NOPP(12)	DRI	RUT
NOPP(13)	DRP	RUP
NOPP(14)	DRI	RUT & RUP
NOPP(15)	DE1	EEM(1)
NOPP(16)	DE2	EEM(2)

CARD 1700 (Required when NOP(17)=2)

AREAP	Cross-sectional area of pile (in. ²).
XLONG	Length of pile (ft).
ELAST	Modulus of elasticity of pile (kip/in. ²).
CENR	Value for use in ENR pile driving formula.
QAVG	Average ground "Quake" (in.).
WRAM	Ram weight (kip).
WPILE	Pile weight (kip).
ENERGY	Actual energy output of the ram (ft lb).

Appendix B

EXAMPLE PROBLEM

Introduction

The following example problem is given to illustrate the steps necessary to arrive at a solution. In the previous chapters, the functional components involved were discussed separately; for example, the driving hammer, pile, soil properties, etc. However, the input data is more easily handled by grouping according to similar physical quantities rather than functional quantities. For example, one series of cards is used to input all segment weights, another for the spring rates. The order in which the input data is set up for the example problems is by no means unique, but it probably should be followed until the programmer becomes familiar with the operations involved.

It should be noted that any variable without a decimal point (such as MP, MH, NR, NSTOP, and NOP(1) on card 101) is always an integer and must be entered as far to the right in its field as possible. Also, the decimal point does not have to be punched for any variable which has a decimal place already shown on the data sheet unless it is desired to change its position. For example, if the initial ram velocity (IVEL on card 101) is 13.48 ft/sec, the numbers 1, 3, 4, and 8 should be punched in columns 19 through 22, respectively. However, to enter a velocity of 127 ft/sec into IVEL, punch 1, 2, and 7 in columns 19, 20, and 21, and punch a decimal point in column 22.

Except for this last case, decimal points need never be punched.

Example Problem

Since case BLTP-6; 57.9 (from the Michigan Pile Study) was one of the problems most often used in this report, the input data required for its solution will be determined first. Figures 3.3 and 3.4 show the real system and the idealized system.

A. Given Information—Case BLTP-6; 57.9

1. Hammer Data-Vulcan #1
 - a. Manufacturer's Rated Energy = 15,000 ft lb, normal stroke = 3 ft.
 - b. Ram Weight = 5,000 lb, velocity at impact not measured.
 - c. Driving Cap Weight = 1,000 lb.
 - d. Cushion Data = Oak block, 6-1/4 in. deep by 11-1/4 in. in diameter, direction of grain unknown, condition of cushion unknown (somewhere between new and "crushed and badly burnt").
2. Pile Data-CBP 124 H-section
 - a. Area = 15.58 in.².
 - b. Weight = 53 lb/ft.
 - c. Total Length = 72.5 ft.
 - d. Driven Length = 57.9 ft.
 - e. Modulus of Elasticity = 30 x 10⁶.
3. Soil Data
 - a. Ultimate Soil Resistance = 300 kip (static value from load test after soil "set-up").
 - b. From driving log, 75 percent of the soil resistance is assumed point bearing and 25 percent side resistance.

c. Soil damping factor "J" and soil quake "Q"—not known.

4. Miscellaneous Data

- a. Load Cell Weight = 580 lb.
- b. Additional Helmet Weight = 1,080 lb.

B. Input Data Calculations

Card 101

1. ID1—Identification Tag, use BLTP-6
2. ID2—Identification Tag, use 57.9.
3. Segment Lengths—Although segment lengths of 10 ft are usually satisfactory, a 5 ft length will be used to increase the accuracy of the solution.
4. Time Interval—The normal time interval of 1/4000 to 1/5000 iterations/sec must be halved since the normal segment length of 10 ft was reduced by half. Therefore, use $\Delta t = 1/10,000$ sec or $1/\Delta t = 10,000$.
5. MP—The total number of segments as shown in Figure 3.4 is 3 above the pile plus 14 pile segments. Thus, MP = 17.
6. Since the ram velocity at impact was not recorded, the following ram velocities will be studied: IVEL = 8, 12, 16, and 20 ft/sec.
7. MH—The first pile segment weight = 4.
8. NR—Number of divisions of the ram = 1.
9. EEMI—Coefficient of restitution of cushion = 0.4, EEM2—coefficient of restitution of load cell = 1.0.
10. Since springs 1, 2, and 3 cannot transmit tensile forces, GAMMA(1), (2), and (3) are 0.0. The remaining GAMMA (I) are set equal to -1.0. This is done by setting GAMMA1 = GAMMA2 = 0.0 and designating NOP(5) = 3 so that GAMMA(3) will also be set = 0.0.
11. To allow the wave time to make two complete passes up and down the pile, NSTOP is set = 173 iterations. This is found from the velocity of travel of the stress wave and the value of Δt .

$$V_{\text{wave}} = \sqrt{E/p} = \sqrt{\frac{30,000,000}{(0.283/386)}}$$

$$= 202,000 \text{ ips or}$$

$$V_{\text{wave}} = \frac{202,000}{12} = 16,800 \text{ ft/sec.}$$

$$\text{Total distance wave must travel} = 4(72.5) = 290 \text{ ft.}$$

$$\text{Total time required} = \frac{290 \text{ ft}}{16,800 \text{ ft/sec}} = .0173 \text{ sec.}$$

$$\text{NSTOP} = \frac{\text{Total time}}{\Delta t}$$

$$= \frac{.0173 \text{ sec}}{(1/10,000) \text{ sec/iteration}} = 173 \text{ iterations.}$$

Therefore, use NSTOP = 173 iterations.

12. Option Calculations—NOP(I)

- a. NOP(1)—No header cards to be read in and printed out, so $NOP(1) = 1$.
- b. NOP(2)—Read segment weights from card series 200 (long form), so $NOP(2) = 1$.
- c. NOP(3)—Read spring constants from card series 300 (long form), so $NOP(3) = 1$.
- d. NOP(4)—Assume triangular soil distribution along the side of the pile, so $NOP(4) = 4$.
- e. NOP(5)—Since $GAMMA(3)$ is to be set equal to 0.0, $NOP(5) = 3$.
- f. NOP(6)—Since all the internal springs are considered perfectly elastic, except for the first one or two for which values of "c" are given by EEM1 and EEM2, set $NOP(6) = 1$ (short form, no series 600 cards).
- g. NOP(7)—Assume zero internal damping in the steel pile, thus set $NOP(7) = 1$ and do not include the 700 card series.
- h. NOP(8)—Only the ram has an initial velocity, so $NOP(8) = 1$, no 800 card series.
- i. NOP(9) and NOP(10)—Since more exact soils information is not available, Smith's recommended values for Q and J will be used and input on card 102 (short form). Thus, $NOP(9) = NOP(10) = 1$.
- j. NOP(11)—No damping, set $NOP(11) = 1$.
- k. NOP(12)—Use a single factor to change force to stress for all springs— $NOP(12) = 1$.
- l. NOP(13)—Use the damping procedure illustrated in Figure 5.13(a), so $NOP(13) = 1$.
- m. NOP(14)—Calculate the force at the pile head from the action of the ram so $NOP(14) = 1$.
- n. NOP(15)—Neglect gravity effects— $NOP(15) = 1$.
- o. NOP(16)—Since several parameters are to be varied, set $NOP(16) = 2$, thus card 1600 must be included in the data.
- p. NOP(17)—Do not calculate driving resistance predicted by pile driving equations. $NOP(17) = 1$.

Card 102

1. ID3—Identification Tag, use 12H53.
2. ID4—Identification Tag, use L = 72.
3. RUT—Since the Michigan Report noted a soil "set-up" of about 2.0, the static resistance actually encountered during driving was probably around half of the measured 400 kip, so $RUT = 200$ kip.
4. RUP—Assuming 75 percent of the total soil resistance at the point, $RUP = 150$ kip.

5. MO—Since the length of pile in the ground was 57.9 ft, the first segment upon which soil resistance acts is given by:

$$MO = MP + 1 - \left(\frac{\text{Depth Driven}}{\text{Segment Length}} \right)$$

$$= 17 + 1 - \frac{57.9}{5.0}$$

$$= 18 - 11.6$$

$$= 18 - 12$$

so $MO = 6$

6. QSIDE and QPOINT—Smith's recommended value of 0.1 in. will be used due to lack of better soils data.
7. SIDEJ and POINTJ—For the same reasons above for values of Q, use $SIDEJ = 0.05$ sec/ft and $POINTJ = 0.15$ sec/ft.
8. NUMR—Since the soil springs all act as shown in Figure 6.1(a), $NUMR = 0$.
9. Set IPRINT = 5 to print out the solution at every 5th iteration.
10. AREA—A single factor will be used to change all forces from lb to kip, thus $AREA = 1000.0$.
11. NS1 through NS6—In this case, the solutions for segments 1, 2, 3, 4, 11, and 17 are desired and, therefore, NS1 through NS6 are given these values.

Cards 201-202

Segment Weights—As shown in Figure 3.4, several weights normally present during driving have been added between the pile and the driving cap to obtain experimental data.

- a. $W(1) = \text{ram weight} = 5.0$ kip.
- b. $W(2) = \text{driving cap weight} + \frac{1}{2}$ of the load cell weight = 1.29 kip.
- c. $W(3) = \frac{1}{2}$ load cell weight + helmet = 1.37 kip.
- d. $W(4)$ through $W(17) = \text{pile segment weights} = (53 \text{ lb/ft}) (5 \text{ ft}) = 0.265$ kip.

Cards 301-302

Segment Stiffness

- a. Because of the lack of data concerning cushion stiffness, several values of $K(1)$ will be run: $K(1) = 500, 1,000,$ and $1,500$ kip. in.
- b. The helmet was found to be extremely stiff compared to the load cell, so $K(2)$ was taken as the stiffness of the load cell alone. From dimensions of the load cell given in the Michigan Report and using $K = AE/L$, the spring rate of the load cell was found to be 86,500 kip/in.
- c. The spring rate of each 5 ft pile segment is found by:

$$K = \frac{AE}{L} = \frac{(15.58) (30 \times 10^3)}{5 \times 12}$$

$$= 7,790 \text{ kip/in.}$$

So $K(3)$ through $K(16) = 7,790$ kip/in.

Card 1600

1. Parameter Options—NOPP(I)—Note that all values of NOPP(I) are set = 1 except when an option is used to vary its assigned parameter, in which case NOPP(I) can equal 2 through 9.
 - a. Since IVEL is to be given the four values of 8, 12, 16, and 20 ft/sec, NOPP(1) = 4.
 - b. NOPP(2) through NOPP(4) = 1 since no segment weights are to be varied.
 - c. NOPP(5) = 3 since three different cushion stiffnesses are to be used (K(1) = 500, 1,000, and 1,500 kip/in.)
 - d. NOPP(6) through NOPP(7)—1 since no other parameter changes are required.

2. Parameter Change Constants—DV1, DE1, DE2, etc. These values specify the desired increase in a given parameter based on the parameter's original value. They may be calculated from the equation:

$$\text{Constant} = \frac{\text{Second Value} - \text{Initial Value}}{\text{Initial Value}}$$

Thus, since the initial value of IVEL is 8 ft/sec and the second value is 12 ft/sec

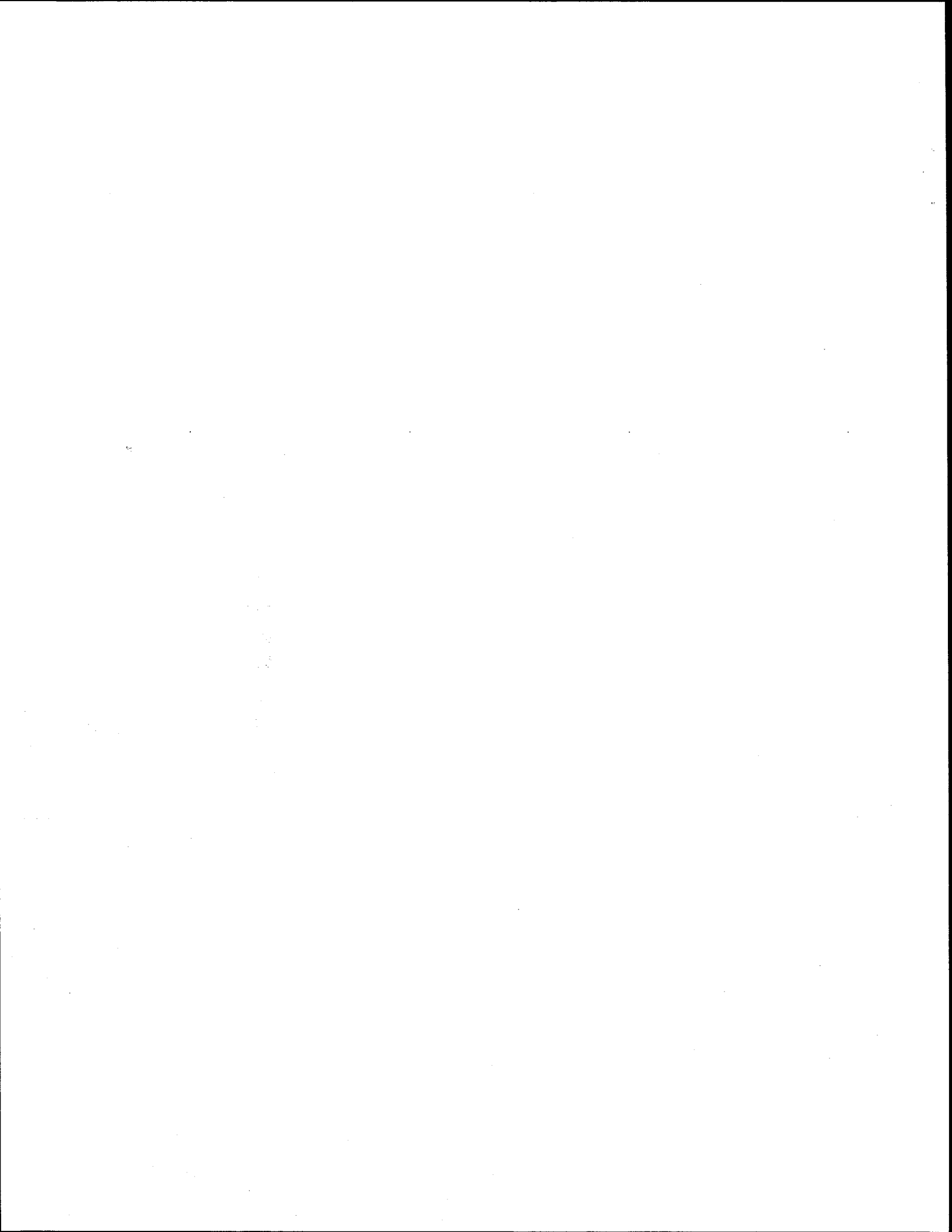
$$DV1 = \frac{12-8}{8} = \frac{4}{8} = 1.0$$

The value for DK1 is therefore given by

$$DK1 = \frac{1000-500}{500} = \frac{500}{500} = 1.0$$

All other values such as DW1, DW2, etc., may be left blank or given any value for later use since they are not used as long as the corresponding NOPP(I) = 1.

Appendix C
PROGRAM LISTING



```

$EXECUTE      IBJOB
$IBJOB
$IBFTC MAIN
C - PROGRAM CONSISTS OF APPROXIMATELY 1200 LINES OUTPUT
C - LINES/PROBLEM = 50 +2*MP +NSTOP/IPRINT (UNLESS J5 CHANGES)
C - RUN TIME FOR PROGRAM IS ABOUT 1 MINUTE
C - RUM TIME FOR ONE PROBLEM IS ABOUT = (MP*NSTOP)/60,000 (MINUTES)
C NOP(1) = 0,1,NO IDENTIFICATION CARDS (SERIES 103)
C          = 2, READ IDENTIFICATION CARD 103 (72 COLS OF ALPHAMERIC POOP)
C          = 3, READ 2 IDENTIFICATION CARDS
C          = 4, ETC. UP TO 4 CARDS
C NOP(2) = 0
C          = 1,READ NEW WAM(I),I=1,MP
C          = 2, READ CARD 200 MAXIMUM DIFFERENT WAM(I) = TEN
C NOP(3) = 0
C          = 1,READ NEW XKAM(I),I=1,N
C          = 2, READ CARD 300 MAXIMUM DIFFERENT XKAM(I) = TEN
C NOP(4) = 0,USE OLD SOIL RESISTANCE VALUES,STANDARD OR GENERAL METHOD
C          = 1,READ NEW STANDARD RUM(I),I=1,MPP
C          = 2,ZERO SIDE RESISTANCE, SET RUM(MPP) = RUT
C          = 2,ZERO SIDE RESISTANCE, SET RUM(MPP) = RUP
C          = 3,UNIFORM SIDE RESISTANCE(RUT-RUP) WITH RUM(MPP) = RUP
C          = 4,TRIANGULAR SIDE RESISTANCE(RUT-RUP) WITH RUM(MPP) = RUP
C          = 5,READ NUMR CARDS AND USE GENERAL SOIL BEHAVIOR ROUTINE
C NOP(5) = 0,USE OLD GAMMA(I)
C          = 1,2 SET GAMMA(NR)=GAMMA1 AND GAMMA(NR+1)=GAMMA2 (SOP)
C          = 3, USE SOP ABOVE AND SET GAMMA(NR+2) = 0.0
C          = 4, USE SOP ABOVE AND SET GAMMAS(NR+2) AND (NR+3) = 0.0
C          = 4, ETC.
C          = 9, USE LONG FORM INPUT
C          NOTE THAT NOP(5) IS USED TO SET ADDITIONAL GAMMA(I)S = 0.0
C NOP(6) = 0, USE OLD EEM(I),I=1,N
C          = 1,USE SHORT FORM INPUT
C          = 2, USE LONG FORM INPUT
C NOP(7) = 0, USE OLD BEEM(I), I=1,N

```

```
C          = 1,USE SHORT FORM INPUT
C          = 2, USE LONG FORM INPUT
C  NOP(8)  = 0,USE OLD VEL(I), I=1,MP
C          = 1,USE SHORT FORM INPUT
C          = 2, USE LONG FORM INPUT
C  NOP(9)  = 0,USE OLD Q(I), I=1,MPP
C          = 1,USE SHORT FORM INPUT
C          = 2, USE LONG FORM INPUT
C  NOP(10) = 0,USE OLD SJ(I), I=1,MPP
C          = 1,USE SHORT FORM INPUT
C          = 2, USE LONG FORM INPUT
C  NOP(11) = 0,USE OLD DYNAMK(I), I=1,N
C          = 1,DYNAMK=0.0
C          = 2, USE LONG FORM INPUT
C  NOP(12) = 0,USE OLD A(I), I=1,N
C          = 1,USE SHORT FORM INPUT
C          = 2, USE LONG FORM INPUT
C  NOP(13) = 0,1,USE SMITHS EEM ROUTINE
C          = 2, USE LINEAR SOLID DAMPING
C  NOP(14) = 0,1,USE FOM(MI) COMPUTED FROM RAMS BEHAVIOR
C          = 2, READ NSTOP VALUES OF FORCIN(INTV) (CARD SERIES 1300)
C          = 3,READ HEADER CARD + NSTOP GALVO DEFLECTIONS(IN.) CARDS 1400
C          = 4,READ CARD 1500 AND USE PARABOLIC FOM(1) VS. CEEM(1)
C  NOP(15) = 1,NO GRAVITY
C          = 2,GRAVITY WITH DEM(I,0) = 0.0
C          = 3,GRAVITY WITH DEM(I,0) BY SMITH
C          = 4,GRAVITY WITH DEM(I,0) BY EXACT
C          = 5,GRAVITY WITH DEM(I,0) AS USED FOR PREVIOUS PROBLEM
C  NOP(16) = 0,1,NO PARAMETER CHANGES
C          = 2, READ CARD 1600 WITH PARAMETER CHANGES
C  NOP(17) = 0,1,NO PILE DRIVING FORMULA OUTPUT
C          = 2, READ CARD 1700 WITH PILE DRIVING CONSTANTS
C
C
C  NUMBER OF CASES = NOPP(1)*NOPP(2)* ... * NOPP(14)
```

C
 C NOPP(1) = 1, RAM VELOCITY = VELMI
 C = 2, RAM VELOCITY=VELMI,(1.0+DV1)*VELMI
 C = 3, RAM VELOCITY=VELMI,(1.0+DV1)*VELMI,(1.0+2.*DV1)*VELMI
 C = 4, ETC.
 C NOPP(2) = WAM(1) CHANGE
 C NOPP(3) = WAM(2) CHANGES
 C NOPP(4) = WAM(3,MP) CHANGES
 C NOPP(5) = XKAM(1) CHANGES
 C NOPP(6) = XKAM(2) CHANGES
 C NOPP(7) = XKAM(3,N) CHANGES
 C NOPP(8) = QSIDE CHANGES
 C NOPP(9) = QPOINT CHANGES
 C NOPP(10) = SIDEJ CHANGES
 C NOPP(11) = POINTJ CHANGES
 C NOPP(12) = RUM(1,MP) CHANGES
 C NOPP(13) = RUM(MPP) CHANGES
 C NOPP(14) = BOTH RUM(1,MP) AND RUM(MPP) CHANGE
 C NOPP(15) = EEM(1) CHANGES
 C NOPP(16) = EEM(2) CHANGES

C
 C
 C

COMMON	WAM(100),	XKAM(100),	RUM(100),	BEEM(100),	EEM(100)	1		
COMMON	GAMMA(100),	XKIM(100),	CEEMAS(100),	NFOM(100),	XDEM(100)	2		
COMMON	DEM(100),	XCEEM(100),	CEEM(100),	FOM(100),	XFOM(100)	3		
COMMON	VEL(100),	DIM(100),	RAM(100),	RMAX(100),	RSTAT(100)	4		
COMMON	R(100,10)	, ITRIG(100),	Q(100),	FORCIN(100),	DFOM(100)	5		
COMMON	FOMAX(100),	IFOMAX(100),	FOMIN(100),	IFOMIN(100),	A(100)	6		
COMMON	DEMAX(100),	IDEMAX(100),	SJ(100),	NOP(22),	DYNAMK(100)	7		
COMMON	CEEMIN(100),	HOLDEM(100),	ANSVEC(50),	SE(50,51)	, IROW(51)	8		
COMMON	RUMA(100),	WAMC(100),	XKAMC(100),	QA(100),	SJA(100)	9		
COMMON	ICOL(51),	NOPP(20),	ENTHRU(100),	ENTMAX(100),	IDS(50)	10		
COMMON	QSIDE	, QPOINT,	SIDEJ	, POINTJ,	NQDIV	, NORAMS,	NSTOP	50
COMMON	INTV	, ISECTN,	NUMR	, F1	, F2	, C1	, C2	51

```

COMMON IPRINT, DELTEE, EEM1 , EEM2 , GAMMA1, GAMMA2, INT          52
COMMON INTT , I , ITST , IX , NR , MO , MP                      53
COMMON NPAGE , N , QUAKE , RUP , RUT , VELMI , ID1              54
COMMON ID2 , ID3 , ID4 , IDW1 , IDW2 , IDK1 , IDK2             55
COMMON IDRL1 , IDRL2 , IDG1 , IDG2 , IDE1 , IDE2 , IDB1        56
COMMON IDB2 , IDV1 , IDV2 , IDQ1 , IDQ2 , IDJ1 , IDJ2          57
COMMON IDDK1 , IDDK2 , IDA1 , IDA2 , KGRADD, J5 , TMIN          58
COMMON TMAX , SMIN , SMAX , NOPNTS, AREA , NS1 , NS2,NS6       59
COMMON NS3 , NS4 , NS5 , IDEEM , MH , VEL1 , ACCEL R           60
COMMON B , C , AREAP , XLONG , ELAST , ACELMX                  61
COMMON DV1,DE1,DE2,DRI,DRP,DQI,DQP,DJI,DJP,DW1,DW2,DWI,DK1,DK2,DKI

```

C
C
C
C

```

NPAGE = 0
9 CONTINUE
NS1 = 0
CALL INPUT
MP = MP
MO = MO
NR = NR
MH = MH
N = MP - 1
MPP = MP + 1

```

C

INITIALIZE PARAMETER CONSTANTS

```

DELTA A = DELTEE
WAMA = WAM(1)
WAMB = WAM(2)
XKAMA = XKAM(1)
XKAMB = XKAM(2)
DO I I=1,MP
RUMA(I) = RUM(I)
WAMC(I) = WAM(I)
XKAMC(I) = XKAM(I)

```

```
QA(I) = Q(I)
SJA(I) = SJ(I)
1 CONTINUE
NOPA = NOPP( 1)
NOPB = NOPP( 2)
NOPC = NOPP( 3)
NOPD = NOPP( 4)
NOPE = NOPP( 5)
NOPF = NOPP( 6)
NOPG = NOPP( 7)
NOPH = NOPP( 8)
NOPI = NOPP( 9)
NOPJ = NOPP(10)
NOPK = NOPP(11)
NOPL = NOPP(12)
NOPM = NOPP(13)
NOPN = NOPP(14)
NOPO = NOPP(15)
NOPQ = NOPP(16)
```

C

```
DO 98 IQ = 1,NOPQ
DO 98 IO = 1,NOPO
11 DO 98 IN = 1,NOPN
IM = IN
IL = IN
DO 98 IK = 1,NOPK
DO 98 IJ = 1,NOPJ
DO 98 II = 1,NOPI
DO 98 IH = 1,NOPH
DO 98 IG = 1,NOPG
DO 98 IF = 1,NOPF
DO 98 IE = 1,NOPE
DO 98 ID = 1,NOPD
DO 98 IC = 1,NOPC
DO 98 IB = 1,NOPB
```

BEGIN PARAMETER VARIATIONS

```

DO 98 IA = 1,NOPA
DELTEE = DELTAA
DO 4 I=1,MP
VEL(I) = 0.0
WAM(I) = WAMC(I)      *(1.0 + FLOAT(ID-1) * DWI)
XKAM(I) = XKAMC(I)   *(1.0 + FLOAT(IG-1) * DK1)
Q(I) = QA(I)         *(1.0 + FLOAT(IH-1) * DQ1)
SJ(I) = SJA(I)      *(1.0 + FLOAT(IJ-1) * DJ1)
RUM(I) = RUMA(I)    *(1.0 + FLOAT(IL-1) * DRI)
4 CONTINUE
DO 3 I=1,NR
VEL(I) = VELMI      *(1.0 + FLOAT(IA-1) * DV1)
3 CONTINUE
VEL1 = VEL(1)
WAM(1) = WAMA      *(1.0 + FLOAT(IB-1) * DW1)
WAM(2) = WAMB      *(1.0 + FLOAT(IC-1) * DW2)
XKAM(1) = XKAMA    *(1.0 + FLOAT(IE-1) * DK1)
XKAM(2) = XKAMB    *(1.0 + FLOAT(IF-1) * DK2)
Q(MPP) = QPOINT    *(1.0 + FLOAT(II-1) * DQP)
SJ(MPP) = POINTJ   *(1.0 + FLOAT(IK-1) * DJP)
RUM(MPP) = RUP     *(1.0 + FLOAT(IM-1) * DRP)
EEM(NR) = EEM1     *(1.0 + FLOAT(IO-1) * DE1)
EEM(NR+1) = EEM2   *(1.0 + FLOAT(IQ-1) * DE2)
IF(NOP(4)-5)13,16,13
13 DO 15 I=1,MPP
15 XKIM(I) = RUM(I)/Q(I)
16 CONTINUE
C IF DELTEE IS LEFT BLANK, 1/2 THE CRITICAL TIME INTERVAL WILL BE USED
IF(DELTEE)32,32,31
32 DO 33 I=1,N
33 DELTEE = AMAX1(DELTEE,39.296*SQRT(XKAM(I)/WAM(I)),
1          39.296*SQRT(XKAM(I)/WAM(I+1)))
31 CONTINUE
C
END PARAMETER VARIATIONS
C1PC2 = 0.0

```



```

ACELMX = 0.0
CALL PRINT 1
CALL REP 1
J5 = IPRINT
KXT=1
INTV = 0
INTT =1
MP = MP
N = MP-1
MPP = MP+1
NOP15P = NOP(15)+1
GO TO(50,50,49,48,47,43,50,50,50),NOP15P
43 DO 42 I = 1,MP
42 DEM(I) = HOLDEM(I)
44 RAM(MP) = DEM(MP)*XKIM(MP)
RAM(MP+1) = DEM(MP)*XKIM(MP+1)
HOLDEM(MP) = DEM(MP)
HOLDEM(1) = DEM(1)
CEEM(1) = DEM(1) - DEM(2)
FOM(1) = CEEM(1)*XKAM(1)
DO 45 I = 2,N
HOLDEM(I) = DEM(I)
CEEM(I) = DEM(I)-DEM(I+1)
FOM(I) = CEEM(I)*XKAM(I)
45 RAM(I) = FOM(I-1)-FOM(I)+WAM(I)
GO TO 49
47 CALL EXACTG
GO TO 49
48 CALL SMITH
49 CONTINUE
WRITE(6,8002)(DEM(I),I=1,MP)
WRITE(6,8001)(DIM(I),I=1,MP)
WRITE(6,8003)(FOM(I),I=1,MP)
WRITE(6,8004)(CEEM(I),I=1,N)
WRITE(6,8005)(RAM(I),I=1,MPP)

```

```

WRITE(6,8006)(XKIM(I),I=1,MPP)
50 CONTINUE
NSM = MP-1
NSM=MINO(NS6,NSM)
WRITE(6,1104)NS1,NS2,NS3,NS4,NS5,NSM,NS1,NS2,NS3,NS4,NS5,NS6,MPP
C BEGIN ITERATION LOOP
12 CALL REP N
INTT=INTT
GO TO(22,9 ),INTT
22 CONTINUE
CMAX = 0.0
DO 24 I=NR,N
24 CMAX = CMAX+CEEM(I)
C1PC2 = AMAX1(C1PC2,CMAX)
IF(INTV-999)25,23,25
23 J5 = 25
25 CONTINUE
IF(((INTV/J5)*J5)-INTV)94,26,94
26 CONTINUE
27 FOMA = FOM(NS1)/A(NS1)
FOMB = FOM(NS2)/A(NS2)
FOMC = FOM(NS3)/A(NS3)
FOMD = FOM(NS4)/A(NS4)
FOME = FOM(NS5)/A(NS5)
FOMF = FOM(NSM)/A(NSM)
RAMP = RAM(MP)/1000.0
C WRITE(6,99)INTV ,FOMA,FOMB,FOMC,FOMD,FOME, CEEM(1),DEM(NS3),
C 1 DEM(NS4),DEM(NS5),DEM(NS5P),(ENTHRU(I),I=2,4),ENTHRU(N),ACCEL R
WRITE(6,99)INTV,FOMA,FOMB,FOMC,FOMD,FOME,FOMF,DEM(NS1),DEM(NS2),
1DEM(NS3),DEM(NS4),DEM(NS5),DEM(NS6),RAMP
94 CONTINUE
IF(INTV-NSTOP )12,14,14
14 WRITE(6,105)
MP = MP
N = MP-1

```

```

MH = MH
DO 20 I=1,N
FOMAX(I) = FOMAX(I)/A(I)
FOMIN(I) = FOMIN(I)/A(I)
WRITE(6,106)I,IFOMAX(I),FOMAX(I),IFOMIN(I),FOMIN(I),
1      ENTHRU(I),ENTMAX(I)
20 CONTINUE
C      BLOWS = 1.0/DIM(MP)          OLD STATEMENT
C      WRITE(6,2107)DIM(MP),BLOWS  OLD STATEMENT
      WRITE(6,2108)DEMAX(MH-1),DEMAX(MP)
      SMIN = SMIN/12.0
      SMAX = SMAX/12.0
      ERES1 = SQRT(SMIN/SMAX)
      WRITE(6,109)SMIN,SMAX,ERES1
      EINPUT = (WAM(1)*VEL1**2)/64.4
      WRITE(6,110)EINPUT
      WRITE(6,111)ACELMX
C
C      BEGIN ULTIMATE LOAD FORMULAS
      IF(NOP(17)-1)98,98,5
5 CONTINUE
      C4 = 0.1
      AEL = AREAP*ELAST/XLONG
      NRP = NR+1
      C3 = QAVG
      S = DIM(MPP)
      W = WRAM
      U = ENERGY
      P = WPILE
      RWAVE = 0.0
      DO 6 I=1,MPP
      RWAVE = RWAVE+RUM(I)/1000.0
6 CONTINUE
      SEGL = XLONG/(FLOAT(MP-MH+1))
      SUMR = 0.0
      DO 10 I=MH,MP

```

```

10 SUMR = SUMR+RUM(I)*SEGL*(FLOAT(I -MH)+0.5)
    SUMR = SUMR+RUM(MPP)*XLONG
    HILEYL = SUMR/RWAVE
    RENEWS = U/(S+CENR)
    REYTEL = U/(S+(C4*P/W))
    RTERZG = AEL*(-S+SQRT(S**2+(2.0*U*(W+P*EEM1**2)/(AEL*(W+P))))))
    REDTEN = AEL*(-S+SQRT(S**2+(2.0*U*W/(AEL*(W+P))))))
    RHILYD = AEL*(-(S+C3)+SQRT((S+C3)**2+(2.0*U*(W+P*EEM1**2)/
1      (AEL*(W+P))))))
    RHILYC=U*(W+P*EEM1**2)/((S+0.5*(C1PC2+C3))*(W+P))
    RCOAST = (AEL/2.)*(-S+SQRT(S**2+(4.*U*(W+P*EEM1**2)/(AEL*(W+P))))))
    WRITE(6,107)
    WRITE(6,108)RENEWS,REYTEL,RTERZG,REDTEN,RHILYD,RHILYC,RCOAST,RWAVE
C                                     END ULTIMATE LOAD FORMULAS

```

```

98 CONTINUE
GO TO 9

```

```

99 FORMAT(1X,I3,6F9.2,6F9.3,F9.1)

```

```

C 99 FORMAT(1X, I3, 5F10.2, 5F11.7,F9.1)

```

```

105 FORMAT(1H0,/, 18X, 63HMAXIMUM COMPRESSIVE AND TENSILE STRESSES (
1PSI) IN THE SEGMENTS ,/,19X, 7HSEGMENT , 1X, 5H TIME ,
2 3X, 6HSTRESS , 5X, 4HTIME,3X,6HSTRESS,7X,6HENTHRU,7X,
3 10HMAX ENTHRU , //)

```

```

106 FORMAT(20X,I4,I8,F9.1,I9,F9.1,2F13.1)

```

```

107 FORMAT( 16X,30H ULTIMATE PILE LOADS (KIPS) )

```

```

108 FORMAT( 21X,25H BY ENG NEWS FORMULA = , F15.3,/ ,

```

```

1 22X,25H BY EYTELWEIN = , F15.3,/ ,

```

```

2 22X,25H BY TERZAGHI = , F15.3,/ ,

```

```

3 22X,25H BY REDTENBACHER = , F15.3,/ ,

```

```

4 22X,25H BY HILEY (DUNHAM) = , F15.3,/ ,

```

```

5 22X,25H BY HILEY (CHELLIS) = , F15.3,/ ,

```

```

6 22X,25H BY PACIFIC COAST = , F15.3,/ ,

```

```

7 22X,25H BY THE WAVE EQUATION = , F15.3)

```

```

109 FORMAT(17X,7HSMIN = F10.1, 7HSMAX = F10.1, 10HERES(1) = F10.7)

```

```

110 FORMAT(16X,18H EINPUT (FT LBS) = F9.1)

```

```

111 FORMAT(16X,24H MAX ACCELERATION (GS) = F9.1)

```

```

1104 FORMAT(3H T,6(6X,1HF,I2),1X, 6(6X,1HD,I2) ,6X,1HR,I2,/)
C1104 FORMAT(115H TIME F(1) F(2) F(3) F(4) F(5) D(2) D(3) D(
C 14) D(5) D(P) ENT(2) ENT(3) ENT(4) ENT(N) ACC(MH-1) )
C1104 FORMAT(5H TIME,5(2X,4HFOM( I3, 1H) ) ,5(3X,4HDEM( I3, 1H) ) ,
C 1 3X, 12HENTHRU (1) //)
2107 FORMAT(1H / ,17X,24HPERMANENT SET OF PILE = F13.8,8H INCHES/
1 ,17X,27HNUMBER OF BLOWS PER INCH = F13.8)
2108 FORMAT(1H / ,17X,24HLIMSET FOR (MH-1) = F13.8,8H INCHES/
1 ,17X,27HMAX DISPLACEMENT OF POINT= F13.8)
8001 FORMAT(33HOINITIAL VALUES FOR DIM(I),I=1,MP /(6E19.8))
8002 FORMAT(33HOINITIAL VALUES FOR DEM(I),I=1,MP /(6E19.8))
8003 FORMAT(33HOINITIAL VALUES FOR FOM(I),I=1,MP /(6E19.8))
8004 FORMAT(33HOINITIAL VALUES FOR CEEM(I),I=1,N /(6E19.8))
8005 FORMAT(35HOINITIAL VALUES FOR RAM(I),I=1,MP+1 /(6E19.8))
8006 FORMAT(38HOCONSTANT VALUES FOR XKIM(I),I=1,MP+1 /(6E19.8))
END

```

\$IBFTC INPUT

SUBROUTINE INPUT

```

COMMON WAM(100), XKAM(100), RUM(100), BEEM(100), EEM(100) 1
COMMON GAMMA(100), XKIM(100),CEEMAS(100), NFOM(100), XDEM(100) 2
COMMON DEM(100), XCEEM(100), CEEM(100), FOM(100), XFOM(100) 3
COMMON VEL(100), DIM(100), RAM(100), RMAX(100), RSTAT(100) 4
COMMON R(100,10) , ITRIG(100), Q(100),FORCIN(100), DFOM(100) 5
COMMON FOMAX(100),IFOMAX(100), FOMIN(100),IFOMIN(100), A(100) 6
COMMON DEMAX(100),IDEMAX(100), SJ(100), NOP( 22),DYNAMK(100) 7
COMMON CEEMIN(100),HOLDDEM(100),ANSVEC( 50),SE(50,51) , IROW( 51) 8
COMMON RUMA(100), WAMC(100), XKAMC(100), QA(100), SJA(100) 9
COMMON ICOL( 51), NOPP( 20),ENTHRU(100),ENTMAX(100), IDS( 50) 10
COMMON QSIDE , QPOINT, SIDEJ , POINTJ, NQDIV , NGRAMS, NSTOP 50
COMMON INTV , ISECTN, NUMR , F1 , F2 , C1 , C2 51
COMMON IPRINT, DELTEE, EEM1 , EEM2 , GAMMA1, GAMMA2, INT 52
COMMON INTT , I , ITST , IX , NR , MO , MP 53
COMMON NPAGE , N , QUAKE , RUP , RUT , VELMI , ID1 54
COMMON ID2 , ID3 , ID4 , IDW1 , IDW2 , IDK1 , IDK2 55
COMMON IDRL1 , IDRL2 , IDG1 , IDG2 , IDE1 , IDE2 , IDB1 56

```

```

COMMON IDB2 , IDV1 , IDV2 , IDQ1 , IDQ2 , IDJ1 , IDJ2      57
COMMON IDDK1 , IDDK2 , IDA1 , IDA2 , KGRADD, J5 , TMIN      58
COMMON TMAX , SMIN , SMAX , NOPNTS, AREA , NS1 , NS2,NS6    59
COMMON NS3 , NS4 , NS5 , IDEEM , MH , VEL1 , ACCELR        60
COMMON B , C , AREAP , XLONG , ELAST , ACELMX              61
COMMON DV1,DE1,DE2,DRI,DRP,DQI,DQP,DJI,DJP,DW1,DW2,DWI,DK1,DK2,DKI

```

C

```

READ(5,100)ID1,ID2,DELTEE,MP,VELMI,MH,NR,EEM1,EEM2,GAMMA1,
1 GAMMA2,NSTOP,(NOP(I),I=1,20)
READ(5,101)ID3,ID4,RUT,RUP,MO,QSIDE,QPOINT,SIDEJ,POINTJ,NUMR,
1 IPRINT,AREA,NS1,NS2,NS3,NS4,NS5,NS6
RUT = RUT*1000.0
RUP = RUP*1000.0
NR = MAX0(NR,1)
N = MP-1
MPP = MP+1
WAM(MPP) = -0.0
XKAM(MP) = -0.0
XKAM(MPP) = -0.0
IF(NOP(1)-2)9,7,7
7 NOIDS = 12*(NOP(1)-1)
READ(5,103)(IDS(I),I=1,NOIDS)
9 CONTINUE
IF(NOP(2)-1) 1,1,14
1 READ(5,102)IDW1,IDW2,(WAM(I),I=1,MP)
GO TO 2
14 NRP1 = NR+1
NRP5 = NR+5
NRP6 = NR+6
MPM3 = MP-3
READ(5,111)IDW1,IDW2,WAM(1),(WAM(I),I=NRP1,NRP5),
1 (WAM(I),I=MPM3,MP)
111 FORMAT(A5,A4,-3P10F6.4)
DO 76 I=1,NR
76 WAM(I) = WAM(1)

```

```

DO 77 I=NRP6,MPM3
77 WAM(I) = WAM(NRP5)
2 CONTINUE
IF(NOP(3)-1) 3,3,15
3 READ(5,104)IDK1,IDK2,(XKAM(I),I=1,N)
GO TO 4
15 NRM1 = NR-1
NRP5 = NR+5
NRP6 = NR+6
MPM3 = MP-3
READ(5,112)IDK1,IDK2,XKAM(1),(XKAM(I),I=NR,NRP5),
1 (XKAM(I),I=MPM3,N)
112 FORMAT(A5,A4,-3P10F6.0)
DO 78 I=1,NRM1
78 XKAM(I) = XKAM(1)
DO 79 I=NRP6,MPM3
79 XKAM(I) = XKAM(MPM3)
4 CONTINUE
IF(NOP(4)-1)22,5,5
5 NOP4 = NOP(4)
DO 6 I=1,MP
6 RUM(I) = 0.0
RUM(MPP) = RUP
GO TO(10,22,11,13,17,22,22,22,22),NOP4
10 READ(5,106)IDRL1,IDRL2,(RUM(I),I=1,MPP)
C INPUT RUM(I) IN UNITS OF KIPS - THE COMPUTER WILL CONVERT TO LBS.
GO TO 22
11 RCONST = (RUT-RUP)/FLOAT(MPP-MO)
DO 12 I=MO,MP
12 RUM(I) = RCONST
GO TO 22
13 DO 16 I=MO,MP
16 RUM(I) = (2.0*(RUT-RUP)*(FLOAT(I-MO)+0.5))/(FLOAT(MPP-MO))**2
GO TO 22
C GENERAL R(I,J) INPUT

```

```
17 DO 20 I=1,MPP
20 XKIM(I) = 0.0
   DO 21 K=1,NUMR
21 READ(5,115)I, XKIM(I),(R(I,J),J=1,10)
22 CONTINUE
C THE R(I,J) INPUT CARDS CAN BE IN RANDOM ORDER
C THE R(I,J) ARRAY NEED NOT BE ZEROED SINCE IF XKIM(I)=0 THE GENERAL
C SOIL RESISTANCE ROUTINE FOR SEGMENT(I) IS NOT CONSIDERED
C NUMR = TOTAL NUMBER OF SEGMENTS W/GEN. R (DONT FORGET TO ADD MPP)
CC I = THE SEGMENT NUMBER FOR WHICH R(I,J) VALUES ARE BEING INPUT
C R(I,J) = STATIC RESISTANCE ON SEGMENT I AT EACH OF TEN POINTS J
   IF(NOP(5)-1)29,27,26
26 IF(NOP(5)-9)24,25,24
25 READ(5,106)IDG1,IDG2,(GAMMA(I),I=1,N)
   GO TO 29
24 IGAMMA = NOP(5)+NR-1
   DO 23 I=1,N
23 GAMMA(I) = -1000.0
   DO 19 I=NR,IGAMMA
19 GAMMA(I) = 0.0
   GAMMA(NR) = GAMMA1
   GAMMA(NR+1) = GAMMA2
   GO TO 29
27 DO 28 I=1,N
28 GAMMA(I) = -1000.0
   GAMMA(NR) = GAMMA1
   GAMMA(NR+1) = GAMMA2
29 GAMMA(MP) = -0.0
   GAMMA(MPP) = -0.0
   IF(NOP(6)-1)33,31,30
30 READ(5,107)IDE1,IDE2,(EEM(I),I=1,N)
   GO TO 33
31 DO 32 I=1,N
32 EEM(I) = 1.0
   EEM(NR) = EEM1
```



```

EEM(NR+1) = EEM2
33 EEM(MP) = -0.0
EEM(MPP) = -0.0
IF(NOP(7)-1)37,35,34
34 READ(5,107)IDB1,IDB2,(BEEM(I),I=1,N)
GO TO 37
35 DO 36 I=1,N
36 BEEM(I) = 0.0
37 BEEM(MP) = -0.0
BEEM(MPP) = -0.0
C DO NOT TRY TO USE LAST PROBLEMS VALUES OF VEL(I)
IF(NOP(8)-1)39,39,38
38 READ(5,108)IDV1,IDV2,(VEL(I),I=1,MP)
GO TO 71
39 DO 40 I=NR,MPP
40 VEL(I) = 0.0
DO 41 I=1,NR
41 VEL(I) = VELMI
71 VEL(MPP) = -0.0
IF(NOP(9)-1)45,43,42
42 READ(5,107)IDQ1,IDQ2,(Q(I),I=1,MPP)
GO TO 45
43 DO 44 I=1,MPP
Q(I) = QSIDE
44 CONTINUE
Q(MPP) = QPOINT
45 IF(NOP(10)-1)49,47,46
46 READ(5,107)IDJ1,IDJ2,(SJ(I),I=1,MPP)
GO TO 49
47 DO 48 I=1,MP
48 SJ(I) = SIDEJ
SJ(MPP) = POINTJ
49 IF(NOP(11)-1)53,51,50
50 READ(5,104)IDDK1,IDDK2,(DYNAMK(I),I=1,N)
DO 72 I=1,N

```

```
72 DYNAMK(I) = DYNAMK(I)-XKAM(I)
   GO TO 53
51 DO 52 I=1,N
52 DYNAMK(I) = 0.0
C STATEMENT 52 SETS DYNAMK(I) = 0.0 SO SMITHS ROUTINE WILL BE USED
53 DYNAMK(MP) = -0.0
   DYNAMK(MPP) = -0.0
   IF(NOP(12)-1)57,55,54
54 READ(5,109)IDA1,IDA2,(A(I),I=1,N)
   GO TO 57
55 DO 56 I=1,N
56 A(I) = AREA
57 A(MP) = -0.0
   A(MPP) = -0.0
   IF(NOP(4)-1)61,58,58
58 IF(NOP(4)-5)59,61,61
59 DO 60 I=1,MPP
60 XKIM(I) = RUM(I)/Q(I)
61 CONTINUE
   NOP14 = NOP(14)+1
   GO TO(65,65,62,63,65),NOP14
C READ NSTOP VALUES OF FOM(1,T) - MAXIMUM NSTOP = 300
62 READ(5,120)(FORCIN(I),I=1,NSTOP)
   GO TO 65
63 READ(5,122)AREAP,EMODUL,RGAGE,RCAL,ACTIVG,GFACTR,D1,D2,D3,D4,D5
   READ(5,121)(FORCIN(I),I=1,NSTOP)
   CE = (AREAP*EMODUL*RGAGE*1000.0)/(ACTIVG*GFACTR*RCAL)
   A(NS1) = CE/D1
   A(NS2) = CE/D2
   A(NS3) = CE/D3
   A(NS4) = CE/D4
   A(NS5) = CE/D5
   DO 64 I=1,NSTOP
64 FORCIN(I) = FORCIN(I)*A(I)
65 CONTINUE
```

```

        IF(NOP(14)-4)67,66,67
66 READ(5,123)F1,F2,C1,C2
67 CONTINUE
        DO 90 I=1,20
90 NOPP(I) = 1
        IF(NOP(16)-2)69,68,69
68 READ(5,124)(NOPP(I),I=1,20),DV1,DW1,DW2,DWI,DK1,DK2,DKI,DQI,
1   DQP,DJI,DJP,DRI,DRP,DE1,DE2
69 CONTINUE
        DO 8 I=1,20
        NOPP(I) = MAX0(NOPP(I),1)
8 CONTINUE
        IF(NOP(17)-1)74,74,73
73 READ(5,125)AREAP,XLONG,ELAST,CENR,QAVG,WRAM,WPILE,ENERGY
        XLONG = XLONG*12.0
74 CONTINUE
100 FORMAT(A5,A4,F6.0,I3,F4.2,2I3,2F4.3,2F6.0,I4,20I1)
101 FORMAT(A5,A4,2F7.2,I3,4F4.3,2I3,F6.2,6I3)
102 FORMAT(A5,A4,-3P10F6.4,/(9X,-3P10F6.4))
103 FORMAT(12A6)
104 FORMAT(A5,A4,-3P10F6.0,/(9X,-3P10F6.0))
106 FORMAT(A5,A4,-3P10F6.1,/(9X,-3P10F6.1))
107 FORMAT(A5,A4, 10F6.5,/(9X, 10F6.5))
108 FORMAT(A5,A4, 10F6.3,/(9X, 10F6.3))
109 FORMAT(A5,A4, 10F6.2,/(9X, 10F6.2))
115 FORMAT(I3,-3P11F6.1)
120 FORMAT(-3P10F6.1)
121 FORMAT( 10F6.4)
122 FORMAT(F7.2,3F7.0,7F4.2)
123 FORMAT(-3P2F6.1,0P2F6.5)
124 FORMAT(20I1,17F3.2)
125 FORMAT(F6.2,F5.2,F7.2)
        RETURN
        END
$IBFTC PRINT

```

C
C

PRINT 1 IS A SUBROUTINE TO PRINT INPUT DATA.

SUBROUTINE PRINT 1

```

COMMON  WAM(100),  XKAM(100),  RUM(100),  BEEM(100),  EEM(100)      1
COMMON  GAMMA(100),  XKIM(100),  CEEMAS(100),  NFOM(100),  XDEM(100)  2
COMMON  DEM(100),  XCEEM(100),  CEEM(100),  FOM(100),  XFOM(100)    3
COMMON  VEL(100),  DIM(100),  RAM(100),  RMAX(100),  RSTAT(100)     4
COMMON  R(100,10) ,  ITRIG(100),  Q(100),  FORCIN(100),  DFOM(100)   5
COMMON  FOMAX(100),  IFOMAX(100),  FOMIN(100),  IFOMIN(100),  A(100)  6
COMMON  DEMAX(100),  IDEMAX(100),  SJ(100),  NOP( 22),  DYNAMK(100)   7
COMMON  CEEMIN(100),  HOLDEM(100),  ANSVEC( 50),  SE(50,51) ,  IROW( 51)  8
COMMON  RUMA(100),  WAMC(100),  XKAMC(100),  QA(100),  SJA(100)     9
COMMON  ICOL( 51),  NOPP( 20),  ENTHRU(100),  ENTMAX(100),  IDS( 50)  10
COMMON  QSIDE ,  QPOINT,  SIDEJ ,  POINTJ,  NQDIV ,  NORAMS,  NSTOP    50
COMMON  INTV ,  ISECTN,  NUMR ,  F1 ,  F2 ,  C1 ,  C2                51
COMMON  IPRINT,  DELTEE,  EEM1 ,  EEM2 ,  GAMMA1,  GAMMA2,  INT       52
COMMON  INTT ,  I ,  ITST ,  IX ,  NR ,  MO ,  MP                    53
COMMON  NPAGE ,  N ,  QUAKE ,  RUP ,  RUT ,  VELMI ,  ID1            54
COMMON  ID2 ,  ID3 ,  ID4 ,  IDW1 ,  IDW2 ,  IDK1 ,  IDK2            55
COMMON  IDRL1 ,  IDRL2 ,  IDG1 ,  IDG2 ,  IDE1 ,  IDE2 ,  IDB1       56
COMMON  IDB2 ,  IDV1 ,  IDV2 ,  IDQ1 ,  IDQ2 ,  IDJ1 ,  IDJ2        57
COMMON  IDDK1 ,  IDDK2 ,  IDA1 ,  IDA2 ,  KGRADD,  J5 ,  TMIN         58
COMMON  TMAX ,  SMIN ,  SMAX ,  NOPNTS,  AREA ,  NS1 ,  NS2,  NS6    59
COMMON  NS3 ,  NS4 ,  NS5 ,  IDEEM ,  MH ,  VEL1 ,  ACCEL           60
COMMON  B ,  C ,  AREAP ,  XLONG ,  ELAST ,  ACELMX                 61
COMMON  DV1,  DE1,  DE2,  DRI,  DRP,  DQ1,  DQP,  DJI,  DJP,  DW1,  DW2,  DWI,  DK1,  DK2,  DK I

```

C

```

NPAGE = NPAGE+1
WRITE(6,102)NPAGE
IF(NOP(1)-2)3,2,2
2 NOIDS = 12*(NOP(1)-1)
WRITE(6,101)
WRITE(6,103 )(IDS(I),I=1,NOIDS)
WRITE(6,101)
3 CONTINUE

```

```

MPP=MP+1
RCT = 0.0
DO 6 I= 1,MPP
RCT = RCT+RUM(I)/1000.0
6 CONTINUE
RCP = RUM(MPP)/1000.0
WRITE(6,105)DELTEE,NOP(1),NOP(16)
DELTEE = 1.0/DELTEE
WRITE(6,106)MP,NOP(2),NOP(17)
WRITE(6,107)ID1,ID2,VELMI,NOP(3),NOP(18)
WRITE(6,108)ID3,ID4,NSTOP,NOP(4),NOP(19)
WRITE(6,110)IDW1,IDW2,RCT,NOP(5),NOP(20)
WRITE(6,111)IDK1,IDK2,RCP,NOP(6)
WRITE(6,112)IDRL1,IDRL2,MO,NOP(7)
WRITE(6,113)IDG1,IDG2,QSIDE,NOP(8)
WRITE(6,114)IDE1,IDE2,QPOINT,NOP(9)
WRITE(6,115)IDB1,IDB2,SIDEJ,NOP(10)
WRITE(6,116)IDV1,IDV2,POINTJ,NOP(11)
WRITE(6,117)IDQ1,IDQ2,NUMR,NOP(12)
WRITE(6,118)IDJ1,IDJ2,IPRINT,NOP(13)
WRITE(6,119)IDDK1,IDDK2,AREA,NOP(14)
WRITE(6,120)IDA1,IDA2,NR,NOP(15)
WRITE(6,101)
WRITE(6,121)
MPP = MP+1
LINES = 19
DO 5 I=1,MPP
WRITE(6,122)I,WAM(I),XKAM(I),RUM(I),GAMMA(I),EEM(I),BEEM(I),
1 VEL(I),Q(I), SJ(I),DYNAMK(I),A(I)
LINES = LINES+1
IF(LINES-58)5,4,4
4 NPAGE = NPAGE
LINES = 5
WRITE(6,102)NPAGE
WRITE(6,101)

```

```
WRITE(6,121)
5 CONTINUE
  IF(NOP(4)-5)30,7,30
7 IF(LINES-50)9,9,8
8 NPAGE = NPAGE
  LINES = -1
  WRITE(6,102)NPAGE
  GO TO 10
9 WRITE(6,101)
10 WRITE(6,123)(J,J=1,10)
  LINES = LINES+6
  LINADD = NQDIV/10
  IF(NQDIV-LINADD*10)13,14,13
13 LINADD = LINADD+1
14 LINADD = LINADD+1
  DO 29 I=1,MPP
  IF(XKIM(I)-0.0)29,29,20
20 LINES = LINES+LINADD
  IF(LINES-59)24,24,23
23 NPAGE = NPAGE
  WRITE(6,102)NPAGE
  WRITE(6,123)(J,J=1,10)
  LINES = 6
24 WRITE(6,124)I,(R(I,J),J=1,10)
29 CONTINUE
  WRITE(6,101)
  LINES = LINES+2
30 WRITE(6,101)
  LINES = LINES+2
  LINADD = MP/8
  IF(MP-LINADD*8)40,41,40
40 LINADD = LINADD+1
41 LINADD = LINADD+2
101 FORMAT(1H0)
```

```

102 FORMAT(1H1, 20H                                66X,7HPROBLEM 14)
103 FORMAT(1X,12A6)
123 FORMAT(85H      R(M,N) = STATIC SOIL RESISTANCE FOR GIVEN SEGMENTS -
1  OTHERS HAVE R(I,J) = 0.0      // 5X,10(8X,I2) )
105 FORMAT(4X,29H CARD  ID1  ID2  1/DELTEE =  F8.0,12H  NOP(1) =
1  I2, 12H  NOP(16) =  I2)
106 FORMAT(28X, 5H MP = 18,12H  NOP(2) =I2,12H  NOP(17) =I2)
107 FORMAT(11H      101  A6,A4,12H  VELMI =F8.2,12H  NOP(3) =
1  I2, 12H  NOP(18) =  I2)
108 FORMAT(11H      102  A6,A4,12H  NSTOP = 18 ,12H  NOP(4) =
1  I2, 12H  NOP(19) =  I2)
110 FORMAT(11H      WAM  A6,A4,12H      RUT =F8.1,12H  NOP(5) =I2,
1  12H  NOP(20) =  I2)
111 FORMAT(11H      XKAM A6,A4,12H      RUP =F8.1,12H  NOP(6) =I2)
112 FORMAT(11H      RUM  A6,A4,12H      MO =18 ,12H  NOP(7) =I2)
113 FORMAT(11H      GAMMA A6,A4,12H      QSIDE =F8.4,12H  NOP(8) =I2)
114 FORMAT(11H      EEM  A6,A4,12H      QPOINT =F8.4,12H  NOP(9) =I2)
115 FORMAT(11H      BEEM A6,A4,12H      SIDEJ =F8.4,12H  NOP(10) =I2)
116 FORMAT(11H      VEL  A6,A4,12H      POINTJ =F8.4,12H  NOP(11) =I2)
117 FORMAT(11H      Q    A6,A4,12H      NUMR =18 ,12H  NOP(12) =I2)
118 FORMAT(11H      SOILJ A6,A4,12H      IPRINT =18 ,12H  NOP(13) =I2)
119 FORMAT(11H      DYNAMK A6,A4,12H      AREA =F8.2,12H  NOP(14) =I2)
120 FORMAT(11H      A    A6,A4,12H      NR =18 ,12H  NOP(15) =I2)
121 FORMAT(116H      M    WAM(M)  XKAM(M)  RUM(M)  GAMMA(M)  EEM(M)
1  BEEM(M)  VEL(M)      Q(M)  SOILJ(M) DYNAMK(M)  A(M)  /,
2  116H      (KIPS)  (KIPS/IN)  (KIPS)  (KIPS)  (NONE) (SECIN/
3FT)  (FT/SEC)  (IN)  (SEC/FT) (KIPS/IN)  (SQ IN)  )
122 FORMAT(14,-3PF10.4,3F10.1,0P2F10.6,F10.3,2F10.6,-3PF10.3,0PF12.3)
124 FORMAT(/4H 7 = 13,2X,10F10.1,(/9X,10F10.1))
RETURN
END

```

```

$IBFTC REPONE
SUBROUTINE REP1
COMMON  WAM(100),  XKAM(100),  RUM(100),  BEEM(100),  EEM(100)  1
COMMON  GAMMA(100),  XKIM(100),CEEMAS(100),  NFOM(100),  XDEM(100)  2

```

```

COMMON  DEM(100), XCEEM(100), CEEM(100), FOM(100), XFOM(100)      3
COMMON  VEL(100), DIM(100), RAM(100), RMAX(100), RSTAT(100)      4
COMMON  R(100,10) , ITRIG(100), Q(100),FORCIN(100), DFOM(100)    5
COMMON  FOMAX(100),IFOMAX(100), FOMIN(100),IFOMIN(100), A(100)  6
COMMON  DEMAX(100),IDEMAX(100), SJ(100), NOP( 22),DYNAMK(100)   7
COMMON  CEEMIN(100),HOLDEM(100),ANSVEC( 50),SE(50,51) , IROW( 51) 8
COMMON  RUMA(100), WAMC(100), XKAMC(100), QA(100), SJA(100)     9
COMMON  ICOL( 51), NOPP( 20),ENTHRU(100),ENTMAX(100), IDS( 50)  10
COMMON  QSIDE , QPOINT, SIDEJ , POINTJ, NQDIV , NORAMS, NSTOP    50
COMMON  INTV , ISECTN, NUMR , F1 , F2 , C1 , C2                  51
COMMON  IPRINT, DELTEE, EEM1 , EEM2 , GAMMA1, GAMMA2, INT        52
COMMON  INTT , I , ITST , IX , NR , MO , MP                      53
COMMON  NPAGE , N , QUAKE , RUP , RUT , VELMI , ID1              54
COMMON  ID2 , ID3 , ID4 , IDW1 , IDW2 , IDK1 , IDK2              55
COMMON  IDRL1 , IDRL2 , IDG1 , IDG2 , IDE1 , IDE2 , IDB1         56
COMMON  IDB2 , IDV1 , IDV2 , IDQ1 , IDQ2 , IDJ1 , IDJ2          57
COMMON  IDDK1 , IDDK2 , IDA1 , IDA2 , KGRADD, J5 , TMIN          58
COMMON  TMAX , SMIN , SMAX , NOPNTS, AREA , NS1 , NS2,NS6       59
COMMON  NS3 , NS4 , NS5 , IDEEM , MH , VEL1 , ACCELR            60
COMMON  B , C , AREAP , XLONG , ELAST , ACELMX                   61
COMMON  DV1,DE1,DE2,DRI,DRP,DQI,DQP,DJI,DJP,DW1,DW2,DWI,DK1,DK2,DKI

```

C

```

MP = MP
MPP = MP+1
SMAX = 0.0
SMIN = 0.0
DO 64 I = 1,MPP
ITRIG(I) = 1
DEM(I) = 0.0
XDEM(I) = 0.0
DEMAX(I) = 0.0
IDEMAX(I) = 0
CEEM(I) = 0.0
XCEEM(I) = 0.0
CEEMAS(I) = 0.0

```



```

FOM(I) = 0.0
XFOM(I) = 0.0
FOMAX(I) = 0.0
FOMIN(I) = 0.0
IFOMAX(I) = 0
IFOMIN(I) = 0
NFOM(I) = 1
RAM(I) = 0.0
RMAX(I) = 0.0
RSTAT(I) = 0.0
DIM(I) = 0.0
ENTHRU(I) = 0.0
ENTMAX(I) = 0.0
64 CONTINUE
IF(NOP(14)-4)18,65,18
65 CONTINUE
C = (F1*C2 - F2*C1)/(C1*C2*(C1-C2))
B = (F2*C1**2 - F1*C2**2)/(C1*C2*(C1-C2))
IF(B)22,22,18
22 IF(F1-F2)24,23,23
23 C = F1/C1**2
GO TO 25
24 C = F2/C2**2
25 B = 0.0
WRITE(6,104)
104 FORMAT(47HOPARABOLA BASED ON F2 AND C2 ONLY MUST BE USED )
18 CONTINUE
RETURN
END
$IBFTC REPREP
SUBROUTINE REP N
COMMON WAM(100), XKAM(100), RUM(100), BEEM(100), EEM(100) 1
COMMON GAMMA(100), XKIM(100), CEEMAS(100), NFOM(100), XDEM(100) 2
COMMON DEM(100), XCEEM(100), CEEM(100), FOM(100), XFOM(100) 3
COMMON VEL(100), DIM(100), RAM(100), RMAX(100), RSTAT(100) 4

```

```

COMMON R(100,10) , ITRIG(100),      Q(100),FORCIN(100),  DFOM(100)      5
COMMON FOMAX(100),IFOMAX(100), FOMIN(100),IFOMIN(100),  A(100)      6
COMMON DEMAX(100),IDEMAX(100),      SJ(100),  NOP( 22),DYNAMK(100)  7
COMMON CEEMIN(100),HOLDEM(100),ANSVEC( 50),SE(50,51) ,  IROW( 51)    8
COMMON RUMA(100), WAMC(100), XKAMC(100),  QA(100),  SJA(100)    9
COMMON ICOL( 51), NOPP( 20),ENTHRU(100),ENTMAX(100),  IDS( 50)   10
COMMON QSIDE , QPOINT, SIDEJ , POINTJ, NQDIV , NORAMS, NSTOP    50
COMMON INTV , ISECTN, NUMR , F1 , F2 , C1 , C2    51
COMMON IPRINT, DELTEE, EEM1 , EEM2 , GAMMA1, GAMMA2, INT    52
COMMON INTT , I , ITST , IX , NR , MO , MP    53
COMMON NPAGE , N , QUAKE , RUP , RUT , VELMI , ID1    54
COMMON ID2 , ID3 , ID4 , IDW1 , IDW2 , IDK1 , IDK2    55
COMMON IDRL1 , IDRL2 , IDG1 , IDG2 , IDE1 , IDE2 , IDB1    56
COMMON IDB2 , IDV1 , IDV2 , IDQ1 , IDQ2 , IDJ1 , IDJ2    57
COMMON IDDK1 , IDDK2 , IDA1 , IDA2 , KGRADD, J5 , TMIN    58
COMMON TMAX , SMIN , SMAX , NOPNTS, AREA , NS1 , NS2,NS6    59
COMMON NS3 , NS4 , NS5 , IDEEM , MH , VEL1 , ACCELR    60
COMMON B , C , AREAP , XLONG , ELAST , ACELMX    61
COMMON DV1,DE1,DE2,DRI,DRP,DQI,DQP,DJI,DJP,DW1,DW2,DWI,DK1,DK2,DKI

```

C

```

INTV = INTV+1
MP=MP
MPP = MP+1
NOP(4) = NOP(4)
NOP(13) = NOP(13)
NOP(14) = NOP(14)
NOP(15) = NOP(15)
ITEST1 = 1
ITESTP = 1
DO 68 I = 1, MP
I=I
IF(I-MP)18,I7,18
17 ITESTP = 2
18 CONTINUE
XDEM(I) = DEM(I)

```

```

    DEM(I) = XDEM(I) +VEL(I)*12.0*DELTEE
    IF(DEMAX(I)-DEM(I))20,21,21
20  DEMAX(I)= DEM(I)
    IDEMAX(I) = INTV
21  GO TO(34,19),ITESTP
34  XCEEM(I) = CEEM(I)
C   STATEMENT 34 MUST USE A COMPUTED VALUE FOR THE ACTUAL DEM(I+1)
    CEEM(I) = DEM(I) -DEM(I+1) -VEL(I+1)*12.0*DELTEE
    XFOM(I) = FOM(I)
    IF(BEEM(I)-0.000001)36,36,30
30  IF(DYNAMK(I))31,31,32
C
31  DFOM(I) = BEEM(I)*XKAM(I)*((CEEM(I)-XCEEM(I))/(DELTEE*IZ.0)
    GO TO 33
C
32  DFOM(I) = (DFOM(I)+DYNAMK(I)*((CEEM(I)-XCEEM(I)))/
1      (1.0+DYNAMK(I)*DELTEE/(1000.0*BEEM(I))))
C   STANDARD LINEAR SOLID DAMPING
33  FOM(I) = CEEM(I)*XKAM(I) + DFOM(I)
    GO TO 43
36  IF(0.99999-EEM(I))38,38,39
38  FOM(I) = CEEM(I)*XKAM(I)
    CEEMAS(I) = AMAX1(CEEMAS(I),XCEEM(I))
    GO TO 43
39  CEEMAS(I) = AMAX1(CEEMAS(I),XCEEM(I))
    CEEMIN(I) = AMIN1(CEEMIN(I),XCEEM(I))
    IF(CEEM(I))13,43,5
5   IF(CEEM(I)-CEEMAS(I))11,11,38
11  FOM(I)=AMAX1(XKAM(I)*((CEEMAS(I)-((CEEMAS(I)-CEEM(I))/EEM(I)**2),0.)
    GO TO 43
13  IF (CEEM(I)-CEEMIN(I))38,14,14
14  FOM(I)=AMIN1(XKAM(I)*((CEEMIN(I)-((CEEMIN(I)-CEEM(I))/EEM(I)**2),0.)
43  CONTINUE
C
    IF NOP(14)=2, SET FOM(1) = FORCIN(INTV)
    GO TO(1,16),ITEST1
1   NOP14 = NOP(14)+1

```

```

      GO TO(6,6,2,2,6),NOP14
2  FOM(1) = FORCIN(INTV)
   IF(FOM(1)-1.0)3,3,4
3  DEM(1) = XDEM(1)
   CEEM(1) = XCEEM(1)
   GO TO 16
C IF NOP(14) = 4, USE PARABOLIC FOM(1) VS. CEEM(1) CURVE
C THE RAM MUST BE A SINGLE MASS IF FOM VS. DEM IS PARABOLIC
6  IF(NOP(14)-4)4,7,4
7  IF(CEEM(1) - CEEMAS(1))9,8,8
8  FOM(1) = C*CEEM(1)**2 + B*CEEM(1)
   GO TO 12
4  IF(CEEM(1)-CEEMAS(1))16,12,12
9  FOMAX(1) = AMAX1(XFOM(1),FOMAX(1))
   FOM(1) = FOMAX(1)-((CEEMAS(1)-CEEM(1))*FOMAX(1)**2)/(2.0*SMAX*
1  EEM(1)**2)
   GO TO 16
12 SMAX = SMAX+((FOM(1)+XFOM(1))/2.0)*(CEEM(1)-XCEEM(1))
16 CONTINUE
   IF(GAMMA(I))46,44,45
44 FOM(I) =AMAX1 (.0, FOM(I))
   GO TO 46
45 IF(FOM(I) - XFOM(I))48,47,47
48 NFOM(I) = 2
47 IX = NFOM(I)
   GO TO (46,49),IX
49 HOLDF = FOM(I)
   FOM(I) = AMAX1(FOM(I),GAMMA(I))
COMMENT THE .01 HOLDS MIN. PRESSURE AT GAMMA(I) FOR .01 SECONDS WHILE THE
COMMENT .0025 REDUCES THE PRESSURE TO ZERO IN .0025 ADDITIONAL SECONDS.
   TINT = INTV
   IF(TINT - .01/DELTEE)46,46,90
90 FOM(I) = AMAX1(0.0, GAMMA(I)*((1.0-(DELTEE*TINT-.01)/.0025),HOLDF)
46 CONTINUE
   ENTHRU(I) = ENTHRU(I)+(FOM(I)+XFOM(I))*(DEM(I+1)-XDEM(I+1))/24.0

```

```

ENTMAX(I) = AMAX1(ENTMAX(I),ENTHRU(I))
GO TO(22,19),ITEST1
22 IF(CEEM(1) - CEEMAS(1))15,19,19
15 SMIN = SMIN-((FOM(1)+XFOM(1))/2.0)*(CEEM(1)-XCEEM(1))
19 CONTINUE
IF(NOP(4)-5)29,28,29

```

C

```

28 CALL GENRAM
GO TO 55
29 CONTINUE

```

GENERALIZED SOIL RESISTANCE

C

```

IF(XKIM(I))50,155,50
155 GO TO(55,156),ITESTP
156 IF(XKIM(MPP ))50,55,50
50 IF(DIM(I) -DEM(I) +Q(I) )51,52,52
51 DIM(I) = DEM(I) -Q(I)
52 CONTINUE
70 IF(DIM(I) -DEM(I) -Q(I) )53,53,54
54 DIM(I) = DEM(I) +Q(I)
53 CONTINUE
DIM(MPP ) =AMAX1 (DIM(MP),DIM(MPP ))
ITST = ITRIG(I)
GO TO(10,57),ITST
10 IF(DEM(I) -DIM(I) -Q(I) )56,57,57
56 RAM(I) = (DEM(I)-DIM(I))*XKIM(I)*(1.0+(SJ(I) *VEL(I)))
GO TO(55,171),ITESTP
171 RAM(MP) = RAM(MP)+(DEM(MP)-DIM(MPP ))*XKIM(MPP )*
1 (1.0+(SJ(MPP)*VEL(MP)))

```

SMITHS SOIL RESISTANCE

C

C

```

GO TO 55
57 RAM(I) = (DEM(I)-DIM(I)+ SJ(I) *Q(I) *VEL(I))*XKIM(I)
ITRIG(I) = 2
GO TO(55,172),ITESTP
172 RAM(MP)=RAM(MP)+(DEM(I)-DIM(MPP)+SJ(MPP)*Q(MPP)*VEL(MP))*XKIM(MPP)

```

SEGMENT MP HAS RAM(MP) + RAM(MP+1) APPLIED
RAM(MP+1) MAY BE TENSILE

```
55 CONTINUE
   GO TO(58,72), ITEST1
58 VEL(I) = VEL(I) - (FOM(I) + RAM(I)) * 32.17 * DELTEE / WAM(I)
   ITEST1 = 2
   GO TO 59
72 VEL(I) = VEL(I) + (FOM(I-1) - FOM(I) - RAM(I)) * 32.17 * DELTEE / WAM(I)
59 CONTINUE
   IF(NOP(15) - 1) 85, 85, 83
83 VEL(I) = VEL(I) + 32.17 * DELTEE
85 CONTINUE
65 IF(FOMAX(I) - FOM(I)) 67, 67, 66
67 FOMAX(I) = FOM(I)
   IFOMAX(I) = INTV
66 IF(FOMIN(I) - FOM(I)) 68, 69, 69
69 FOMIN(I) = FOM(I)
   IFOMIN(I) = INTV
68 CONTINUE
   IF(VEL(2) / VEL1 - 2.1) 61, 60, 60
60 WRITE(6, 105)
   INTT = 2
   RETURN
105 FORMAT(76H0 THE RATIO OF THE VELOCITY OF W(2) TO THE VELOCITY OF
   1THE RAM EXCEEDS 2.1. )
61 IF(VEL(MP) / VEL1 - 2.1) 63, 62, 62
62 WRITE(6, 106)
106 FORMAT(76H0 THE RATIO OF THE VELOCITY OF W(P) TO THE VELOCITY OF
   1THE RAM EXCEEDS 2.1. )
   INTT = 2
   RETURN
63 CONTINUE
   LDCELL = MH - 1
   ACCELR = (FOM(LDCELL - 1) - FOM(LDCELL)) / WAM(LDCELL)
71 ACELMX = AMAX1(ACELMX, ACCELR)
73 CONTINUE
   RETURN
```

END
 \$IBFTC RAMGEN
 SUBROUTINE GENRAM

C
 C NQDIV = NO. OF EQUAL SEGMENTS INTO WHICH Q(I) IS DIVIDED = 10
 C RSTAT(I) = STATIC SOIL RESISTANCE NEGLECTING THE SOIL DAMPING EFFECTS
 C RMAX(I) = A TEMPORARY MAXIMUM STATIC SOIL RESISTANCE
 C PERCQ = DISTANCE FROM ZERO DISPLACEMENT TO DEM(I) IN UNITS (1.732,..)
 C

COMMON	WAM(100),	XKAM(100),	RUM(100),	BEEM(100),	EEM(100)	1		
COMMON	GAMMA(100),	XKIM(100),	CEEMAS(100),	NFOM(100),	XDEM(100)	2		
COMMON	DEM(100),	XCEEM(100),	CEEM(100),	FOM(100),	XFOM(100)	3		
COMMON	VEL(100),	DIM(100),	RAM(100),	RMAX(100),	RSTAT(100)	4		
COMMON	R(100,10)	, ITRIG(100),	Q(100),	FORCIN(100),	DFOM(100)	5		
COMMON	FOMAX(100),	IFOMAX(100),	FOMIN(100),	IFOMIN(100),	A(100)	6		
COMMON	DEMAX(100),	IDEMAX(100),	SJ(100),	NOP(22),	DYNAMK(100)	7		
COMMON	CEEMIN(100),	HOLDEM(100),	ANSVEC(50),	SE(50,51)	, IROW(51)	8		
COMMON	RUMA(100),	WAMC(100),	XKAMC(100),	QA(100),	SJA(100)	9		
COMMON	ICOL(51),	NOPP(20),	ENTHRU(100),	ENTMAX(100),	IDS(50)	10		
COMMON	QSIDE ,	QPOINT,	SIDEJ ,	POINTJ,	NQDIV ,	NORAMS ,	NSTOP	50
COMMON	INTV ,	ISECTN,	NUMR ,	F1 ,	F2 ,	C1 ,	C2	51
COMMON	IPRINT,	DELTEE,	EEM1 ,	EEM2 ,	GAMMA1,	GAMMA2,	INT	52
COMMON	INTT ,	I ,	ITST ,	IX ,	NR ,	MO ,	MP	53
COMMON	NPAGE ,	N ,	QUAKE ,	RUP ,	RUT ,	VELMI ,	ID1	54
COMMON	ID2 ,	ID3 ,	ID4 ,	IDW1 ,	IDW2 ,	IDK1 ,	IDK2	55
COMMON	IDRL1 ,	IDRL2 ,	IDG1 ,	IDG2 ,	IDE1 ,	IDE2 ,	IDB1	56
COMMON	IDB2 ,	IDV1 ,	IDV2 ,	IDQ1 ,	IDQ2 ,	IDJ1 ,	IDJ2	57
COMMON	IDDK1 ,	IDDK2 ,	IDA1 ,	IDA2 ,	KGRADD,	J5 ,	TMIN	58
COMMON	TMAX ,	SMIN ,	SMAX ,	NOPNTS,	AREA ,	NS1 ,	NS2,NS6	59
COMMON	NS3 ,	NS4 ,	NS5 ,	IDEEM ,	MH ,	VEL1 ,	ACCELR	60
COMMON	B ,	C ,	AREAP ,	XLONG ,	ELAST ,	ACELMX		61
COMMON	DV1,DEL,	DE2,DRI,	DRP,DQI,	DQP,DJI,	DJP,DW1,	DW2,DW1,	DK1,DK2,DKI	

C
 MP = MP
 K = I

```

QDIV = 10.0
NQDIV = 10
IF(XKIM(K)-0.1) 1,2,2
1 RAM(K) = 0.0
GO TO 70
2 IF(DEM(K)-DIM(K))32,3,3
3 DIM(K) = DEM(K)
IF(DEM(K)-Q(K))7,6,6
6 RSTAT(K) = R(K,NQDIV)
GO TO 50
7 PERCQ = DEM(K)/(Q(K)/QDIV)
IPERCQ = PERCQ
XPERCQ = IPERCQ
IF(IPERCQ)8,8,9
8 RSTAT(K) = PERCQ*R(K,1)
GO TO 50
9 RSTAT(K) = R(K,IPERCQ)+(PERCQ-XPERCQ)*(R(K,IPERCQ+1)-R(K,IPERCQ))
GO TO 50
32 RMAX(K) = AMAX1(RMAX(K),RSTAT(K))
RSTAT(K) = RMAX(K)-(DIM(K)-DEM(K))*XKIM(K)
C THE STATIC FORCE SHOULD REALLY LEAVE THE XKIM(I) SLOPE AND REMAIN
C CONSTANT IF RMAX(I)+RSTAT(I) EVER EXCEEDS 0.0
IF(RMAX(K)+RSTAT(K))39,50,50
39 WRITE(6,200)RMAX(K),RSTAT(K),K
200 FORMAT(11HORMAX(I) = F10.2, 6X, 12H RSTAT(I) = F10.2,6X,4H I =I6)
C STATEMENTS 50 THRU 70 INCLUDE THE SOIL DAMPING EFFECT
50 ITST = ITRIG(K)
GO TO(51,57),ITST
51 IF(DEM(K)-Q(K))56,57,57
56 RAM(K) = RSTAT(K)+RSTAT(K)*SJ(K)*VEL(K)
GO TO 70
57 RAM(K) = RSTAT(K)+R(K,NQDIV)*SJ(K)*VEL(K)
ITRIG(K) = 2
GO TO 70
70 IF(K-MP)80,71,73

```



```

71 CONTINUE
   K = MP+1
   IF(XKIM(K)-0.01)80,80,72
72 DEM(K) = DEM(MP)
   VEL(K) = VEL(MP)
   GO TO 2
73 CONTINUE
C 73 IF(RAM(K))74,75,75      (OLD STATEMENT)
C 74 RAM(K) = 0.0 (OLD STATEMENT)      1
74 CONTINUE
75 RAM(MP) = RAM(MP)+RAM(MP+1)
C
80 RETURN                      RAM(MP+1) CAN      GO INTO TENSION
   END

```

\$IBFTC EXCTG

```

SUBROUTINE EXACTG
COMMON   WAM(100),  XKAM(100),  RUM(100),  BEEM(100),  EEM(100)      1
COMMON   GAMMA(100),  XKIM(100),CEEMAS(100),  NFUM(100),  XDEM(100)      2
COMMON   DEM(100),  XCEEM(100),  CEEM(100),  FOM(100),  XFOM(100)      3
COMMON   VEL(100),  DIM(100),  RAM(100),  RMAX(100),  RSTAT(100)      4
COMMON   R(100,10)  ,  ITRIG(100),  Q(100),FORCIN(100),  DFOM(100)      5
COMMON   FOMAX(100),IFOMAX(100), FOMIN(100),IFOMIN(100),  A(100)      6
COMMON   DEMAX(100),IDEMAX(100),  SJ(100),  NOP( 22),DYNAMK(100)      7
COMMON   CEEMIN(100),HOLDEM(100),ANSVEC( 50),SE(50,51)  ,  IROW( 51)      8
COMMON   RUMA(100),  WAMC(100),  XKAMC(100),  QA(100),  SJA(100)      9
COMMON   ICOL( 51),  NOPP( 20),ENTHRU(100),ENTMAX(100),  IDS( 50)     10
COMMON   QSIDE  ,  QPOINT,  SIDEJ  ,  POINTJ,  NQDIV  ,  NORAMS,  NSTOP     50
COMMON   INTV  ,  ISECTN,  NUMR  ,  F1  ,  F2  ,  C1  ,  C2     51
COMMON   IPRINT,  DELTEE,  EEM1  ,  EEM2  ,  GAMMA1,  GAMMA2,  INT     52
COMMON   INTT  ,  I  ,  ITST  ,  IX  ,  NR  ,  MO  ,  MP     53
COMMON   NPAGE ,  N  ,  QUAKE  ,  RUP  ,  RUT  ,  VELMI  ,  ID1     54
COMMON   ID2  ,  ID3  ,  ID4  ,  IDW1  ,  IDW2  ,  IDK1  ,  IDK2     55
COMMON   IDRL1 ,  IDRL2 ,  IDG1  ,  IDG2  ,  IDE1  ,  IDE2  ,  IDB1     56
COMMON   IDB2  ,  IDV1  ,  IDV2  ,  IDQ1  ,  IDQ2  ,  IDJ1  ,  IDJ2     57
COMMON   IDDK1 ,  IDDK2 ,  IDA1  ,  IDA2  ,  KGRADD,  J5  ,  TMIN     58

```

```

COMMON TMAX , SMIN , SMAX , NOPNTS, AREA , NS1 , NS2,NS6      59
COMMON NS3 , NS4 , NS5 , IDEEM , MH , VEL1 , ACCEL R          60
COMMON B , C , AREAP , XLONG , ELAST , ACELMX                 61
COMMON DVI,DE1,DE2,DRI,DRP,DQI,DQP,DJI,DJP,DW1,DW2,DWI,DK1,DK2,DKI

```

C

```

MP = MP
MO = MO
MMO = MO-1
MMOO = MO - 2
MAO = MP - MO
NSDD = MP-MO+1
DO 6 NSEW = 1,NSDD
DO 6 NSE = 1,NSDD
6 SE(NSEW,NSE) = 0.0
SE(1,1) = XKAM(MO) + XKIM(MO)
SE(2,1) = -XKAM(MO)
DO 13 K = 2,MAO
NN = K + MMOO
NNN = K + MMO
SE(K-1,K) = SE(K,K-1)
SE(K,K) = XKAM(NN) + XKAM(NNN) + XKIM(NNN)
SE(K+1,K) = -XKAM(NNN)
13 CONTINUE
SE(MAO,NSDD) = SE(NSDD,MAO)
SE(NSDD,NSDD) = XKAM(MP-1)+XKIM(MP) + XKIM(MP+1)
DET = TAMINV(SE,ICOL,NSDD,50,0.00001)
IF(0.00001 - ABS(DET))14,12,12
12 WRITE(6,100)DET
100 FORMAT(33H0THE VALUE OF THE DETERMINANT = F10.7)
INTF = 2
RETURN
14 CONTINUE
WAMTL = 0.0
DO 15 NSEW = 2,MO
15 WAMTL = WAMTL + WAM(NSEW)

```

```

SE(1,NSDD+1) = WAMTL
DO 16 NSEW = 2,NSDD
NUTZ = MMO+NSEW
16 SE(NSEW,NSDD+1) = WAM(NUTZ)
DO 17 IANS = 1,NSDD
17 ANSVEC(IANS) = 0.0
DO 23 IM1 = 1,NSDD
DO 23 IM2 = 1,NSDD
23 ANSVEC(IM1) = ANSVEC(IM1)+SE(IM1,IM2)*SE(IM2,NSDD+1)
NAT = 0
DO 26 NST = MO,MP
NAT = NAT+1
DEM(NST) = ANSVEC(NAT)
HOLDEM(NST) = DEM(NST)
26 CONTINUE
WOS = 0.0
DO 27 NST = 2,MMO
WOS = WOS+WAM(NST)
CEEM(NST) = WOS/XKAM(NST)
FOM(NST) = WOS
27 CONTINUE
DO 28 NST = 1,MMO
NEL = MO-NST
DEM(NEL) = DEM(NEL+1) + CEEM(NEL)
HOLDEM(NEL) = DEM(NEL)
28 CONTINUE
MAM = MP-1
DO 29 NST = MO,MAM
CEEM(NST) = DEM(NST) - DEM(NST+1)
FOM(NST) = CEEM(NST)*XKAM(NST)
RAM(NST) = DEM(NST)*XKIM(NST)
29 CONTINUE
RAM(MP) = DEM(MP)*XKIM(MP)
RAM(MP+1) = DEM(MP)*XKIM(MP+1)
RETURN

```

```

END
$IBFTC SMTH
SUBROUTINE SMITH
COMMON WAM(100), XKAM(100), RUM(100), BEEM(100), EEM(100) 1
COMMON GAMMA(100), XKIM(100), CEEMAS(100), NFOM(100), XDEM(100) 2
COMMON DEM(100), XCEEM(100), CEEM(100), FOM(100), XFOM(100) 3
COMMON VEL(100), DIM(100), RAM(100), RMAX(100), RSTAT(100) 4
COMMON R(100,10), ITRIG(100), Q(100), FORCIN(100), DFOM(100) 5
COMMON FOMAX(100), IFOMAX(100), FOMIN(100), IFOMIN(100), A(100) 6
COMMON DEMAX(100), IDEMAX(100), SJ(100), NOP( 22), DYNAMK(100) 7
COMMON CEEMIN(100), HOLDEM(100), ANSVEC( 50), SE(50,51), IROW( 51) 8
COMMON RUMA(100), WAMC(100), XKAMC(100), QA(100), SJA(100) 9
COMMON ICOL( 51), NOPP( 20), ENTHRU(100), ENTMAX(100), IDS( 50) 10
COMMON QSIDE, QPOINT, SIDEJ, POINTJ, NQDIV, NQRAMS, NSTOP 50
COMMON INTV, ISECTN, NUMR, F1, F2, C1, C2 51
COMMON IPRINT, DELTEE, EEM1, EEM2, GAMMA1, GAMMA2, INT 52
COMMON INTT, I, ITST, IX, NR, MO, MP 53
COMMON NPAGE, N, QUAKE, RUP, RUT, VELMI, ID1 54
COMMON ID2, ID3, ID4, IDW1, IDW2, IDK1, IDK2 55
COMMON IDRL1, IDRL2, IDG1, IDG2, IDE1, IDE2, IDB1 56
COMMON IDB2, IDV1, IDV2, IDQ1, IDQ2, IDJ1, IDJ2 57
COMMON IDDK1, IDDK2, IDA1, IDA2, KGRADD, J5, TMIN 58
COMMON TMAX, SMIN, SMAX, NOPNTS, AREA, NS1, NS2, NS6 59
COMMON NS3, NS4, NS5, IDEEM, MH, VEL1, ACCELR 60
COMMON B, C, AREAP, XLONG, ELAST, ACELMX 61
COMMON DV1, DE1, DE2, DRI, DRP, DQI, DQP, DJI, DJP, DW1, DW2, DWI, DK1, DK2, DKI

```

C

```

MP = MP
N = MP-1
WAMTL = 0.0
RAMTL = 0.0
DO 5 JT = 2, MP
WAMTL = WAMTL + WAM(JT)
5 RAMTL = RAMTL + RUM(JT)
RAMTL = RAMTL + RUM(MP+1)

```

```

DO 8 JT = 2,N
RAM(JT) = (RUM(JT)*WAMTL)/RAMTL
8 FOM(JT) = FOM(JT-1)+WAM(JT)-RAM(JT)
RAM(1) = RUM(1)*WAMTL/RAMTL
RAM(MP) = RUM(MP)*WAMTL/RAMTL
RAM(MP+1) = RUM(MP+1)*WAMTL/RAMTL
DEM(MP) = (RAM(MP)+RAM(MP+1))/(XKIM(MP)+XKIM(MP+1))
HOLDEM(MP) = DEM(MP)
DO 11 JT = 1,N
JTM = MP-JT
CEEM(JTM) = FOM(JTM)/XKAM(JTM)
DEM(JTM) = DEM(JTM+1) + CEEM(JTM)
HOLDEM(JTM) = DEM(JTM)
DIM(JTM)=DEM(JTM)-WAMTL*Q(JTM)/RAMTL
11 CONTINUE
RETURN
END
SDATA

```

